

Covariance Matrix Estimation for High-Throughput Biomedical Data with Interconnected Communities

Yifan Yang

Department of Mathematics, University of Maryland, College Park, MD

and

Chixiang Chen

School of Medicine, University of Maryland, Baltimore, MD

and

Shuo Chen *

School of Medicine, University of Maryland, Baltimore, MD

November 17, 2023

Abstract

Estimating a covariance matrix is central to high-dimensional data analysis. Empirical analyses of high-dimensional biomedical data, including genomics, proteomics, microbiome, and neuroimaging, among others, consistently reveal strong modularity in the dependence patterns. In these analyses, intercorrelated high-dimensional biomedical features often form communities or modules that can be interconnected with others. While the interconnected community structure has been extensively studied in biomedical research (e.g., gene co-expression networks), its potential to assist in the estimation of covariance matrices remains largely unexplored. To address this gap, we propose a procedure that leverages the commonly observed interconnected community structure in high-dimensional biomedical data to estimate large covariance and precision matrices. We derive the uniformly minimum variance unbiased estimators for covariance and precision matrices in closed forms and provide theoretical results on their asymptotic properties. Our proposed method enhances the accuracy of covariance- and precision-matrix estimation and demonstrates superior performance compared to the competing methods in both simulations and real data analyses.

Keywords: Closed-form estimate; Interconnected community network; Precision matrix; Structured covariance matrix; Uniform blocks

*Emails: yiorfun@umd.edu; chixiang.chen@som.umaryland.edu; shuochen@som.umaryland.edu; and * is for the corresponding author

1 Introduction

Technological innovations in biomedicine have facilitated the generation of high-dimensional datasets with simultaneous measurements of up to millions of biological features (Fan and Lv, 2008). In the past few decades, numerous statistical methods have been developed to analyze these large-dimensional datasets. Estimating a covariance matrix (or a precision matrix) is fundamental to these analyses (Fan et al., 2016; Cai et al., 2016; Wainwright, 2019) because a covariance matrix not only describes the complex interactive relations among variables but also leads to accurate inferential and predictive results for clinical outcomes (He et al., 2019; Ke et al., 2022). Since the dimensionality of the variables is much larger than the sample size, we resort to advanced statistical methods rather than traditional covariance estimation strategies (Johnstone, 2001; Johnstone and Paul, 2018). The shrinkage and thresholding methods can provide a reliable and robust covariance estimator under the sparsity assumption (Ledoit and Wolf, 2004; Bickel and Levina, 2008b; Rothman et al., 2009; Cai and Liu, 2011). In addition, prior knowledge of a covariance structure can greatly improve the accuracy of estimation and statistical inference (Fan, 2005; Bien, 2019). For example, recent methods can accommodate Toeplitz, banded, block-diagonal, or separable covariance structures (Cai et al., 2013; Bickel and Levina, 2008a; Devijver and Gallopin, 2018; Kong et al., 2020; Zhang et al., 2022).

In the present research, we consider a well-organized block structure named *interconnected community structure* that holds considerable importance in biomedical applications due to its widespread prevalence across diverse fields and its challenges in accurate estimation. The interconnected community structure is commonly found in a wide range of high-dimensional datasets with various data types, including genetics, proteomics, brain imaging, and RNA expression data, among others (Spellman et al., 1998; Yildiz et al., 2007; Chiappelli et al., 2019; Chen et al., 2016; He et al., 2019, 2015; Wu et al., 2021, please see the examples in Figure 1). Although latent, this structure can be accurately extracted using recently developed network pattern detection methods, as proposed by Magwene (2021) and Wu et al. (2021). However, the potential of utilizing this structure to enhance large covariance matrix estimation remains unexplored, making it a primary motivation for our current research.

An interconnected community structure exhibits several properties of highly organized networks. For example, it demonstrates high modality as some variables are clustered in

the multiple and coherently correlated communities; it exhibits small-worldness as these communities are interconnected; and the network is scale-free as the remaining variables are isolated if singletons (see the right parts of B, D, E, F, and G in Figure 1) are detected (Newman, 2006). Therefore, we can specify this interconnected community structure by assigning the high-dimensional variables to multiple interconnected communities, which are more informative, and a set of singletons. The interconnected community structures might not be directly available from the high-dimensional biomedical data, but they can be estimated by several clustering algorithms and network detection methods (Magwene, 2021; Wu et al., 2021). Although there are potential benefits to leveraging the estimated interconnected community structure to enhance the estimation of large covariance matrices, existing statistical methods are restricted to establishing a connection between this structure and the covariance or precision parameters and providing precise estimates. To address this methodological gap, we propose a novel statistical procedure that enables closed-form estimators of large covariance and precision matrices and supports robust statistical inference.

We propose a parametric covariance model that subdivides the covariance matrix into blocks or submatrices and assigns each block to either a community or the interconnection between two communities based on the observed interconnected community structure. By linking the covariance parameters and the underlying network topological structure, we can facilitate a closed-form estimator for each covariance parameter (focusing solely on the elements within the corresponding block) and establish the asymptotic properties for the proposed estimators. Specifically, we derive explicit estimators employing advanced matrix theories, i.e., the block Hadamard product representation of a covariance matrix with the above structure, and the covariance matrix regularization in the high-dimensional setting, where the number of diagonal blocks exceeds the sample size.

Our method makes at least three novel contributions. Firstly, we have developed a fast, closed-form, and accurate procedure for estimating a large covariance (and precision) matrix with a particular structure that is applicable to various high-throughput biomedical data, including genomics, metabolomics, proteomics, neuroimaging, and others. Our method quantitatively characterizes the interconnected community structure by estimating parameters in both diagonal submatrices (i.e., correlations among features within communities) and off-diagonal submatrices (i.e., interactions among features between communities). Thus, it offers better insights into the interactive mechanisms of a complex biosystem. By

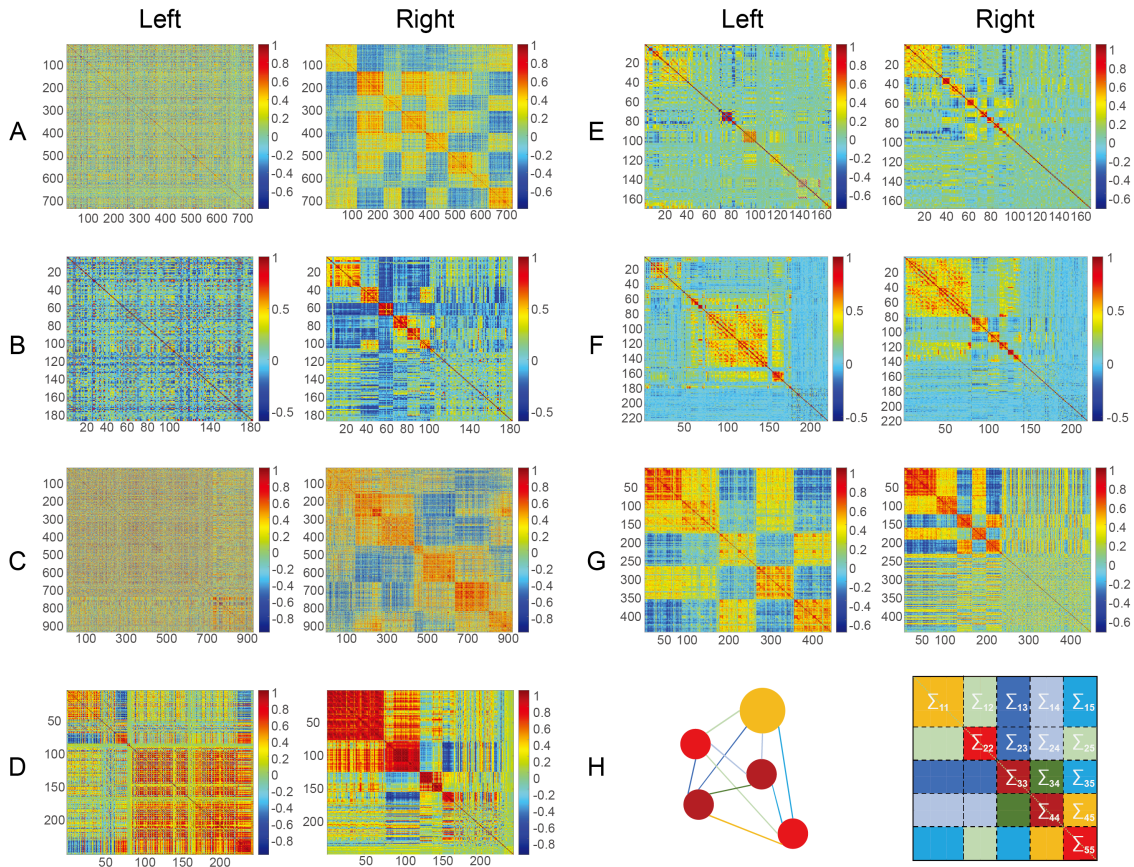


Figure 1: We demonstrate that the interconnected community structure is widespread across various types of high-throughput biomedical data, including genomics (A; Spellman et al., 1998), proteomics (B; Yildiz et al., 2007), multi-omics (C; Perrot-Dockès et al., 2022), nuclear magnetic resonance plasma metabolomics (D; Ritchie et al., 2023), exposome (E; ISGlobal, 2021), liquid chromatography-tandem mass spectrometry serum metabolomics (F; ISGlobal, 2021), brain imaging (G; Chiappelli et al., 2019), where the left plots are the heatmaps of correlation matrices of raw variables, and the right plots are the heatmaps of correlation matrices of reordered variables (as the results of applying the community detection or clustering algorithms). The left plot in H illustrates a network model with 5 interconnected communities, and the right plot in H displays the corresponding population matrix.

utilizing this interconnected community structure, our large covariance matrix estimation procedure outperforms comparable methods in terms of accuracy and is numerically robust to model misspecification. Consequently, our approach can lead to a more precise selection of biological features (e.g., cancer-related gene expressions) in the context of multiple testing, which relies on accurate and reliable large covariance- and precision-matrix estimation (Fan et al., 2012; Fan and Han, 2017). Secondly, we have derived the exact

variance estimators and established the asymptotic properties for the covariance parameter estimators, which enables us to evaluate covariance patterns and provide confidence intervals. Lastly, we have extended our method to accommodate scenarios where the number of diagonal blocks exceeds the sample size, allowing for scalability to accommodate ultra-high-dimensional datasets.

The rest of the paper is organized as follows. Section 2 introduces our proposed method. We first mathematically define the interconnected community structure (with uniform blocks) and the uniform-block matrix in Section 2.1. In Section 2.2, we derive the uniformly minimum variance unbiased covariance- and precision-matrix estimators for the “small number of communities” case by taking advantage of the block Hadamard product representation. We generalize the estimating procedure to the “large number of communities” case with a diverging number of diagonal blocks in Section 2.3. Section 3 contains thorough numerical evaluations of our method under various scenarios. Section 4 illustrates the use of our method in two real-world applications. We provide a discussion in Section 5. The properties of uniform-block matrices, the exact covariance estimators for the proposed estimators, additional simulation studies, and all the technical proofs are provided in the [Supplementary Material](#).

2 Methodology

2.1 A Parametric Covariance Model with the Uniform-Block Structure

Suppose $\mathbf{X} \in \mathbb{R}^{n \times p}$ is an n by p observed data matrix containing n independent and identically distributed p -variate normal vectors $\mathbf{X}_1, \dots, \mathbf{X}_n \sim N(\boldsymbol{\mu}, \boldsymbol{\Sigma})$ with mean $\boldsymbol{\mu} := E(\mathbf{X}_1) \in \mathbb{R}^p$, positive definite covariance matrix $\boldsymbol{\Sigma} := \text{cov}(\mathbf{X}_1) \in \mathbb{R}^{p \times p}$, and precision matrix $\boldsymbol{\Omega} := \boldsymbol{\Sigma}^{-1}$. Without loss of generality, let $\boldsymbol{\mu} = \mathbf{0}_{p \times 1}$ be known, where $\mathbf{0}_{r \times s}$ denotes an r by s zero matrix. Furthermore, let $\mathbf{S} := n^{-1} \mathbf{X}^\top \mathbf{X} \in \mathbb{R}^{p \times p}$ denote the unbiased sample covariance matrix, where \mathbf{M}^\top denotes the transpose of a matrix (or a vector) \mathbf{M} . Moreover, we require that the covariance matrix has the *interconnected community structure with uniform blocks* (abbreviated as the *uniform-block structure*, distinguishing it from cases with singletons), as described below. The parameterization of this covariance structure is illustrated in two steps.

We specify the parametric covariance matrix based on our previous discussions of the uniform-block structure. First, we use a vector to characterize the community sizes. Specif-

ically, given the dimension p of the covariance matrix Σ and the number of communities K , let p_1, \dots, p_K be positive integers satisfying $p_k > 1$ ($k = 1, \dots, K$) and $p = p_1 + \dots + p_K$ and let $\mathbf{p} := (p_1, \dots, p_K)^\top$ be the *partition-size vector*, which is assumed to remain fixed throughout this paper. Given \mathbf{p} , we can express Σ *partitioned by \mathbf{p} in block form*:

$$(\Sigma_{kk'}) := \begin{pmatrix} \Sigma_{11} & \Sigma_{12} & \dots & \Sigma_{1K} \\ \Sigma_{21} & \Sigma_{22} & \dots & \Sigma_{2K} \\ \vdots & \vdots & \ddots & \vdots \\ \Sigma_{K1} & \Sigma_{K2} & \dots & \Sigma_{KK} \end{pmatrix}, \quad (1)$$

where $\Sigma_{kk'} \in \mathbb{R}^{p_k \times p_{k'}}$ ($k, k' = 1, \dots, K$). Second, following (1), we specify the diagonal submatrix $\Sigma_{kk} := a_{kk}\mathbf{I}_{p_k} + b_{kk}\mathbf{J}_{p_k}$ for every k and the off-diagonal submatrix $\Sigma_{kk'} := b_{kk'}\mathbf{1}_{p_k \times p_{k'}}$ with $b_{kk'} = b_{k'k}$ for every $k \neq k'$, where \mathbf{I}_s , \mathbf{J}_s , and $\mathbf{1}_{r \times s}$ are an s by s identity matrix, an s by s all-one matrix, and an r by s all-one matrix, respectively. Using $K < p_1 + \dots + p_K = p$, we can represent a large covariance matrix Σ by a smaller diagonal matrix $\mathbf{A} := \text{diag}(a_{11}, \dots, a_{KK})$, a smaller symmetric matrix $\mathbf{B} := (b_{kk'})$ with $b_{kk'} = b_{k'k}$ for every $k \neq k'$, and a known vector \mathbf{p} :

$$\Sigma(\mathbf{A}, \mathbf{B}, \mathbf{p}) := (\Sigma_{kk'}) = \begin{pmatrix} a_{11}\mathbf{I}_{p_1} + b_{11}\mathbf{J}_{p_1} & b_{12}\mathbf{1}_{p_1 \times p_2} & \dots & b_{1K}\mathbf{1}_{p_1 \times p_K} \\ b_{21}\mathbf{1}_{p_2 \times p_1} & a_{22}\mathbf{I}_{p_2} + b_{22}\mathbf{J}_{p_2} & \dots & b_{2K}\mathbf{1}_{p_2 \times p_K} \\ \vdots & \vdots & \ddots & \vdots \\ b_{K1}\mathbf{1}_{p_K \times p_1} & b_{K2}\mathbf{1}_{p_K \times p_2} & \dots & a_{KK}\mathbf{I}_{p_K} + b_{KK}\mathbf{J}_{p_K} \end{pmatrix}. \quad (2)$$

In this paper, we say that the pattern in (2) is the *uniform-block structure*. If a matrix has the structure in (2), it is called a *uniform-block matrix*. This covariance parameterization strategy for Σ_{kk} and $\Sigma_{kk'}$ has been widely employed in the field of statistics. For example, the generalized estimation equations where the working correlation structure has a compound symmetry as well as linear mixed-effects models with a random intercept both have this pattern. In practice, this parameterization strategy can characterize the covariance knowledge well using a parsimonious model (as shown in Figure 1). In Section 3, we demonstrate that the performance of this parameterization remains robust under misspecification and matrix perturbation. By building the parsimonious and effective covariance-matrix specification, we can develop reliable and accurate covariance-matrix estimations using a likelihood-based approach and achieve optimistic theoretical properties.

Notice that the partition-size vector \mathbf{p} is assumed to be known throughout this article. In practice, it can be learned using a preliminary algorithm (e.g., a K -medoids clustering

algorithm by Magwene (2021) or a network detection algorithm by Wu et al. (2021)) before estimating the covariance matrix. Alternatively, given the heatmap, community sizes can be consistently estimated using a least-square approach (Brault et al., 2017). Also, the above definition of a uniform-block matrix does not guarantee its positive definiteness in general. Thus, additional constraints should be imposed on the uniform-block matrix $\Sigma(\mathbf{A}, \mathbf{B}, \mathbf{p})$ in (2) to ensure that it is a valid covariance matrix. We defer the discussion of these constraints to the next section.

2.2 Matrix Estimation for the Uniform-Block Structure with a Small K

Given a partition-size vector \mathbf{p} and the parametric covariance matrix $\Sigma(\mathbf{A}, \mathbf{B}, \mathbf{p})$ with the uniform-block structure (2), we define a q -dimensional parameter vector

$$\boldsymbol{\theta} := (a_{11}, \dots, a_{KK}, b_{11}, \dots, b_{1K}, b_{22}, \dots, b_{KK})^\top$$

that includes all the covariance parameters in the blocks. That is, the parameters of interest are in the upper triangular part of $\Sigma(\mathbf{A}, \mathbf{B}, \mathbf{p})$. Also, $q = K + K(K + 1)/2$. Thus, the problem of estimating a p by p symmetric covariance matrix reduces to the estimation of the q -dimensional parameter vector $\boldsymbol{\theta}$. In practice, q is considerably smaller than $p(p+1)/2$, thereby remarkably reducing the dimensionality of the parameters of interest.

The small K setting can be specified as follows: $q < n$ while K , p , and q are fixed and p can be greater than n . In other words, both the number of diagonal blocks K and the number of parameters in the blocks $q = K + K(K + 1)/2$ are smaller than the sample size n . Moreover, we require that K and the dimension of the covariance matrix p , which is proportional to K , are fixed, so that q is also fixed. Also, p can be large enough to exceed n with a small K . In this section, we first introduce an explicit maximum likelihood estimator of $\boldsymbol{\theta}$ with asymptotic properties and then show it to be the uniformly minimum variance unbiased estimator (UMVUE), for which we also provide the exact variance estimator in closed form. Finally, we present the uniformly minimum variance unbiased covariance- and precision-matrix estimators for the case of a small K .

We begin with the maximum likelihood estimation. Specifically, let $(\mathbf{S}_{kk'})$ be the block form of \mathbf{S} partitioned by \mathbf{p} . Since the data \mathbf{X} are normally distributed, the log-likelihood function of the data can be expressed by

$$\ell_n(\boldsymbol{\theta}; \mathbf{X}) \propto \frac{n}{2} \log (\det [\{\Sigma(\mathbf{A}, \mathbf{B}, \mathbf{p})\}^{-1}]) - \frac{n}{2} \text{tr} [(\mathbf{S}_{kk'}) \{\Sigma(\mathbf{A}, \mathbf{B}, \mathbf{p})\}^{-1}].$$

A typical approach in the literature to estimate $\boldsymbol{\theta}$ is to derive the score function by taking the first-order partial derivative of the log-likelihood function with respect to $\boldsymbol{\theta}_j$:

$$\frac{\partial}{\partial \boldsymbol{\theta}_j} \ell_n(\boldsymbol{\theta}; \mathbf{X}) = \frac{n}{2} \operatorname{tr} \left[\left\{ \boldsymbol{\Sigma}(\mathbf{A}, \mathbf{B}, \mathbf{p}) - (\mathbf{S}_{kk'}) \right\} \frac{\partial \left\{ \boldsymbol{\Sigma}(\mathbf{A}, \mathbf{B}, \mathbf{p}) \right\}^{-1}}{\partial \boldsymbol{\theta}_j} \right] \quad (j = 1, \dots, q), \quad (3)$$

where $\boldsymbol{\theta}_j \in \{a_{11}, \dots, a_{KK}, b_{11}, \dots, b_{1K}, b_{22}, \dots, b_{KK}\}$ denotes the j th element of $\boldsymbol{\theta}$ and $\partial \left\{ \boldsymbol{\Sigma}(\mathbf{A}, \mathbf{B}, \mathbf{p}) \right\}^{-1} / \partial \boldsymbol{\theta}_j \in \mathbb{R}^{p \times p}$ is a matrix whose entries are functions of these $\boldsymbol{\theta}_j$.

However, solving the score equation derived from (3) is challenging. Although the unknown entries a_{kk} and $b_{kk'}$ are uniformly and elegantly arranged in $\boldsymbol{\Sigma}(\mathbf{A}, \mathbf{B}, \mathbf{p})$, they become entangled in a complex way in the precision matrix $\boldsymbol{\Omega} = \left\{ \boldsymbol{\Sigma}(\mathbf{A}, \mathbf{B}, \mathbf{p}) \right\}^{-1}$. In other words, $\boldsymbol{\theta}_j$ is implicit in $\boldsymbol{\Omega}$, making the closed form of $\boldsymbol{\Omega}$ generally inaccessible. The complexity of the calculation increases as the dimension of the precision matrix grows. Alternatively, existing numerical algorithms for solving $\boldsymbol{\theta}$ (e.g., the method of averaging proposed by Szatrowski (1980)) rely on iterative updating schemes, which demand a long computational time and may lead to unstable estimates. These facts motivate us to reconsider the possibility of deriving a closed-form estimator of $\boldsymbol{\theta}$. Therefore, we aim to find an explicit expression for $\boldsymbol{\Omega}$ in terms of a_{kk} and $b_{kk'}$ by taking advantage of the special covariance structure in (2). More precisely, we speculate that $\boldsymbol{\Omega}$ has an analogous form to (2), which can indeed be fulfilled by realizing the following representation of the block Hadamard product.

Lemma. *Given a partition-size vector $\mathbf{p} = (p_1, \dots, p_K)^\top$ satisfying $p_k > 1$ for every k and $p = p_1 + \dots + p_K$, suppose a p by p matrix \mathbf{N} partitioned by \mathbf{p} has the uniform-block structure in (2), expressed by $\mathbf{N}(\mathbf{A}, \mathbf{B}, \mathbf{p})$, then the following representation is unique,*

$$\mathbf{N}(\mathbf{A}, \mathbf{B}, \mathbf{p}) = \mathbf{A} \circ \mathbf{I}(\mathbf{p}) + \mathbf{B} \circ \mathbf{J}(\mathbf{p}),$$

where $\mathbf{I}(\mathbf{p}) := \mathbf{I}_p(\mathbf{I}_K, \mathbf{0}_{K \times K}, \mathbf{p}) = \text{Bdiag}(\mathbf{I}_{p_1}, \dots, \mathbf{I}_{p_K})$, $\mathbf{J}(\mathbf{p}) := \mathbf{J}_p(\mathbf{0}_{K \times K}, \mathbf{J}_K, \mathbf{p}) = (\mathbf{1}_{p_k \times p_{k'}})$, $\text{Bdiag}(\cdot)$ denotes a block-diagonal matrix, and \circ denotes the block Hadamard product satisfying that $\mathbf{A} \circ \mathbf{I}(\mathbf{p}) := \text{Bdiag}(a_{11} \mathbf{I}_{p_1}, \dots, a_{KK} \mathbf{I}_{p_K})$ and $\mathbf{B} \circ \mathbf{J}(\mathbf{p}) := (b_{kk'} \mathbf{1}_{p_k \times p_{k'}})$.

Based on the lemma, we derive several basic properties of a uniform-block matrix, which are summarized in the [Supplementary Material](#). These properties reveal how \mathbf{A} , \mathbf{B} , and \mathbf{p} determine the algebraic operations for a uniform-block matrix $\mathbf{N}(\mathbf{A}, \mathbf{B}, \mathbf{p})$ and how a collection of uniform-block matrices with the same \mathbf{p} forms a quadratic subspace (Seely, 1971). If we view \mathbf{A} , \mathbf{B} , and \mathbf{p} as the coordinates of a uniform-block matrix, then using the notation $\mathbf{N}(\mathbf{A}, \mathbf{B}, \mathbf{p})$ can simplify the mathematical operations between p by p

uniform-block matrices into those between their corresponding lower-dimensional K by K coordinates. Following these properties of uniform-block matrices, we obtain a useful result for the precision matrix.

Corollary. *Suppose $\Sigma(\mathbf{A}, \mathbf{B}, \mathbf{p}) = \mathbf{A} \circ \mathbf{I}(\mathbf{p}) + \mathbf{B} \circ \mathbf{J}(\mathbf{p})$ is positive definite and $\Omega = \{\Sigma(\mathbf{A}, \mathbf{B}, \mathbf{p})\}^{-1}$ is the precision matrix, then, Ω partitioned by \mathbf{p} is a uniform-block matrix with expression $\Omega(\mathbf{A}_\Omega, \mathbf{B}_\Omega, \mathbf{p}) = \mathbf{A}_\Omega \circ \mathbf{I}(\mathbf{p}) + \mathbf{B}_\Omega \circ \mathbf{J}(\mathbf{p})$, where $\mathbf{A}_\Omega = \mathbf{A}^{-1}$, $\mathbf{B}_\Omega = -\Delta^{-1}\mathbf{B}\mathbf{A}^{-1}$, $\Delta := \mathbf{A} + \mathbf{B}\mathbf{P}$, and $\mathbf{P} := \text{diag}(p_1, \dots, p_K)$.*

The above corollary finalizes that $\Sigma(\mathbf{A}, \mathbf{B}, \mathbf{p})$ is positive definite if and only if \mathbf{A} is positive definite (i.e., $a_{kk} > 0$ for all k) and Δ has only positive eigenvalues. It also confirms that the precision matrix $\Omega = \{\Sigma(\mathbf{A}, \mathbf{B}, \mathbf{p})\}^{-1}$, partitioned by \mathbf{p} , is a uniform-block matrix, expressed by $\Omega(\mathbf{A}_\Omega, \mathbf{B}_\Omega, \mathbf{p})$. Furthermore, it provides the relations between \mathbf{A}_Ω , \mathbf{B}_Ω , and \mathbf{A}, \mathbf{B} .

Therefore, applying the representation of the precision matrix in the corollary, we can rewrite the partial derivative of the log-likelihood in (3) as

$$\frac{\partial}{\partial \theta_j} \ell_n(\boldsymbol{\theta}; \mathbf{X}) = \frac{n}{2} \text{tr} \left[\left\{ \Sigma(\mathbf{A}, \mathbf{B}, \mathbf{p}) - (\mathbf{S}_{kk'}) \right\} \left\{ \frac{\partial \mathbf{A}_\Omega}{\partial \theta_j} \circ \mathbf{I}(\mathbf{p}) + \frac{\partial \mathbf{B}_\Omega}{\partial \theta_j} \circ \mathbf{J}(\mathbf{p}) \right\} \right], \quad (4)$$

for $j = 1, \dots, q$, where $\boldsymbol{\theta}_j \in \{a_{11}, \dots, a_{KK}, b_{11}, \dots, b_{1K}, b_{22}, \dots, b_{KK}\}$. In contrast to (3), the derivatives in (4) can be calculated using explicit expressions of \mathbf{A}, \mathbf{B} , and \mathbf{p} (details are provided in the [Supplementary Material](#)). The explicit forms of the derivatives highlight the advantage of (4) over (3). With (4), we can explicitly derive the analytic form of the maximum likelihood estimator for $\boldsymbol{\theta}$:

$$\tilde{a}_{kk} := \frac{\text{tr}(\mathbf{S}_{kk})}{p_k} - \tilde{b}_{kk}, \quad \tilde{b}_{kk'} := \begin{cases} \frac{\text{sum}(\mathbf{S}_{kk'})}{p_k p_{k'}}, & k \neq k' \\ \frac{\text{sum}(\mathbf{S}_{kk'}) - \text{tr}(\mathbf{S}_{kk'})}{p_k(p_{k'} - 1)}, & k = k' \end{cases}, \quad (5)$$

for $k, k' = 1, \dots, K$, where $\text{sum}(\mathbf{M}) = \sum_{j=1}^r \sum_{j'=1}^s m_{jj'}$ denotes the sum of all entries in $\mathbf{M} := (m_{jj'}) \in \mathbb{R}^{r \times s}$. Technical details are referred to the [Supplementary Material](#). From (5), the maximum likelihood estimators are identical to the moment estimators: the estimator $\tilde{b}_{kk'}$ is the average of all elements of $\mathbf{S}_{kk'}$ for $k \neq k'$; the estimator \tilde{b}_{kk} is the average of all off-diagonal elements of \mathbf{S}_{kk} , and the estimator $\tilde{a}_{kk} + \tilde{b}_{kk}$ is the average of all diagonal elements of \mathbf{S}_{kk} for $k' = k$.

We denote the maximum likelihood estimator of $\boldsymbol{\theta}$ as

$$\tilde{\boldsymbol{\theta}} := (\tilde{a}_{11}, \dots, \tilde{a}_{KK}, \tilde{b}_{11}, \dots, \tilde{b}_{1K}, \tilde{b}_{22}, \dots, \tilde{b}_{KK})^\top.$$

The strong consistency, asymptotic efficiency, and asymptotic normality for $\tilde{\boldsymbol{\theta}}$ can similarly be derived using standard procedures in the literature (Ferguson, 1996; Van Der Vaart and Wellner, 1996; Van Der Vaart, 2000). Please refer to the [Supplementary Material](#) for more details. Moreover, the following theorem summarizes the optimal properties of the plug-in covariance- and precision-matrix estimators.

Theorem 1 (Optimal properties of the proposed estimators). (1) $\tilde{\boldsymbol{\theta}}$ is the UMVUE of $\boldsymbol{\theta}$.
(2) The plug-in covariance-matrix estimator

$$\tilde{\boldsymbol{\Sigma}}(\tilde{\mathbf{A}}, \tilde{\mathbf{B}}, \mathbf{p}) = \tilde{\mathbf{A}} \circ \mathbf{I}(\mathbf{p}) + \tilde{\mathbf{B}} \circ \mathbf{J}(\mathbf{p}) \quad (6)$$

is the UMVUE of $\boldsymbol{\Sigma}(\mathbf{A}, \mathbf{B}, \mathbf{p})$, where $\tilde{\mathbf{A}} := \text{diag}(\tilde{a}_{11}, \dots, \tilde{a}_{KK})$ and $\tilde{\mathbf{B}} := (\tilde{b}_{kk'})$ with $\tilde{b}_{kk'} = \tilde{b}_{k'k}$ for every $k \neq k'$ are the UMVUEs of \mathbf{A} and \mathbf{B} , respectively.

(3) If $\tilde{\mathbf{A}}$ is positive definite and $\tilde{\boldsymbol{\Delta}} := \tilde{\mathbf{A}} + \tilde{\mathbf{B}}\mathbf{P}$ has only positive eigenvalues, then the plug-in precision-matrix estimator

$$\tilde{\boldsymbol{\Omega}}(\tilde{\mathbf{A}}_{\Omega}, \tilde{\mathbf{B}}_{\Omega}, \mathbf{p}) = \tilde{\mathbf{A}}_{\Omega} \circ \mathbf{I}(\mathbf{p}) + \tilde{\mathbf{B}}_{\Omega} \circ \mathbf{J}(\mathbf{p}) \quad (7)$$

is the UMVUE of $\boldsymbol{\Omega}(\mathbf{A}_{\Omega}, \mathbf{B}_{\Omega}, \mathbf{p})$ with $\tilde{\mathbf{A}}_{\Omega} = \tilde{\mathbf{A}}^{-1}$ and $\tilde{\mathbf{B}}_{\Omega} = -\tilde{\boldsymbol{\Delta}}^{-1}\tilde{\mathbf{B}}\tilde{\mathbf{A}}^{-1}$.

Geisser (1963) and Morrison (1972) derived the same estimator $\tilde{\boldsymbol{\theta}}$ based on an analysis of the variance table, but they did not show the above optimal properties.

The covariance matrix of the proposed estimator $\tilde{\boldsymbol{\theta}}$ can be calculated from the Fisher information matrix based on the asymptotic normality. Given a small K (say, $K \leq 3$, empirically), the Fisher information matrix and its inverse may have explicit expressions. However, for some real applications with relatively large K 's (say, $K > 3$), calculating the inverse of the Fisher information matrix might be burdensome and unstable. Alternatively, we provide the exact variance and covariance estimators of the elements of $\tilde{\boldsymbol{\theta}}$ in the [Supplementary Material](#) for finite sample sizes.

2.3 Matrix Estimation for the Uniform-Block Structure with a Large K

In Section 2.2, we estimated the covariance matrix with the uniform-block structure and its precision matrix for a small K . However, there are applications where the covariance matrices are uniform-block matrices with more diagonal blocks than the sample size. More specifically, a large K occurs when $K, q > n$ and K, p , and q grow with n . In other words, the number of diagonal blocks K is greater than the sample size n , and so is the number of

covariance parameters in the blocks: $q = K + K(K + 1)/2$. Moreover, we require that K , the dimension p of the covariance matrix (which is proportional to K), and q grow with n and diverge as n goes to infinity. In this section, we generalize the proposed estimation procedure for a small K and introduce a consistent covariance-matrix estimator by modifying the hard-thresholding method for a large K . Denote $\|\mathbf{M}\|_F = (\sum_{j=1}^r \sum_{j'=1}^r m_{jj'}^2)^{1/2}$ and $\|\mathbf{M}\|_S = \max_{\|\mathbf{x}\|_2=1} \|\mathbf{M}\mathbf{x}\|_2$ as the Frobenius norm and spectral norm of $\mathbf{M} := (m_{jj'}) \in \mathbb{R}^{r \times r}$ respectively, where $\|\mathbf{x}\|_2 := (\sum_{j=1}^r x_j^2)^{1/2}$ for $\mathbf{x} := (x_1, \dots, x_r)^\top \in \mathbb{R}^r$.

For normal data $\mathbf{X} \in \mathbb{R}^{n \times p}$ with the population mean $\boldsymbol{\mu} = \mathbf{0}_{p \times 1}$, the unbiased sample covariance matrix $\mathbf{S} = n^{-1} \mathbf{X}^\top \mathbf{X}$, and the population covariance matrix with the uniform-block structure $\boldsymbol{\Sigma}(\mathbf{A}, \mathbf{B}, \mathbf{p})$ for a large K , we propose a new thresholding approach based on the work by [Bickel and Levina \(2008b\)](#). Since covariance matrix $\boldsymbol{\Sigma}(\mathbf{A}, \mathbf{B}, \mathbf{p})$ is fully determined by \mathbf{A} , \mathbf{B} , and \mathbf{p} according to the lemma, we threshold the estimates of \mathbf{A} and \mathbf{B} , rather than \mathbf{S} , to yield a covariance-matrix estimate. Specifically, given a thresholding level $\lambda = \lambda_n > 0$, let

$$\widehat{a}_{kk}(\lambda) := \widetilde{a}_{kk} \times \mathbb{I}(|\widetilde{a}_{kk}| > \lambda), \quad \widehat{b}_{kk'}(\lambda) := \widetilde{b}_{kk'} \times \mathbb{I}(|\widetilde{b}_{kk'}| > \lambda)$$

be the hard-thresholding estimators of a_{kk} and $b_{kk'}$, respectively, where \widetilde{a}_{kk} and $\widetilde{b}_{kk'}$ are the UMVUEs defined in (5) for every k and k' and $\mathbb{I}(\cdot)$ is the indicator function. We regard the new covariance-matrix estimator

$$\widehat{\boldsymbol{\Sigma}}_\lambda(\widehat{\mathbf{A}}_\lambda, \widehat{\mathbf{B}}_\lambda, \mathbf{p}) = \widehat{\mathbf{A}}_\lambda \circ \mathbf{I}(\mathbf{p}) + \widehat{\mathbf{B}}_\lambda \circ \mathbf{J}(\mathbf{p}) \tag{8}$$

as the *modified hard-thresholding estimator* of $\boldsymbol{\Sigma}(\mathbf{A}, \mathbf{B}, \mathbf{p})$, where $\widehat{\mathbf{A}}_\lambda := \text{diag}\{\widehat{a}_{11}(\lambda), \dots, \widehat{a}_{KK}(\lambda)\}$, $\widehat{\mathbf{B}}_\lambda := \{\widehat{b}_{kk'}(\lambda)\}$ with $\widehat{b}_{kk'}(\lambda) = \widehat{b}_{k'k}(\lambda)$ for every $k \neq k'$. The consistency of this modified hard-thresholding estimator is summarized below.

Theorem 2 (Consistency of the modified hard-thresholding estimator). *Suppose positive definite $\boldsymbol{\Sigma}(\mathbf{A}, \mathbf{B}, \mathbf{p})$ defined in (2). If we choose $\lambda = C\{\log(K)/n\}^{1/2}$ for some positive constant C and some mild regularity conditions are satisfied, then $\widehat{\boldsymbol{\Sigma}}_\lambda(\widehat{\mathbf{A}}_\lambda, \widehat{\mathbf{B}}_\lambda, \mathbf{p})$ defined in (8) is (weakly) consistent in both Frobenius and spectral norms as $K > n$, $\log(K)/n \rightarrow 0$, $K, n \rightarrow \infty$.*

The performance of the modified hard-thresholding estimator (8) relies on the choice of λ , which can be determined by applying the resampling rule outlined in [Bickel and Levina \(2008a,b\)](#).

As demonstrated in B, D, E, F, and G in Figure 1, the high-dimensional features comprise a set of interconnected communities and a set of singletons. Therefore, we represent their covariance matrix $\Sigma_\star := \{\Sigma(\mathbf{A}, \mathbf{B}, \mathbf{p}), \mathbf{D}_1; \mathbf{D}_1^\top, \mathbf{D}_2\}$, where $\mathbf{D}_1 \in \mathbb{R}^{p \times d}$, $\mathbf{D}_2 \in \mathbb{R}^{d \times d}$, and $\Sigma_\star \in \mathbb{R}^{(p+d) \times (p+d)}$, and d denotes the number of singletons. We estimate Σ_\star in two steps. First, we compute and partition the sample covariance matrix $\mathbf{S}_\star := \{(\mathbf{S}_{kk'}), \mathbf{S}_1; \mathbf{S}_1^\top, \mathbf{S}_2\}$ based on the covariance structure. Next, we calculate $\tilde{\Sigma}(\tilde{\mathbf{A}}, \tilde{\mathbf{B}}, \mathbf{p})$ using the consistent estimators in (5) regarding $(\mathbf{S}_{kk'})$ and (6), while performing conventional soft- or hard-thresholding on the singleton-related sample covariance matrix $\{\mathbf{0}_{p \times p}, \mathbf{S}_1; \mathbf{S}_1^\top, \mathbf{S}_2\}$ (Bickel and Levina, 2008b). Jointly, these two steps provide a consistent estimator of Σ_\star .

3 Numerical Studies

3.1 Simulations

To evaluate the performance of the proposed method comprehensively, we simulate data and benchmark them against comparable estimation methods for large covariance (and precision) matrices in the following three scenarios.

In Scenario 1 (Section 3.2), we generate normal data using a covariance matrix with a uniform-block structure $\Sigma_{0,1}(\mathbf{A}_0, \mathbf{B}_0, \mathbf{p}_1)$ for n subjects with a small K . We first focus on evaluating the finite-sample performance of the parameter vector estimator $\tilde{\boldsymbol{\theta}}$ in (5) by comparing the estimates with the ground truth. Additionally, we assess the accuracy of the exact covariance estimator for $\tilde{\boldsymbol{\theta}}$, as presented in the [Supplementary Material](#). Subsequently, we present the performance of the covariance estimator $\tilde{\Sigma}_1(\tilde{\mathbf{A}}_1, \tilde{\mathbf{B}}_1, \mathbf{p}_1)$ in (6) and the precision estimator $\tilde{\Omega}_1(\tilde{\mathbf{A}}_{\Omega,1}, \tilde{\mathbf{B}}_{\Omega,1}, \mathbf{p}_1)$ in (7) by comparing their losses in the matrix norms with those of existing covariance- and precision-matrix estimators.

In Scenario 2 (Section 3.3), we simulate normal data using the covariance matrix $\Sigma_{0,2}(\mathbf{A}_0, \mathbf{B}_0, \mathbf{p}_2)$ with the structure of uniform blocks for a large K . Next, we compare the modified hard-thresholding estimator $\hat{\Sigma}_2(\hat{\mathbf{A}}_2, \hat{\mathbf{B}}_2, \mathbf{p}_2)$ in (8) with several competing methods by computing the losses in the matrix norms.

In Scenario 3 (Section 3.4), we perform a misspecification analysis for $\tilde{\Sigma}_3(\tilde{\mathbf{A}}_3, \tilde{\mathbf{B}}_3, \mathbf{p}_3)$ and $\tilde{\Omega}_3(\tilde{\mathbf{A}}_{\Omega,3}, \tilde{\mathbf{B}}_{\Omega,3}, \mathbf{p}_3)$ when the covariance matrix does not adhere to the uniform-block structure.

3.2 Scenario 1: Comparison for Covariance Matrices with a Small K

We first set the true covariance uniform-block matrix as $\Sigma_{0,1}(\mathbf{A}_0, \mathbf{B}_0, \mathbf{p}_1) = \mathbf{A}_0 \circ \mathbf{I}(\mathbf{p}_1) + \mathbf{B}_0 \circ \mathbf{J}(\mathbf{p}_1)$, where the number of diagonal blocks $K = 5$; the partition-size vector

$$\mathbf{p}_1 := (p_{\text{ind}}, p_{\text{ind}}, p_{\text{ind}}, p_{\text{ind}}, p_{\text{ind}})^\top = p_{\text{ind}} \mathbf{1}_{K \times 1}$$

with individual component $p_{\text{ind}} = 30, 45, \text{ or } 60$; the number of covariance parameters in the blocks $q = K + K(K + 1)/2 = 20$; the dimension of the covariance matrix $p = Kp_{\text{ind}} = 150, 225, \text{ or } 300$; and $\mathbf{A}_0 := \text{diag}(a_{0,11}, \dots, a_{0,KK})$ and $\mathbf{B}_0 := (b_{0,kk'})$ with $b_{0,kk'} = b_{0,k'k}$ for $k \neq k'$:

$$\mathbf{A}_0 = \text{diag}(0.016, 0.214, 0.749, 0.068, 0.100), \quad \mathbf{B}_0 = \begin{pmatrix} 6.731 & -1.690 & 0.696 & -2.936 & 1.913 \\ & 5.215 & 3.815 & -1.010 & 0.703 \\ & & 4.328 & -3.357 & -0.269 \\ & & & 6.788 & 0.000 \\ & & & & 3.954 \end{pmatrix}.$$

The true precision matrix $\Omega_{0,1}(\mathbf{A}_{\Omega,0}, \mathbf{B}_{\Omega,0}, \mathbf{p}_1) = \mathbf{A}_{\Omega,0} \circ \mathbf{I}(\mathbf{p}_1) + \mathbf{B}_{\Omega,0} \circ \mathbf{J}(\mathbf{p}_1)$ is given by $\mathbf{A}_{\Omega,0} := \mathbf{A}_0^{-1}$ and $\mathbf{B}_{\Omega,0} := -(\mathbf{A}_0 + \mathbf{B}_0 \mathbf{P}_{0,1})^{-1} \mathbf{B}_0 \mathbf{A}_0^{-1}$, where $\mathbf{P}_{0,1} := \text{diag}(p_{\text{ind}}, p_{\text{ind}}, p_{\text{ind}}, p_{\text{ind}}, p_{\text{ind}})$. Specifically, we choose $n = 50, 100, \text{ or } 150$, while ensuring that $q = 20 < n$. We generate the data matrix \mathbf{X} by drawing an independent and identically distributed sample from $N(\mathbf{0}_{p \times 1}, \Sigma_{0,1}(\mathbf{A}_0, \mathbf{B}_0, \mathbf{p}_1))$ and repeat this procedure 1000 times.

For each replicate, we calculate \tilde{a}_{kk} and $\tilde{b}_{kk'}$ using (5) to obtain $\tilde{\mathbf{A}}_1 := \text{diag}(\tilde{a}_{11}, \dots, \tilde{a}_{KK})$, $\tilde{\mathbf{B}}_1 := (\tilde{b}_{kk'})$, $\tilde{\mathbf{A}}_{\Omega,1} := \tilde{\mathbf{A}}_1^{-1}$, and $\tilde{\mathbf{B}}_{\Omega,1} := -(\tilde{\mathbf{A}}_1 + \tilde{\mathbf{B}}_1 \mathbf{P}_{0,1})^{-1} \tilde{\mathbf{B}}_1 \tilde{\mathbf{A}}_1^{-1}$ and then calculate their standard errors by substituting the estimates \tilde{a}_{kk} and $\tilde{b}_{kk'}$ for a_{kk} and $b_{kk'}$, respectively, (please see the formulas in the [Supplementary Material](#)). We also calculate the estimates of the covariance matrix and precision matrices using (6) and (7) and denote them by $\tilde{\Sigma}_{\text{prop.}} := \tilde{\Sigma}_1(\tilde{\mathbf{A}}_1, \tilde{\mathbf{B}}_1, \mathbf{p}_1)$ and $\tilde{\Omega}_{\text{prop.}} := \tilde{\Omega}_1(\tilde{\mathbf{A}}_{\Omega,1}, \tilde{\mathbf{B}}_{\Omega,1}, \mathbf{p}_1)$, respectively. In addition, we estimate the covariance matrix using conventional methods, which include the soft-thresholding method (soft; [Antoniadis and Fan, 2001](#)), the hard-thresholding method (hard), the adaptive-thresholding method (adaptive), and the principal orthogonal complement thresholding method (POET), as shown in Figure 2. We also estimate the precision matrix using the graphical lasso method (glasso; [Friedman et al., 2008](#)), the bandwidth test (banded; [An et al., 2014](#)), Bayesian frameworks with G-Wishart prior (BayesG; [Banerjee and Ghosal, 2014](#)) or with the k -banded Cholesky prior (BayesKBC; [Lee and Lee, 2021](#)), as

also illustrated in Figure 2. Finally, we evaluate the performance of all methods using the losses in the Frobenius and spectral norms respectively, that is, $\|\tilde{\Sigma}_* - \Sigma_{0,1}(\mathbf{A}_0, \mathbf{B}_0, \mathbf{p}_1)\|_F$, $\|\tilde{\Sigma}_* - \Sigma_{0,1}(\mathbf{A}_0, \mathbf{B}_0, \mathbf{p}_1)\|_S$, $\|\tilde{\Omega}_* - \Omega_{0,1}(\mathbf{A}_{\Omega,0}, \mathbf{B}_{\Omega,0}, \mathbf{p}_1)\|_F$, and $\|\tilde{\Omega}_* - \Omega_{0,1}(\mathbf{A}_{\Omega,0}, \mathbf{B}_{\Omega,0}, \mathbf{p}_1)\|_S$ for the method $*$.

For the 1000 replicates, we assess the absolute relative (average) bias (%), Monte Carlo standard deviation, average standard error, and empirical coverage probability based on 95% Wald-type confidence intervals for each covariance parameter, as presented in Table 1. The results in Table 1 demonstrate that the proposed estimators \tilde{a}_{kk} and $\tilde{b}_{kk'}$ achieve satisfactory performance: the absolute relative biases in the parameter estimations are generally small in contrast to the Monte Carlo standard deviations; as the sample size n increases, the average standard errors become smaller for all covariance parameters; the average standard errors are approximately equal to the Monte Carlo standard deviations with comparable corresponding 95% empirical coverage probabilities. We demonstrate the performance of covariance- and precision-matrix estimators in terms of the Frobenius and spectral norms, as well as computational times, for both the proposed procedure and competing methods in Figure 2. Our estimating procedure outperforms existing methods, as it is much faster and has smaller matrix norm losses. Compared with conventional precision-matrix estimators, the proposed precision-matrix estimator has much fewer losses. This is probably because the true precision matrix contains many non-sparse blocks (that is, the off-diagonal entries in $\mathbf{B}_{\Omega,0}$ are very small but different from 0). As the dimension p increases, the matrix norm losses between the proposed covariance estimate and $\Sigma_{0,1}(\mathbf{A}_0, \mathbf{B}_0, \mathbf{p}_1)$ increase, while those between the proposed precision estimate and $\Omega_{0,1}(\mathbf{A}_{\Omega,0}, \mathbf{B}_{\Omega,0}, \mathbf{p}_1)$ decrease slightly. One possible explanation is that we fix n and q , then $\tilde{\Sigma}_{\text{prop.}}$ is determined by $\tilde{\mathbf{A}}_1$, $\tilde{\mathbf{B}}_1$, and \mathbf{p}_1 while $\tilde{\Omega}_{\text{prop.}}$ is determined by $\tilde{\mathbf{A}}_1^{-1}$, $\tilde{\mathbf{B}}_1$, $(\tilde{\mathbf{A}}_1 + \tilde{\mathbf{B}}_1 \mathbf{P}_{0,1})^{-1}$, and \mathbf{p}_1 .

3.3 Scenario 2: Comparison for Covariance Matrices with a Large K

The true covariance matrix is $\Sigma_{0,2}(\mathbf{A}_{0,K}, \mathbf{B}_{0,K}, \mathbf{p}_2) = \mathbf{A}_{0,K} \circ \mathbf{I}(p_2) + \mathbf{B}_{0,K} \circ \mathbf{J}(p_2)$, where $K = 30, 40, \text{ or } 50$; $\mathbf{p}_2 := (p_{\text{ind}}, \dots, p_{\text{ind}})^\top = p_{\text{ind}} \mathbf{1}_{K \times 1}$ with the individual component $p_{\text{ind}} = 10$; $q = K + K(K + 1)/2 = 495, 860, \text{ or } 1325$; $p = K p_{\text{ind}} = 300, 400, \text{ or } 500$; and $\mathbf{A}_{0,K}$ and $\mathbf{B}_{0,K}$ are generated depending on the value of K . For each K , we first generate a K by K diagonal matrix $\mathbf{A}_{0,K}$ and a symmetric matrix $\mathbf{B}_{0,K}$ satisfying $\Sigma_{0,2}(\mathbf{A}_{0,K}, \mathbf{B}_{0,K}, \mathbf{p}_2)$ is positive definite, or equivalently, $\mathbf{A}_{0,K}$ is positive definite and $\mathbf{\Delta}_{0,K} := \mathbf{A}_{0,K} + \mathbf{B}_{0,K} \mathbf{P}_{0,K}$

	$p = 150$				$p = 225$				$p = 300$			
	ARB	MCS	ASE	95% CP	ARB	MCS	ASE	95% CP	ARB	MCS	ASE	95% CP
$a_{0,11}$	0.1	0.0	0.0	95.1	0.1	0.0	0.0	94.9	0.1	0.0	0.0	95.2
$a_{0,22}$	0.0	0.6	0.6	95.8	0.0	0.4	0.5	96.2	0.0	0.4	0.4	94.8
$a_{0,33}$	0.0	2.1	2.0	94.2	0.0	1.6	1.6	94.9	0.1	1.4	1.4	95.3
$a_{0,44}$	0.1	0.2	0.2	96.3	0.0	0.1	0.1	95.5	0.0	0.1	0.1	95.4
$a_{0,55}$	0.1	0.3	0.3	95.3	0.1	0.2	0.2	95.1	0.0	0.2	0.2	95.3
$b_{0,11}$	0.1	97.6	95.7	93.5	1.1	97.3	96.7	93.5	0.2	93.7	95.5	94.6
$b_{0,12}$	-0.7	59.6	61.8	95.4	-1.3	61.3	62.4	95.8	-1.4	62.5	61.9	94.7
$b_{0,13}$	1.6	52.2	54.7	96.8	0.6	54.3	55.0	95.6	1.7	55.0	54.8	94.9
$b_{0,14}$	-0.1	72.5	74.1	95.4	-1.1	75.4	74.3	94.3	-0.1	74.5	73.9	94.8
$b_{0,15}$	0.4	55.6	55.2	93.8	1.9	56.0	55.9	96.0	0.4	56.8	55.3	94.8
$b_{0,22}$	0.3	71.5	74.0	95.1	0.5	73.4	74.5	94.0	0.3	76.5	74.4	94.0
$b_{0,23}$	0.6	58.3	61.0	94.1	0.0	60.6	61.3	94.2	0.4	64.3	61.4	93.8
$b_{0,24}$	-1.7	59.9	60.6	95.3	-3.2	61.7	60.6	95.5	-0.1	61.8	60.7	94.5
$b_{0,25}$	2.6	45.4	46.1	95.6	2.7	48.3	46.6	94.8	2.4	46.2	46.3	95.0
$b_{0,33}$	0.6	58.9	61.5	95.3	0.4	60.7	61.5	93.9	0.1	64.0	61.8	94.1
$b_{0,34}$	-0.4	63.3	64.0	94.9	-1.0	62.7	63.7	94.8	-0.2	66.7	64.0	93.5
$b_{0,35}$	-4.6	39.8	41.6	96.2	-5.5	43.9	41.9	94.8	-7.6	41.9	41.7	95.4
$b_{0,44}$	0.1	93.1	96.6	96.3	0.6	93.8	95.9	94.7	0.1	98.8	96.4	93.0
$b_{0,45}$	NA	50.2	52.1	96.0	NA	54.5	52.2	93.3	NA	53.9	52.0	94.7
$b_{0,55}$	0.2	57.1	56.1	94.0	1.0	56.7	56.8	94.9	0.0	56.6	56.2	93.9

Table 1: We assess the estimated covariance parameters ($a_{0,kk}$ and $b_{0,kk'}$) using our proposed method across 1000 simulated datasets under $n = 100$: “ARB” represents the absolute relative bias (in %), calculated as $|\tilde{a}_{11} - a_{0,11}|/a_{0,11} \times 100\%$; “MCS” refers to the Monte Carlo standard deviation ($\times 100$); “ASE” stands for the average calculated standard error ($\times 100$) by Corollary A.2 in the [Supplementary Material](#); “95% CP” represents the empirical coverage probability (in %) based on a 95% Wald-type confidence interval. For the ARB of $b_{0,45}$, denoted as “NA” (not available) due to $b_{0,45} = 0$, the absolute biases ($\times 100$) are 0.0, 1.9, and 1.2 for $p = 150$, 225, and 300, respectively. In all settings, the estimation biases of the covariance parameters are small, generally less than 5%. The standard errors, calculated using both MCS and ASE, are close, indicating that our proposed variance estimators are accurate. This is further supported by the results of the 95% coverage probabilities.

has only positive eigenvalues, where $\mathbf{P}_{0,K} := \text{diag}(p_{\text{ind}}, \dots, p_{\text{ind}}) \in \mathbb{R}^{K \times K}$. Then, we proceed to generate the data matrix \mathbf{X} based on an independently and identically distributed sample of size $n = 30$ from $N(\mathbf{0}_{p \times 1}, \Sigma_{0,2}(\mathbf{A}_{0,K}, \mathbf{B}_{0,K}, \mathbf{p}_2))$, where all $K, p, q \geq n$. For each K , the above generation procedure is repeated 1000 times. To estimate $\Sigma_{0,2}(\mathbf{A}_{0,K}, \mathbf{B}_{0,K}, \mathbf{p}_2)$, we adopt the modified hard-thresholding estimator in (8). The thresholding level λ is chosen by following a similar procedure to that described in [Bickel and Levina \(2008a,b\)](#). We also compare our method with other large covariance matrix estimation techniques used in Scenario 1 (Section 3.2). For 1000 replicates, we visualize the average losses in terms of matrix norms in Figure 2. The results in Figure 2 reveal that the proposed modified

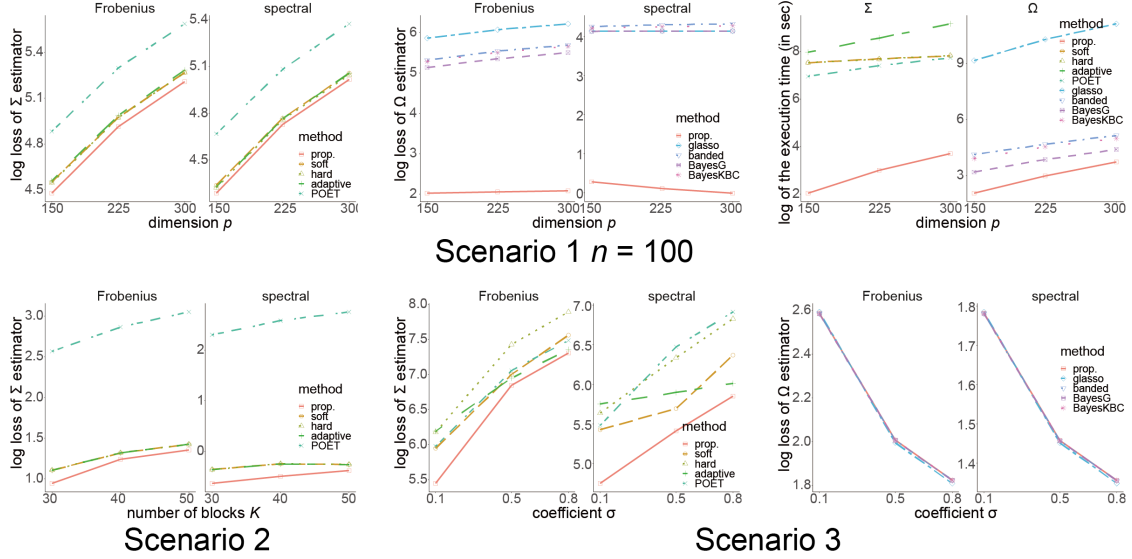


Figure 2: We evaluate the estimated covariance and precision matrices using our approach and compare them with estimates from benchmark methods. In the first row, we present the results for Scenario 1 (the small K setting) under $n = 100$ with various dimensions p (the x -axis). The left two and the middle two subfigures illustrate the logarithmic losses in both Frobenius and spectral norms for covariance matrix Σ and precision matrix Ω estimations for all methods, respectively; and the right two subfigures display the execution time for Σ and Ω estimation. In the second row, the left two subfigures demonstrate the logarithmic losses in both Frobenius and spectral norms for covariance matrix estimation in Scenario 2 (the large K setting). The middle two and the right two subfigures in the second row showcase the results under model misspecification (Scenario 3) by assessing the logarithmic losses in both Frobenius and spectral norms for covariance matrix Σ and precision matrix Ω estimations. In general, our method provides more accurate covariance and precision matrix estimates with reduced computational loads and demonstrates robustness to model specification.

estimator produces the smallest loss by taking advantage of the underlying structure.

3.4 Scenario 3: Simulation Analysis under Model Misspecification

In this scenario, we assess the performance of the proposed covariance- and precision-matrix estimators under model misspecification, where the true covariance matrix does not have a uniform-block structure. Specifically, we set the true positive definite covariance matrix $\Upsilon_{0,\sigma} := \Sigma_{0,3}(\mathbf{A}_0, \mathbf{B}_0, \mathbf{p}_3) + \mathbf{M}_\sigma$, where $K = 5$; $\mathbf{p}_3 := p_{\text{ind}} \mathbf{1}_{K \times 1}$ with $p_{\text{ind}} = 30$; $q = 20$; $p = K p_{\text{ind}} = 150$; and \mathbf{A}_0 and \mathbf{B}_0 are identical to those in Scenario 1 (Section 3.2). Matrix \mathbf{M}_σ follows a Wishart distribution with p degrees of freedom and parameter $\sigma \mathbf{I}_p$, where $\sigma = 0.1, 0.5, \text{ or } 0.8$. It is clear that if $\sigma = 0$, then $\Upsilon_{0,\sigma} = \Sigma_{0,3}(\mathbf{A}_0, \mathbf{B}_0, \mathbf{p}_3)$ is a uniform-block matrix; if $\sigma > 0$, then $\Upsilon_{0,\sigma}$ and the true precision matrix $\Upsilon_{0,\sigma}^{-1}$ are not uniform-block

matrices because uniformity does not hold. For each σ , we generate \mathbf{X} based on a random sample with a size of $n = 50$ (satisfying $q = 20 < n$) drawn from $N(\mathbf{0}_{p \times 1}, \mathbf{\Upsilon}_{0,\sigma})$. We fit the covariance-matrix estimator in (6), the precision-matrix estimator in (7), and the other estimators for large covariance and precision matrices described in Scenario 1 (Section 3.2) to the data. We simulate 1000 replicates for each σ . The average losses $\|\tilde{\Sigma}_* - \mathbf{\Upsilon}_{0,\sigma}\|_F$, $\|\tilde{\Sigma}_* - \mathbf{\Upsilon}_{0,\sigma}\|_S$, $\|\tilde{\Omega}_* - \mathbf{\Upsilon}_{0,\sigma}^{-1}\|_F$, and $\|\tilde{\Omega}_* - \mathbf{\Upsilon}_{0,\sigma}^{-1}\|_S$ are calculated among 1000 replicates for the method $*$. The results are plotted in Figure 2.

The results in Figure 2 show that the proposed covariance-matrix estimator works well under the misspecified covariance structure. Compared with traditional covariance-matrix estimators, our method exhibits smaller losses in terms of matrix norms. The losses in terms of matrix norms for our precision-matrix estimator are comparable to those of the other methods. One possible reason is that the inverse of a non-uniform-block matrix is not a uniform-block matrix, so the proposed precision-matrix estimator cannot benefit from the underlying structure.

In summary, our method can robustly and accurately estimate covariance matrices with the dependence structure of interconnected communities. Since recent multiple testing correction methods, e.g., to control the false discovery proportion (FDP; Fan et al., 2012; Fan and Han, 2017), are based on the covariance-matrix estimate, we also evaluated the influence of covariance estimation on the accuracy of feature selection (please see the details in the additional simulation studies in the [Supplementary Material](#)). Our simulation results showed that our approach can largely improve the sensitivity while preserving the FDP compared to competing methods.

4 Data Examples

4.1 Proteomics Data Analysis

We applied the proposed method to estimate the covariance matrix for high-throughput proteomics data used in cancer research (Yildiz et al., 2007). Specifically, this case-control study involved 288 participants (180 male and 108 female, aged 62.4 ± 9.4 years). Matrix-assisted laser desorption ionization mass spectrometry was employed to identify abundant peptides in human serum samples between case and control groups.

Following preprocessing (Chen et al., 2009) in the preliminary study, we selected 184 features in the serum as candidate proteins and peptides. Out of these, a total of 107

were identified as constituting 7 interconnected communities, while the remaining 77 were considered as singletons according to the network detection algorithm (Chen et al., 2018), as illustrated in the first two subfigures of A in Figure 3.

Our primary objective was to explore the interactive relationships within the 107 features that constituted the interconnected communities through the 107 by 107 correlation matrix, denoted by $\Sigma_0(\mathbf{A}_0, \mathbf{B}_0, \mathbf{p})$, as well as those within all 184 features through the 184 by 184 correlation matrix, denoted as $\Sigma_\star = (\Sigma_0(\mathbf{A}_0, \mathbf{B}_0, \mathbf{p}), \mathbf{D}_1; \mathbf{D}_1^\top, \mathbf{D}_2)$. We estimated both correlation matrices $\Sigma_0(\mathbf{A}_0, \mathbf{B}_0, \mathbf{p})$ and Σ_\star .

Firstly, we employed the proposed estimation procedure to calculate the 107 by 107 covariance matrix $\Sigma_0(\mathbf{A}_0, \mathbf{B}_0, \mathbf{p})$, where $n = 288$, $p = 107$, $K = 7$, $q = 35$, and $\mathbf{p} = (34, 18, 14, 14, 13, 10, 4)^\top$ as provided by the network detection algorithm (Chen et al., 2018). Let $\mathbf{A}_0 = \text{diag}(a_{0,11}, \dots, a_{0,KK})$ and $\mathbf{B}_0 = (b_{0,kk'})$ with $b_{0,kk'} = b_{0,k'k}$ for $k' \neq k$ denote the K by K unknown diagonal matrix and symmetric matrix, respectively. Consequently, all diagonal entries were equal to 1 (i.e., $a_{0,kk} + b_{0,kk} = 1$ for every k). As $q = 35 < n = 288$, we could obtain estimates and standard errors for $a_{0,kk}$ and $b_{0,kk'}$ using (5) and their respective variance estimators. We summarized the results in the third and fourth subfigures of A in Figure 3, noting that the sum of the estimates of $a_{0,kk}$ and $b_{0,kk}$ was 1 for every k because the diagonal entries in the sample correlation matrix were 1. Moreover, the fourth subfigure of A in Figure 3 showed that the 95% confidence intervals of the correlations between the (1, 2), (2, 4), and (6, 7) blocks contained 0. Additionally, the (1, 3), (1, 4), (1, 5), (1, 6), (2, 3), (2, 5), (3, 4), (3, 5), (3, 6), (3, 7), and (5, 7) blocks exhibited negative correlations, while the remaining blocks displayed positive correlations. Lastly, we estimated the correlation matrix Σ_\star for all 184 features by applying the soft-thresholding approach to the singleton-related sample covariance matrix and then merging it with the estimate of $\Sigma_0(\mathbf{A}_0, \mathbf{B}_0, \mathbf{p})$, as illustrated in the last subfigure of A in Figure 3.

4.2 Brain Imaging Data Analysis

The second example is from a brain imaging study based on echo-planar spectroscopic imaging, allowing simultaneous measurements of multiple neurometabolites across whole brain regions (Chiappelli et al., 2019). Data were collected from 78 participants (39 male and 39 female, aged 42.1 ± 18.8 years). This study involved participants' measurements of 5 neurometabolites, which included choline, myo-inositol, creatine-containing compounds,

N-acetylaspartate, and glutamate–glutamine, across 89 brain regions for each participant.

In the preliminary study, we calculated the sample correlation matrix for 445 combinations of neurometabolites and brain regions (i.e., $445 = 5 \times 89$). Employing the approach developed by [Chen et al. \(2018\)](#), we extracted an interconnected community structure consisting of 227 combinations from the initial 445, while the remaining 218 combinations were considered as singletons, as depicted in the first subfigure of B in [Figure 3](#). The interconnected community structure was characterized by 5 diagonal blocks and 10 off-diagonal blocks, as illustrated in the second subfigure of B in [Figure 3](#).

We applied the proposed method to estimate two correlation matrices separately: the 227×227 block-form correlation matrix, denoted as $\Sigma_0(\mathbf{A}_0, \mathbf{B}_0, \mathbf{p})$, and the 445×445 correlation matrix, denoted as $\Sigma_\star = (\Sigma_0(\mathbf{A}_0, \mathbf{B}_0, \mathbf{p}), \mathbf{D}_1; \mathbf{D}_1^\top, \mathbf{D}_2)$.

To estimate $\Sigma_0(\mathbf{A}_0, \mathbf{B}_0, \mathbf{p})$ in this application, we obtained $n = 78$ and $\mathbf{p} = (77, 49, 36, 33, 32)^\top$ from the preliminary network detection algorithm ([Chen et al., 2018](#)). Accordingly, we had $K = 5$, $p = 227$, and $q = 20$. We estimated $a_{0,kk}$ and $b_{0,kk'}$ using (5) and their respective standard errors. The estimated correlations and their corresponding confidence intervals have been presented in the third and fourth subfigures of B in [Figure 3](#). Specifically, combinations within all diagonal blocks and those between the (1, 2), (1, 4), (2, 4), and (3, 5) blocks were positively correlated, with 95% confidence intervals excluding 0, while combinations between the (1, 3), (1, 5), and (2, 5) blocks were negatively correlated, with 95% confidence intervals excluding 0. Conversely, combinations within the (2, 3), (3, 4), and (4, 5) blocks had 95% confidence intervals for their correlations containing 0. Furthermore, the 5 diagonal blocks represented: (1) 74 regions associated with choline (including three regions with other metabolites), (2) 49 regions linked to myo-inositol, (3) 26 regions associated with *N*-acetylaspartate (including 10 regions with glutamate–glutamine), (4) 33 regions related to creatine-containing compounds, and (5) an additional 32 regions associated with *N*-acetylaspartate. The off-diagonal blocks indicated positive relationships among choline, myo-inositol, and creatine-containing compounds, as well as between *N*-acetylaspartate and glutamate–glutamine across the brain. Additionally, a global negative correlation existed between two sets of metabolites across the brain: (1) choline, myo-inositol, and creatine-containing compounds and (2) glutamate–glutamine and *N*-acetylaspartate. The region-level correlations might assist in providing an understanding of the neurophysiological mechanisms relating to metabolites in the central nervous system. We employed a similar approach estimate Σ_\star by combining the estimate of $\Sigma_0(\mathbf{A}_0, \mathbf{B}_0, \mathbf{p})$ with the soft-

thresholding estimate of the singleton-related covariance matrix, as depicted in the last subfigure of B in Figure 3.

For comparison, we also directly applied existing methods for large covariance matrix estimation (e.g., the thresholding approach) to both proteomics and brain imaging datasets. As outlined in an additional figure in the [Supplementary Material](#), these estimated covariance matrices, obtained using existing methods, appeared to miss a large proportion of correlations both within and between communities.

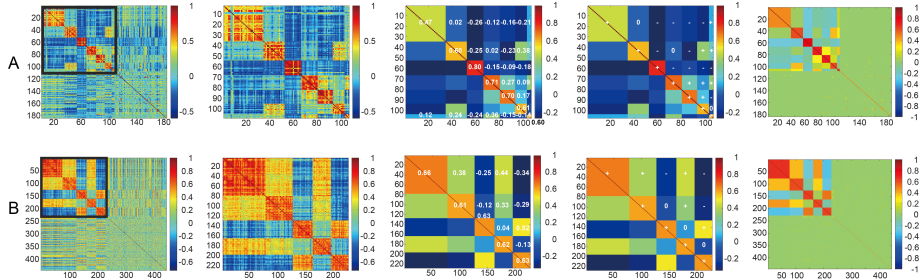


Figure 3: We present the results for proteomics data analysis in the first row (A) and for brain imaging data analysis in the second row (B). A: the first subfigure displays the heatmap of the sample correlation matrix for the proteomics dataset and the second one displays that of 107 features within interconnected communities; the third subfigure exhibits $\tilde{b}_{0,kk'}$ (with their standard errors ranging between 0.03 and 0.07, while for each k , $\tilde{a}_{0,kk} = 1 - \tilde{b}_{0,kk}$ with the standard error around 0.01); the fourth subfigure provides confidence intervals for $b_{0,kk'}$; and the last subfigure exhibits the heatmap of the estimated correlation matrix for all 184 features. B: the first subfigure exhibits the heatmap of the sample correlation matrix for the brain imaging dataset and the second one displays that of 227 combinations within interconnected communities; the third subfigure displays $\tilde{b}_{0,kk'}$ (with their standard errors ranging between 0.07 and 0.11, while for each k , $\tilde{a}_{0,kk} = 1 - \tilde{b}_{0,kk}$ with the standard error around 0.01); the fourth subfigure contains confidence intervals for $b_{0,kk'}$, where “+” indicates the 95% confidence interval to the right of 0, “-” indicates the 95% confidence interval to the left of 0, “0” indicates the 95% confidence interval containing 0; and the last subfigure exhibits the heatmap of the estimated correlation matrix for all 445 combinations.

5 Discussion

We have developed a computationally efficient method for estimating large covariance and precision matrices with interconnected community structures. In our empirical analyses of multiple types of high-throughput biomedical data, we have observed that most of these datasets, including gene expression, proteomics, neuroimaging, exposome, and many others, exhibit a latent yet well-organized block pattern, as demonstrated in the examples in Figure 1. By leveraging the interconnected community structure, we provided an accurate

estimate of the parameter vector for the large covariance matrix with a drastically reduced number of parameters. We further derived the covariance- and precision-matrix estimators in closed forms, significantly reducing the computational burden and improving the accuracy of statistical inference. On the other hand, the proposed estimation procedure relies on the output of the chosen community detection or clustering algorithm. Therefore, we aim to integrate community detection and covariance estimation into a unified framework to achieve more robust and reliable results in future studies.

In a uniform-block structure, we assigned one parameter for the diagonal entries and one parameter for the off-diagonal entries in a diagonal block, and one parameter for all entries in an off-diagonal block. This parameterization strategy is driven by the fact that the intra-block and the inter-block variances in the real applications are relatively small in large sample correlation matrices (for additional results, refer to the [Supplementary Material](#)). Given the strong block patterns in the correlation matrices, as illustrated in the examples in [Figure 1](#), this parameterization strategy appears valid. This strategy is also analogous to the commonly used compound symmetry covariance structure in linear mixed-effect models and generalized estimating equation models. Although our method is developed for the interconnected community structure, it is also applicable to other covariance structures (e.g., the hierarchical community structure; see [Section C.4](#) in the [Supplementary Material](#)). Additionally, we demonstrated that our method generally performs well when there are multiple parameters within each block, as in [Scenario 3](#) ([Section 3.4](#)). Therefore, our approach is robust and computationally efficient for handling high-dimensional biomedical data, taking into account the frequently observed block-wise covariance structures.

References

- An, B., Guo, J., and Liu, Y. (2014). Hypothesis testing for band size detection of high-dimensional banded precision matrices. *Biometrika* **101**, 477–483.
- Antoniadis, A. and Fan, J. (2001). Regularization of wavelet approximations. *Journal of the American Statistical Association* **96**, 939–967.
- Banerjee, S. and Ghosal, S. (2014). Posterior convergence rates for estimating large precision matrices using graphical models. *Electronic Journal of Statistics* **8**, 2111 – 2137.
- Bickel, P. J. and Levina, E. (2008a). Regularized estimation of large covariance matrices. *Annals of Statistics* **36**, 199–227.

- Bickel, P. J. and Levina, E. (2008b). Covariance regularization by thresholding. *Annals of Statistics* **36**, 2577–2604.
- Bien, J. (2019). Graph-guided banding of the covariance matrix. *Journal of the American Statistical Association* **114**, 782–792.
- Brault, V., Delattre, M., Lebarbier, E., Mary-Huard, T., and Lévy-Leduc, C. (2017). Estimating the number of block boundaries from diagonal blockwise matrices without penalization. *Scandinavian Journal of Statistics* **44**, 563–580.
- Cai, T. and Liu, W. (2011). Adaptive thresholding for sparse covariance matrix estimation. *Journal of the American Statistical Association* **106**, 672–684.
- Cai, T. T., Ren, Z., and Zhou, H. H. (2013). Optimal rates of convergence for estimating toeplitz covariance matrices. *Probability Theory and Related Fields* **156**, 101–143.
- Cai, T. T., Ren, Z., and Zhou, H. H. (2016). Estimating structured high-dimensional covariance and precision matrices: Optimal rates and adaptive estimation. *Electronic Journal of Statistics* **10**, 1–59.
- Chen, S., Bowman, F. D., and Mayberg, H. S. (2016). A bayesian hierarchical framework for modeling brain connectivity for neuroimaging data. *Biometrics* **72**, 596–605.
- Chen, S., Kang, J., Xing, Y., Zhao, Y., and Milton, D. K. (2018). Estimating large covariance matrix with network topology for high-dimensional biomedical data. *Computational Statistics and Data Analysis* **127**, 82 – 95.
- Chen, S., Li, M., Hong, D., Billheimer, D., Li, H., Xu, B. J., and Shyr, Y. (2009). A novel comprehensive wave-form MS data processing method. *Bioinformatics* **25**, 808–814.
- Chiappelli, J., Rowland, L. M., Wijtenburg, S. A., Chen, H., Maudsley, A. A., Sheriff, S., Chen, S., Savransky, A., Marshall, W., Ryan, M. C., Bruce, H. A., Shuldiner, A. R., Mitchell, B. D., Kochunov, P., and Hong, L. E. (2019). Cardiovascular risks impact human brain n-acetylaspartate in regionally specific patterns. *Proceedings of the National Academy of Sciences* **116**, 25243–25249.
- Devijver, E. and Gallopin, M. (2018). Block-diagonal covariance selection for high-dimensional gaussian graphical models. *Journal of the American Statistical Association* **113**, 306–314.
- Fan, J. (2005). Rejoinder: A Selective Overview of Nonparametric Methods in Financial Econometrics. *Statistical Science* **20**, 351 – 357.
- Fan, J. and Han, X. (2017). Estimation of the false discovery proportion with unknown dependence. *Journal of the Royal Statistical Society: Series B (Statistical Methodology)* **79**, 1143–1164.
- Fan, J., Han, X., and Gu, W. (2012). Estimating false discovery proportion under arbitrary covariance dependence. *Journal of the American Statistical Association* **107**, 1019–1035.

- Fan, J., Liao, Y., and Liu, H. (2016). An overview of the estimation of large covariance and precision matrices. *The Econometrics Journal* **19**, C1–C32.
- Fan, J. and Lv, J. (2008). Sure independence screening for ultrahigh dimensional feature space. *Journal of the Royal Statistical Society: Series B (Statistical Methodology)* **70**, 849–911.
- Ferguson, T. (1996). *A Course in Large Sample Theory*. Chapman & Hall Texts in Statistical Science Series. Springer US.
- Friedman, J., Hastie, T., and Tibshirani, R. (2008). Sparse inverse covariance estimation with the graphical lasso. *Biostatistics* **9**, 432–441.
- Geisser, S. (1963). Multivariate analysis of variance for a special covariance case. *Journal of the American Statistical Association* **58**, 660–669.
- He, K., Kang, J., Hong, H. G., Zhu, J., Li, Y., Lin, H., Xu, H., and Li, Y. (2019). Covariance-insured screening. *Computational Statistics and Data Analysis* **132**, 100–114.
- He, K., Li, Y., Zhu, J., Liu, H., Lee, J. E., Amos, C. I., Hyslop, T., Jin, J., Lin, H., Wei, Q., and Li, Y. (2015). Component-wise gradient boosting and false discovery control in survival analysis with high-dimensional covariates. *Bioinformatics* **32**, 50–57.
- ISGlobal (2021). Barcelona institute for global health. <https://www.isglobal.org/en>. Accessed: 2022-07-30.
- Johnstone, I. M. (2001). On the distribution of the largest eigenvalue in principal components analysis. *Annals of Statistics* **29**, 295–327.
- Johnstone, I. M. and Paul, D. (2018). Pca in high dimensions: An orientation. *Proceedings of the IEEE* **106**, 1277–1292.
- Ke, H., Ren, Z., Qi, J., Chen, S., Tseng, G. C., Ye, Z., and Ma, T. (2022). High-dimension to high-dimension screening for detecting genome-wide epigenetic and noncoding rna regulators of gene expression. *Bioinformatics* **38**, 4078–4087.
- Kong, D., An, B., Zhang, J., and Zhu, H. (2020). L2rm: Low-rank linear regression models for high-dimensional matrix responses. *Journal of the American Statistical Association* **115**, 403–424.
- Ledoit, O. and Wolf, M. (2004). A well-conditioned estimator for large-dimensional covariance matrices. *Journal of Multivariate Analysis* **88**, 365–411.
- Lee, K. and Lee, J. (2021). Estimating large precision matrices via modified cholesky decomposition. *Statistica Sinica* **31**, 173–196.
- Magwene, P. (2021). Biology 723: Statistical computing for biologists. <https://bio723-class.github.io/Bio723-book/index.html>. Accessed: 2022-07-30.

- Morrison, D. F. (1972). The analysis of a single sample of repeated measurements. *Biometrics* **28**, 55–71.
- Newman, M. E. J. (2006). Modularity and community structure in networks. *Proceedings of the National Academy of Sciences* **103**, 8577–8582.
- Perrot-Dockès, M., Lévy-Leduc, C., and Rajjou, L. (2022). Estimation of large block structured covariance matrices: Application to ‘multi-omic’ approaches to study seed quality. *Journal of the Royal Statistical Society: Series C (Applied Statistics)* **71**, 119–147.
- Ritchie, S. C., Surendran, P., Karthikeyan, S., Lambert, S. A., Bolton, T., Pennells, L., Danesh, J., Di Angelantonio, E., Butterworth, A. S., and Inouye, M. (2023). Quality control and removal of technical variation of nmr metabolic biomarker data in ~ 120,000 uk biobank participants. *Scientific Data* **10**, 64.
- Rothman, A. J., Levina, E., and Zhu, J. (2009). Generalized thresholding of large covariance matrices. *Journal of the American Statistical Association* **104**, 177–186.
- Seely, J. (1971). Quadratic Subspaces and Completeness. *The Annals of Mathematical Statistics* **42**, 710 – 721.
- Spellman, P. T., Sherlock, G., Zhang, M. Q., Iyer, V. R., Anders, K., Eisen, M. B., Brown, P. O., Botstein, D., and Futcher, B. (1998). Comprehensive identification of cell cycle-regulated genes of the yeast *saccharomyces cerevisiae* by microarray hybridization. *Molecular Biology of the Cell* **9**, 3273–3297.
- Szatrowski, T. H. (1980). Necessary and Sufficient Conditions for Explicit Solutions in the Multivariate Normal Estimation Problem for Patterned Means and Covariances. *The Annals of Statistics* **8**, 802 – 810.
- Van Der Vaart, A. W. (2000). *Asymptotic Statistics*. Cambridge University Press.
- Van Der Vaart, A. W. and Wellner, J. A. (1996). *Weak convergence and empirical processes*. Springer.
- Wainwright, M. J. (2019). *High-dimensional statistics: A non-asymptotic viewpoint*, volume 48. Cambridge University Press.
- Wu, Q., Ma, T., Liu, Q., Milton, D. K., Zhang, Y., and Chen, S. (2021). ICN: extracting interconnected communities in gene co-expression networks. *Bioinformatics* **37**, 1997–2003.
- Yildiz, P. B., Shyr, Y., Rahman, J. S., Wardwell, N. R., Zimmerman, L. J., Shakhtour, B., Gray, W. H., Chen, S., Li, M., Roder, H., Liebler, D. C., Bigbee, W. L., Siegfried, J. M., Weissfeld, J. L., Gonzalez, A. L., Ninan, M., Johnson, D. H., Carbone, D. P., Caprioli, R. M., and Massion, P. P. (2007). Diagnostic accuracy of maldi mass spectrometric analysis of unfractionated serum in lung cancer. *Journal of Thoracic Oncology* **2**, 893 – 901.
- Zhang, Y., Shen, W., and Kong, D. (2022). Covariance estimation for matrix-valued data. *Journal of the American Statistical Association* **0**, 1–12.

Supplementary material for *Covariance Matrix Estimation for High-Throughput Biomedical Data with Interconnected Communities*

Yifan Yang^{*} Chixiang Chen[†] Shuo Chen[‡]

Abstract

The present supplementary material contains four sections. Section **A** includes the additional properties of the uniform-block matrices. Section **B** has the additional numerical results for both Numerical Studies and Data Examples sections. Section **C** presents the additional simulation studies. Section **D** provides the technical proofs.

A COROLLARIES

Corollary A.1 (Algebraic properties of uniform-block matrices). *Let $N(\mathbf{A}, \mathbf{B}, \mathbf{p})$, $N_1(\mathbf{A}_1, \mathbf{B}_1, \mathbf{p})$ and $N_2(\mathbf{A}_2, \mathbf{B}_2, \mathbf{p})$ be uniform-block matrices, where $\mathbf{A} = \text{diag}(a_{11}, \dots, a_{KK})$, $\mathbf{A}_1, \mathbf{A}_2$ are diagonal matrices, $\mathbf{B} = (b_{kk'})$ with $b_{kk'} = b_{k'k}$ for $k \neq k'$, $\mathbf{B}_1, \mathbf{B}_2$ are symmetric matrices. additionally, $\mathbf{p} = (p_1, \dots, p_K)^\top$ is the common pre-determined partition-size vector satisfying $p_k > 1$ for every k and $p = p_1 + \dots + p_K$. Let $\mathbf{P} := \text{diag}(p_1, \dots, p_K)$ and $\mathbf{\Delta} := \mathbf{A} + \mathbf{B}\mathbf{P}$.*

(1) *Addition/Subtraction: suppose $\mathbf{N}^* := N_1 \pm N_2$, then \mathbf{N}^* partitioned by \mathbf{p} is a uniform-block matrix, denoted by $\mathbf{N}^*(\mathbf{A}^*, \mathbf{B}^*, \mathbf{p})$ with $\mathbf{A}^* := \mathbf{A}_1 \pm \mathbf{A}_2$ and $\mathbf{B}^* := \mathbf{B}_1 \pm \mathbf{B}_2$.*

^{*}Email: yiorfun@umd.edu

[†]Email: chixiang.chen@som.umaryland.edu

[‡]Email: shuo.chen@som.umaryland.edu

(2) *Square*: suppose $N^* := N^2$, then N^* partitioned by \mathbf{p} is a uniform-block matrix, denoted by $N^*(\mathbf{A}^*, \mathbf{B}^*, \mathbf{p})$ with $\mathbf{A}^* := \mathbf{A}^2$ and $\mathbf{B}^* := \mathbf{A}\mathbf{B} + \mathbf{B}\mathbf{A} + \mathbf{B}\mathbf{P}\mathbf{B}$.

(3) *Eigenvalues*: $N(\mathbf{A}, \mathbf{B}, \mathbf{p})$ has a total of p eigenvalues, comprising a_{kk} with multiplicity $(p_k - 1)$ for $k = 1, \dots, K$ and the remaining K eigenvalues are identical to those of Δ .

(4) *Positive Definiteness*: $N(\mathbf{A}, \mathbf{B}, \mathbf{p})$ is positive definite if and only if \mathbf{A} is positive definite, and Δ has positive eigenvalues only.

(5) *Inverse*: suppose N is invertible, and $N^* := N^{-1}$, then N^* partitioned by \mathbf{p} is a uniform-block matrix, denoted by $N^*(\mathbf{A}^*, \mathbf{B}^*, \mathbf{p})$ with $\mathbf{A}^* = \mathbf{A}^{-1}$ and $\mathbf{B}^* = -\Delta^{-1}\mathbf{B}\mathbf{A}^{-1}$.

Corollary A.2 (Exact variance estimators). *The exact variance estimators of \tilde{a}_{kk} and $\tilde{b}_{kk'}$ are*

$$\begin{aligned} \text{var}(\tilde{a}_{kk}) &= \frac{2a_{kk}^2}{(n-1)(p_k-1)}, \\ \text{var}(\tilde{b}_{kk'}) &= \begin{cases} \frac{2}{(n-1)p_k(p_k-1)} \{(a_{kk} + p_k b_{kk})^2 - (2a_{kk} + p_k b_{kk})b_{kk}\}, & k = k' \\ \frac{1}{2(n-1)p_k p_{k'}} \{p_k p_{k'} (b_{kk'}^2 + b_{k'k}^2) + 2(a_{kk} + p_k b_{kk})(a_{k'k'} + p_{k'} b_{k'k'})\}, & k \neq k' \end{cases} \end{aligned}$$

for every k and k' .

More general, given a partition-size vector $\mathbf{p} = (p_1, \dots, p_K)^\top$ and a uniform-block matrix $\Sigma = (\Sigma_{kk'})$ partitioned by \mathbf{p} , let $\alpha_{kk} = \text{tr}(\Sigma_{kk})/p_k = a_{kk} + b_{kk}$ denote the average of the diagonal entries in Σ_{kk} , let $\beta_{kk} = \text{sum}(\Sigma_{kk})/p_k^2 = a_{kk}/p_k + b_{kk}$ denote the average of all entries in Σ_{kk} for every k , and let $\beta_{kk'} = \text{sum}(\Sigma_{kk'})/(p_k p_{k'}) = b_{kk'}$ denote the average of all entries in $\Sigma_{kk'}$ for every $k \neq k'$. Let $\tilde{\alpha}_{kk} = \text{tr}(\mathbf{S}_{kk})/p_k$, $\tilde{\beta}_{kk} = \text{sum}(\mathbf{S}_{kk})/p_k^2$ for every k , and $\tilde{\beta}_{kk'} = \text{sum}(\mathbf{S}_{kk'})/(p_k p_{k'})$ for every $k \neq k'$. Then,

(1) $\tilde{\alpha}_{kk}$, $\tilde{\beta}_{kk'}$ are the UMVUEs of α_{kk} , $\beta_{kk'}$ for every k and k' ; the variances of $\tilde{\alpha}_{kk}$ and $\tilde{\beta}_{kk'}$ are

$$\begin{aligned} \text{var}(\tilde{\alpha}_{kk}) &= \frac{2}{(n-1)p_k} (a_{kk}^2 + 2a_{kk}b_{kk} + p_k b_{kk}^2), \\ \text{var}(\tilde{\beta}_{kk'}) &= \begin{cases} \frac{2}{(n-1)p_k^2} (a_{kk} + p_k b_{kk})^2, & k = k' \\ \frac{1}{2(n-1)p_k p_{k'}} \{p_k p_{k'} (b_{kk'}^2 + b_{k'k}^2) + 2(a_{kk} + p_k b_{kk})(a_{k'k'} + p_{k'} b_{k'k'})\}, & k \neq k' \end{cases}, \end{aligned}$$

respectively, for every k and k' ; the covariance between $\tilde{\alpha}_{kk}$, $\tilde{\alpha}_{k'k'}$, $\tilde{\beta}_{kk}$, and $\tilde{\beta}_{k'k'}$ are

$$\begin{aligned} \text{cov}(\tilde{\alpha}_{kk}, \tilde{\alpha}_{k'k'}) &= \frac{2}{n-1} b_{kk'} b_{k'k}, & \text{cov}(\tilde{\beta}_{kk}, \tilde{\beta}_{k'k'}) &= \frac{2}{n-1} b_{kk'} b_{k'k}, & k \neq k' \\ \text{cov}(\tilde{\alpha}_{kk}, \tilde{\beta}_{k'k'}) &= \begin{cases} \frac{2}{(n-1)p_k^2} (a_{kk} + p_k b_{kk})^2, & k = k' \\ \frac{2}{n-1} b_{kk'} b_{k'k}, & k \neq k' \end{cases}, \end{aligned}$$

respectively, for every k and k' ; the covariance between $\tilde{\beta}_{kk'}$ and the other estimators are

$$\begin{aligned} \text{cov}(\tilde{\alpha}_{kk}, \tilde{\beta}_{k'k''}) &= \frac{1}{(n-1)p_{k'}p_{k''}} \begin{cases} p_{k'}p_{k''} (b_{k'k} b_{kk''} + b_{k''k} b_{kk'}), & k \neq k', k \neq k'' \\ p_{k''} (b_{k'k''} + b_{k''k'}) (a_{kk} + p_k b_{kk}), & k = k' \\ p_{k'} (b_{k'k''} + b_{k''k'}) (a_{kk} + p_k b_{kk}), & k = k'' \end{cases}, \\ \text{cov}(\tilde{\beta}_{kk}, \tilde{\beta}_{k'k''}) &= \frac{1}{(n-1)p_k} \begin{cases} p_k (b_{k'k} b_{kk''} + b_{k''k} b_{kk'}), & k \neq k', k \neq k'' \\ (a_{kk} + p_k b_{kk}) (b_{k'k''} + b_{k''k'}), & k = k' \\ (a_{kk} + p_k b_{kk}) (b_{k'k''} + b_{k''k'}), & k = k'' \end{cases}, \end{aligned}$$

respectively, for every $k, k' \neq k''$; and

$$\text{cov} \left(\tilde{\beta}_{k_1 k_2}, \tilde{\beta}_{l_1, l_2} \right) = \frac{1}{2(n-1)}$$

$$\left\{ \begin{array}{l} b_{l_1 k_1} b_{k_2 l_2} + b_{l_2 k_1} b_{k_2 l_1} + b_{l_1 k_2} b_{k_1 l_2} + b_{l_2 k_2} b_{k_1 l_1}, \\ \hspace{20em} (I-1) \ k_1 \neq l_1, l_2; k_2 \neq l_1, l_2 \\ \\ \frac{1}{p_{l_1}} (a_{k_2 k_2} b_{l_2 k_1} + a_{k_2 k_2} b_{k_1 l_2}) + b_{l_1 k_1} b_{k_2 l_2} + b_{l_2 k_1} b_{k_2 l_1} + b_{l_1 k_2} b_{k_1 l_2} + b_{l_2 k_2} b_{k_1 l_1}, \\ \hspace{20em} (I-2) \ k_1 \neq l_1, l_2; k_2 = l_1 \\ \\ \frac{1}{p_{l_2}} (a_{k_2 k_2} b_{l_1 k_1} + a_{k_2 k_2} b_{k_1 l_1}) + b_{l_1 k_1} b_{k_2 l_2} + b_{l_2 k_1} b_{k_2 l_1} + b_{l_1 k_2} b_{k_1 l_2} + b_{l_2 k_2} b_{k_1 l_1}, \\ \hspace{20em} (I-3) \ k_1 \neq l_1, l_2; k_2 = l_2 \\ \\ \frac{1}{p_{l_1}} (a_{k_1 k_1} b_{l_2 k_2} + a_{k_1 k_1} b_{k_2 l_2}) + b_{l_1 k_2} b_{k_1 l_2} + b_{l_2 k_2} b_{k_1 l_1} + b_{l_1 k_1} b_{k_2 l_2} + b_{l_2 k_1} b_{k_2 l_1}, \\ \hspace{20em} (2-1) \ k_1 = l_1; k_2 \neq l_1, l_2; \\ \hspace{20em} \text{switch } k_1, k_2 \text{ in (I-2)} \\ \\ (b_{l_1 l_2}^2 + b_{l_2 l_1}^2) + \frac{2}{p_{l_1} p_{l_2}} (a_{l_1 l_1} + p_{l_1} b_{l_1 l_1}) (a_{l_2 l_2} + p_{l_2} b_{l_2 l_2}), \\ \hspace{20em} (2-2) \ k_1 = l_1; k_2 = l_2; \\ \hspace{20em} \text{i.e., var} \left(\tilde{\beta}_{l_1, l_2} \right) \\ \\ \frac{1}{p_{l_2}} (a_{k_1 k_1} b_{l_1 k_2} + a_{k_1 k_1} b_{k_2 l_1}) + b_{l_1 k_2} b_{k_1 l_2} + b_{l_2 k_2} b_{k_1 l_1} + b_{l_1 k_1} b_{k_2 l_2} + b_{l_2 k_1} b_{k_2 l_1}, \\ \hspace{20em} (3-1) \ k_1 = l_2; k_2 \neq l_1, l_2; \\ \hspace{20em} \text{switch } k_1, k_2 \text{ in (I-3)} \\ \\ (b_{l_2 l_1}^2 + b_{l_1 l_2}^2) + \frac{2}{p_{l_2} p_{l_1}} (a_{l_2 l_2} + p_{l_2} b_{l_2 l_2}) (a_{l_1 l_1} + p_{l_1} b_{l_1 l_1}), \\ \hspace{20em} (3-2) \ k_1 = l_2; k_2 = l_1; \\ \hspace{20em} \text{i.e., var} \left(\tilde{\beta}_{l_2, l_1} \right). \end{array} \right.$$

for every $k_1 \neq k_2$ and $l_1 \neq l_2$.

(2) Furthermore, using the below transformations

$$\begin{pmatrix} \tilde{a}_{kk} \\ \tilde{b}_{kk} \end{pmatrix} = \frac{1}{p_k - 1} \begin{pmatrix} p_k & -p_k \\ -1 & p_k \end{pmatrix} \begin{pmatrix} \tilde{\alpha}_{kk} \\ \tilde{\beta}_{kk} \end{pmatrix} \quad \text{for every } k, \quad \tilde{b}_{kk'} = \tilde{\beta}_{kk'} \quad \text{for every } k \neq k',$$

the q by q covariance matrix of $\tilde{\boldsymbol{\theta}}$ consisting the variance and covariance estimators for $\tilde{\boldsymbol{\theta}}$, can be obtained by $\text{var}(\tilde{\boldsymbol{\theta}}) = \mathbf{\Phi}_{\mathbf{p}} \text{var}\{(\tilde{\alpha}_{11}, \dots, \tilde{\alpha}_{KK}, \tilde{\beta}_{11}, \dots, \tilde{\beta}_{1K}, \tilde{\beta}_{22}, \tilde{\beta}_{KK})^\top\} \mathbf{\Phi}_{\mathbf{p}}^\top$, where $\mathbf{\Phi}_{\mathbf{p}} \in \mathbb{R}^{q \times q}$ is a matrix containing the elements of \mathbf{p} only. In particular, by rearranging the order of the elements of $\tilde{\boldsymbol{\theta}}$, we can obtain the results at the beginning.

B ADDITIONAL NUMERICAL RESULTS

B.1 Finite performance of the proposed covariance estimators

We include the additional results from simulation studies for both Scenario 1 and Scenario 2, which are presented in Table B.1, Table B.2, and Table B.3.

B.2 Comparison of the proposed method with existing methods on the simulated datasets

We include the additional results from simulation studies for both Scenario 1 and Scenario 2, which are presented in Figure B.1.

B.3 Comparison of the proposed method with existing methods on the real data examples

We include the additional results for real data examples in Figure B.2.

C ADDITIONAL SIMULATION STUDIES

C.1 Examination of the accuracy of the covariance estimator

Following the setup in Scenario 1, we aimed to assess the accuracy of covariance estimators outlined in Corollary A.2. This evaluation involved examining each pair of $\alpha_{0,11}, \dots, \alpha_{0,KK}$

	$p = 150$				$p = 225$				$p = 300$			
	bias	MCS	ASE	95% CP	bias	MCS	ASE	95% CP	bias	MCS	ASE	95% CP
$a_{0,11}$	0.0	0.1	0.1	95.5	0.0	0.0	0.0	95.2	0.0	0.0	0.0	95.7
$a_{0,22}$	0.0	0.8	0.8	93.9	0.0	0.7	0.7	95.0	0.0	0.6	0.6	94.7
$a_{0,33}$	0.1	2.8	2.8	95.7	0.1	2.3	2.3	95.3	0.0	1.9	2.0	96.3
$a_{0,44}$	0.0	0.3	0.3	94.8	0.0	0.2	0.2	95.3	0.0	0.2	0.2	95.4
$a_{0,55}$	0.0	0.4	0.4	94.6	0.0	0.3	0.3	94.7	0.0	0.3	0.3	94.3
$b_{0,11}$	-1.7	139.4	135.7	91.4	0.8	135.3	136.2	93.1	-0.4	134.1	135.9	93.2
$b_{0,12}$	6.0	86.9	87.5	94.8	4.3	85.7	87.2	95.1	1.0	86.2	88.2	95.0
$b_{0,13}$	5.6	79.4	78.0	95.4	3.5	77.7	77.9	95.9	2.3	75.9	78.0	96.9
$b_{0,14}$	-2.6	110.3	105.1	91.8	-0.8	104.0	105.3	93.7	-0.1	103.6	104.8	95.0
$b_{0,15}$	-2.0	80.7	78.2	93.5	1.9	78.1	78.4	94.0	-3.3	77.6	78.4	93.7
$b_{0,22}$	-0.9	105.7	105.3	93.2	-7.4	105.7	104.0	91.2	5.7	106.3	106.6	93.9
$b_{0,23}$	-0.1	88.6	87.1	92.7	-3.1	86.6	86.3	93.3	4.1	89.5	87.8	93.7
$b_{0,24}$	1.3	85.6	86.1	95.4	-2.7	86.2	85.8	95.3	-0.4	88.7	86.4	95.2
$b_{0,25}$	3.2	66.1	65.5	95.7	-3.3	63.4	64.9	95.4	2.9	67.9	66.1	95.7
$b_{0,33}$	0.7	88.1	88.1	93.6	-0.5	86.6	87.7	93.3	3.3	90.1	88.3	93.5
$b_{0,34}$	0.4	91.6	91.1	94.4	-2.6	91.3	91.3	93.0	1.2	91.4	90.9	93.5
$b_{0,35}$	2.9	61.4	59.3	95.6	-0.9	58.1	59.1	95.8	1.9	60.2	59.5	96.3
$b_{0,44}$	0.1	140.5	137.2	92.1	2.6	137.0	137.7	94.2	-4.9	132.2	136.2	93.1
$b_{0,45}$	-0.5	78.6	74.0	94.2	-1.5	73.5	73.9	96.2	-2.1	73.8	73.8	96.0
$b_{0,55}$	-1.6	80.7	79.6	92.7	-2.2	81.4	79.5	92.7	0.4	80.4	80.0	93.0

Table B.1: We assess the estimated covariance parameters ($a_{0,kk}$ and $b_{0,kk'}$) using our proposed method across 1000 simulated datasets under $n = 50$: “bias” represents the relative bias ($\times 100$); “MCS” refers to the Monte Carlo standard deviation ($\times 100$); “ASE” stands for the average estimated standard error ($\times 100$); “95% CP” represents the empirical coverage probability (in %) based on a 95% Wald-type confidence interval.

and $\beta_{0,11}, \dots, \beta_{0,KK}$ for the sample sizes of $n = 50, 100$, or 150 , with 1000 Monte Carlo replicates. In each replicate, we computed the covariance estimate for every pair of α_0 's and β_0 's by substituting the respective estimates $\tilde{\alpha}_{kk}$ and $\tilde{\beta}_{kk'}$ in Corollary A.2. Averaging the estimated covariances over the 1000 replicates provided the average estimated covariance (denoted as AC) for each pair of α_0 's and β_0 's. Additionally, we calculated the covariances using the actual values in the covariance formulas (denoted as RC) for every pair of α_0 's and β_0 's. To establish a baseline, we computed the Monte Carlo covariance (denoted as MCC) for every pair of α_0 's and β_0 's. The results for pairs involving α_0 's, β_0 's, and α_0 's- β_0 's are tabulated in an Excel file, available at <https://github.com/yiorfun/uniform-blockCovEst>.

The findings in the tables demonstrate that the covariances evaluated at the true values are closely align with the empirical covariances computed using the Monte Carlo method. Moreover, for relatively small sample sizes, say $n = 50$, the proposed method may slightly overestimate the covariances for certain pairs of α_0 's and β_0 's. This occurrence might be attributed

	$p = 150$				$p = 225$				$p = 300$			
	bias	MCSD	ASE	95% CP	bias	MCSD	ASE	95% CP	bias	MCSD	ASE	95% CP
$a_{0,11}$	0.0	0.0	0.0	95.1	0.0	0.0	0.0	94.9	0.0	0.0	0.0	95.2
$a_{0,22}$	0.0	0.6	0.6	95.8	0.0	0.4	0.5	96.2	0.0	0.4	0.4	94.8
$a_{0,33}$	0.0	2.1	2.0	94.2	0.0	1.6	1.6	94.9	0.1	1.4	1.4	95.3
$a_{0,44}$	0.0	0.2	0.2	96.3	0.0	0.1	0.1	95.5	0.0	0.1	0.1	95.4
$a_{0,55}$	0.0	0.3	0.3	95.3	0.0	0.2	0.2	95.1	0.0	0.2	0.2	95.3
$b_{0,11}$	0.3	97.6	95.7	93.5	7.1	97.3	96.7	93.5	-1.1	93.7	95.5	94.6
$b_{0,12}$	1.2	59.6	61.8	95.4	-2.1	61.3	62.4	95.8	2.3	62.5	61.9	94.7
$b_{0,13}$	1.1	52.2	54.7	96.8	-0.4	54.3	55.0	95.6	1.2	55.0	54.8	94.9
$b_{0,14}$	-0.4	72.5	74.1	95.4	-3.1	75.4	74.3	94.3	-0.2	74.5	73.9	94.8
$b_{0,15}$	-0.8	55.6	55.2	93.8	3.7	56.0	55.9	96.0	0.7	56.8	55.3	94.8
$b_{0,22}$	-1.6	71.5	74.0	95.1	2.3	73.4	74.5	94.0	1.8	76.5	74.4	94.0
$b_{0,23}$	-2.3	58.3	61.0	94.1	-0.1	60.6	61.3	94.2	1.5	64.3	61.4	93.8
$b_{0,24}$	1.7	59.9	60.6	95.3	3.3	61.7	60.6	95.5	-0.1	61.8	60.7	94.5
$b_{0,25}$	1.8	45.4	46.1	95.6	1.9	48.3	46.6	94.8	1.7	46.2	46.3	95.0
$b_{0,33}$	-2.6	58.9	61.5	95.3	-1.6	60.7	61.5	93.9	0.5	64.0	61.8	94.1
$b_{0,34}$	1.4	63.3	64.0	94.9	3.5	62.7	63.7	94.8	0.6	66.7	64.0	93.5
$b_{0,35}$	1.2	39.8	41.6	96.2	1.5	43.9	41.9	94.8	2.0	41.9	41.7	95.4
$b_{0,44}$	0.8	93.1	96.6	96.3	-3.9	93.8	95.9	94.7	-0.8	98.8	96.4	93.0
$b_{0,45}$	0.0	50.2	52.1	96.0	-1.9	54.5	52.2	93.3	-1.2	53.9	52.0	94.7
$b_{0,55}$	-0.8	57.1	56.1	94.0	4.1	56.7	56.8	94.9	0.0	56.6	56.2	93.9

Table B.2: We assess the estimated covariance parameters ($a_{0,kk}$ and $b_{0,kk'}$) using our proposed method across 1000 simulated datasets under $n = 100$: “bias” represents the relative bias ($\times 100$); “MCSD” refers to the Monte Carlo standard deviation ($\times 100$); “ASE” stands for the average estimated standard error ($\times 100$); “95% CP” represents the empirical coverage probability (in %) based on a 95% Wald-type confidence interval.

to the number of unknown parameters (i.e., $q = 20$) being comparable to to $n = 50$. As the sample size increases beyond 50, the proposed method becomes more effective in providing reasonable covariance estimation.

C.2 Evaluation of the estimated covariance matrix estimator on multiple testing

We conducted an additional simulation study to investigate the advantage of a covariance matrix estimate with less bias. Specifically, we examined how a covariance matrix estimate with a larger bias might potentially lead to inappropriate type 1 error or a loss in statistical power. For this study, we set $p_{\text{ind}} = 100$ (resulting in $p = 500$) and generated a sample with $n = 50$ from $N(\boldsymbol{\mu}_0, \boldsymbol{\Sigma}_{0,1}(\mathbf{A}_0, \mathbf{B}_0, \mathbf{p}_1))$, where $\boldsymbol{\mu}_0 = (\mu_{01}, \dots, \mu_{0p})^\top$, with $\mu_{0j} = 0.3$ for $j = 1, \dots, 10$ and $\mu_{0j} = 0$ otherwise. The other settings were kept consistent with those in Scenario 1. To

	$p = 150$				$p = 225$				$p = 300$			
	bias	MCSD	ASE	95% CP	bias	MCSD	ASE	95% CP	bias	MCSD	ASE	95% CP
$a_{0,11}$	0.0	0.0	0.0	95.0	0.0	0.0	0.0	96.0	0.0	0.0	0.0	94.6
$a_{0,22}$	0.0	0.5	0.5	93.7	0.0	0.4	0.4	95.5	0.0	0.3	0.3	94.1
$a_{0,33}$	0.0	1.6	1.6	95.1	0.0	1.3	1.3	93.6	0.0	1.1	1.1	96.3
$a_{0,44}$	0.0	0.1	0.1	94.7	0.0	0.1	0.1	95.1	0.0	0.1	0.1	96.0
$a_{0,55}$	0.0	0.2	0.2	95.3	0.0	0.2	0.2	95.2	0.0	0.2	0.2	94.4
$b_{0,11}$	2.6	75.1	78.3	95.6	-2.8	77.3	77.7	94.3	-5.8	76.5	77.3	94.3
$b_{0,12}$	1.1	49.7	50.6	95.1	1.3	49.4	50.2	95.1	1.1	51.6	50.3	93.7
$b_{0,13}$	2.3	44.1	44.9	96.1	1.0	44.4	44.7	96.2	-1.5	45.9	44.4	94.0
$b_{0,14}$	-3.6	58.3	60.6	95.9	-0.5	61.9	60.4	94.2	4.6	60.3	59.8	93.7
$b_{0,15}$	0.6	46.1	45.1	94.5	-1.6	45.9	44.9	94.9	-1.4	44.9	44.9	93.7
$b_{0,22}$	1.1	61.7	60.6	95.0	-2.7	60.5	60.2	93.6	1.2	61.7	60.6	93.9
$b_{0,23}$	1.1	51.4	50.1	94.6	-0.8	49.5	49.9	94.2	0.9	50.0	50.0	94.2
$b_{0,24}$	-0.5	48.6	49.6	95.8	-2.0	48.3	49.5	95.3	-1.2	49.5	49.4	94.4
$b_{0,25}$	1.4	36.7	37.7	95.2	-1.1	37.2	37.5	94.5	2.1	38.7	37.8	95.6
$b_{0,33}$	1.1	52.1	50.6	94.4	1.3	49.5	50.5	94.7	-0.2	49.3	50.3	94.4
$b_{0,34}$	-1.0	52.4	52.4	94.9	-3.6	51.5	52.6	95.1	1.0	51.4	52.1	94.4
$b_{0,35}$	2.3	33.2	34.1	95.6	-1.8	33.7	34.1	95.3	1.0	35.5	34.0	94.1
$b_{0,44}$	1.5	77.2	78.8	95.0	3.2	81.2	79.0	93.9	-3.9	79.7	78.2	93.2
$b_{0,45}$	-2.6	42.3	42.5	95.5	2.7	43.1	42.5	94.5	0.4	42.9	42.4	95.2
$b_{0,55}$	-0.6	46.9	45.8	93.4	-0.7	46.8	45.8	94.2	0.7	46.4	45.9	94.5

Table B.3: We assess the estimated covariance parameters ($a_{0,kk}$ and $b_{0,kk'}$) using our proposed method across 1000 simulated datasets under $n = 150$: “bias” represents the relative bias ($\times 100$); “MCSD” refers to the Monte Carlo standard deviation ($\times 100$); “ASE” stands for the average estimated standard error ($\times 100$); “95% CP” represents the empirical coverage probability (in %) based on a 95% Wald-type confidence interval.

simultaneously perform hypothesis tests

$$H_{0j} : \mu_j = 0, \quad \text{against} \quad H_{1j} : \mu_j \neq 0, \quad j = 1, \dots, p,$$

we utilized the principal factor approximation (PFA) method to estimate the false discovery proportion (FDP) in the presence of dependence among test statistics (Fan et al., 2012; Fan and Han, 2017). Across 100 Monte Carlo replicates, for a sequence of threshold values t , we calculated the medians and standard errors (s.d.) of the total number of rejections $R(t)$, the number of correct rejections $S(t)$, and the false discovery proportion $FDP(t)$ using the true covariance matrix $\Sigma_{0,1}(\mathbf{A}_0, \mathbf{B}_0, \mathbf{p}_1)$, its POET estimator $\tilde{\Sigma}_{\text{POET}}$, and the proposed estimator $\tilde{\Sigma}_{\text{prop.}} = \tilde{\Sigma}_1(\tilde{\mathbf{A}}_1, \tilde{\mathbf{B}}_1, \mathbf{p}_1)$, respectively.

The results presented in Table C.1 demonstrate that the proposed covariance matrix estimator behaves more similarly to the true covariance matrix than the POET estimator, primarily

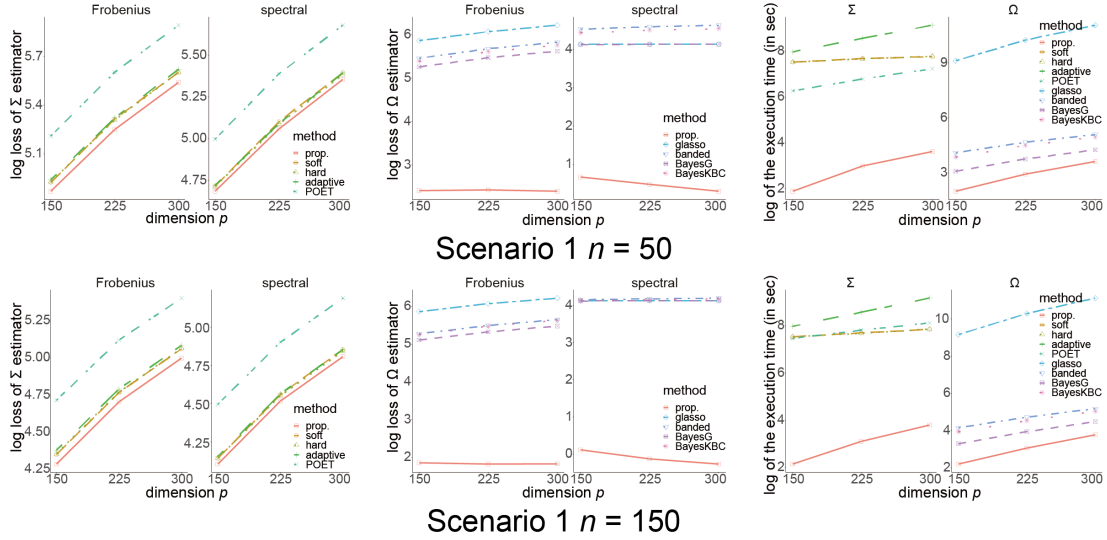


Figure B.1: We evaluate the estimated covariance and precision matrices and compare them with all benchmark estimates. In the first and second rows, we present the results for Scenario 1 (the small K setting) under $n = 50$ and $n = 150$, respectively. The left two and the middle two subfigures illustrate the logarithmic losses in both Frobenius and spectral norms for covariance matrix Σ and precision matrix Ω estimations for all methods, respectively; and the right two subfigures display the execution time for Σ and Ω estimation.

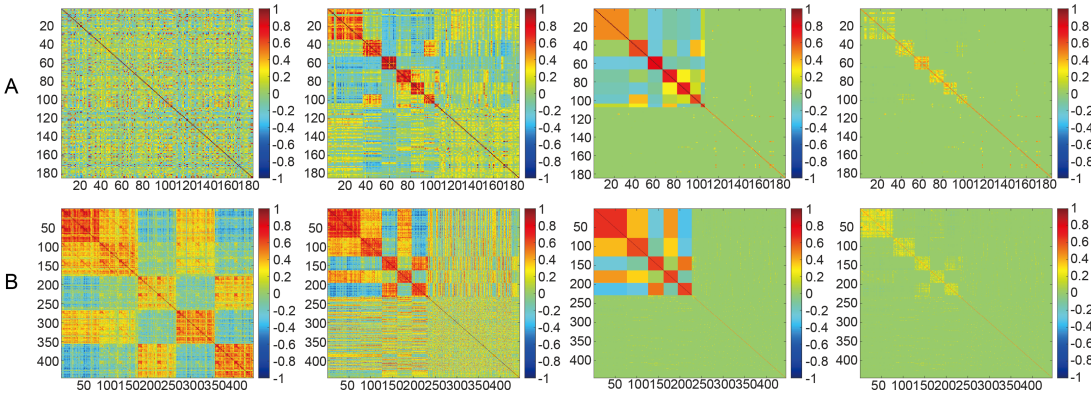


Figure B.2: We compare the proposed covariance estimates for all features in the proteomics and brain imaging studies with the conventional covariance estimates (i.e., the soft-thresholding estimates). The two rows correspond to the two data examples: A, the proteomics dataset; B, the brain imaging dataset. From the left heatmaps to the right, we have: (1) the raw correlation matrix, (2) the correlation matrix produced by a community detection algorithm, (3) the proposed covariance matrix estimate, and (4) the conventional soft-thresholding covariance matrix estimate.

due to its fewer bias. For example, at a threshold value $t = 0.0527$, the approximate FDP(t) are 0.00, 0.79, and 0.13 for the true covariance matrix, the POET estimator, and the proposed

estimator, respectively. This suggests that the bias in the POET estimator may result in an inappropriate PDP. Furthermore, $S(t)$ is estimated by 10, 4, and 10 for the true covariance matrix, the POET estimator, and the proposed estimator, respectively, indicating a loss in statistical power for the POET estimator.

threshold ϵ	true			POET			proposed method					
	median $R(t)$	s.d. $R(t)$	median $S(t)$	median $R(t)$	s.d. $S(t)$	median $FDP(t)$	median $R(t)$	s.d. $R(t)$	median $S(t)$	s.d. $S(t)$	median $FDP(t)$	s.d. $FDP(t)$
0.0001	0.00	0.00	10.00	0.00	0.00	0.00	0.00	0.00	10.00	4.23	0.00	0.00
0.0054	0.00	3.47	10.00	0.00	11.40	0.00	3.21	0.00	10.97	3.18	0.00	0.23
0.0106	0.00	11.96	10.00	0.00	15.95	0.00	3.42	0.00	14.68	2.81	0.00	0.34
0.0159	0.00	20.02	10.00	0.00	24.75	0.00	3.70	0.00	22.95	2.76	0.00	0.39
0.0211	0.00	25.19	10.00	0.00	30.70	0.00	3.78	0.00	30.01	2.70	0.00	0.40
0.0264	0.00	30.84	10.00	0.00	35.79	0.00	3.96	0.00	34.22	2.46	0.00	0.42
0.0316	0.00	36.12	10.00	0.00	39.71	0.00	3.99	0.00	38.52	2.41	0.00	0.43
0.0369	0.00	40.75	10.00	0.00	44.15	0.00	4.19	0.00	42.58	2.36	0.00	0.44
0.0422	0.00	45.65	10.00	0.00	49.61	1.50	4.29	0.00	47.61	2.18	0.00	0.45
0.0474	0.00	49.77	10.00	0.00	55.04	2.00	4.43	0.03	53.13	2.09	0.00	0.45
0.0527	1.00	52.49	10.00	0.00	59.48	4.00	4.52	0.79	57.79	2.04	0.13	0.46
0.0579	1.00	55.14	10.00	0.00	63.10	5.00	4.61	0.85	61.26	1.97	0.42	0.46
0.0632	4.00	57.63	10.00	0.00	65.92	6.50	4.65	0.87	64.55	1.96	0.44	0.46
0.0685	8.00	59.61	10.00	0.00	67.90	7.00	4.63	0.97	66.84	1.96	0.60	0.45
0.0737	10.00	62.86	10.00	0.00	69.55	7.50	4.61	1.00	68.44	1.96	0.73	0.46
0.0790	10.00	65.62	10.00	0.00	71.26	8.00	4.45	1.00	70.06	1.96	0.84	0.45
0.0842	10.50	68.02	10.00	0.00	72.40	9.00	4.37	1.00	71.64	1.94	0.88	0.44
0.0895	10.50	70.18	10.00	0.00	73.83	10.00	4.26	1.00	72.85	1.94	0.82	0.44
0.0947	14.00	71.77	10.00	0.00	75.19	10.00	4.16	1.00	74.40	1.94	0.79	0.43
0.1000	20.00	72.97	10.00	0.00	77.10	10.00	3.95	1.00	75.90	1.93	0.83	0.43

Table C.1: We present the total number of rejections $R(t)$, the number of correct rejections $S(t)$, and the false discovery proportion (FDP) using the true covariance matrix, the POET estimator, and the proposed estimator

C.3 Justification of the proposed parameterization strategy

To validate the proposed parameterization for the uniform-block structure, we compared box plots of the off-diagonal entries in the diagonal blocks and all entries in the off-diagonal blocks, using both the real data examples and simulated datasets from Scenario 3 (Section 3.4). The resulting box plots, shown below, demonstrate that while the true covariance matrix $\Upsilon_{0,\sigma}$ may not precisely follow a uniform-block structure, the proposed estimation procedure can provide a more competitive covariance-matrix estimate and a comparable precision-matrix estimate to conventional methods, especially when variations within blocks are small. These results suggest that considering the structure of uniform blocks for real datasets is reasonable, given that the variations within the blocks closely resemble those observed in the simulated data with $\sigma = 0.8$ for both the proteomics study and the brain imaging study.

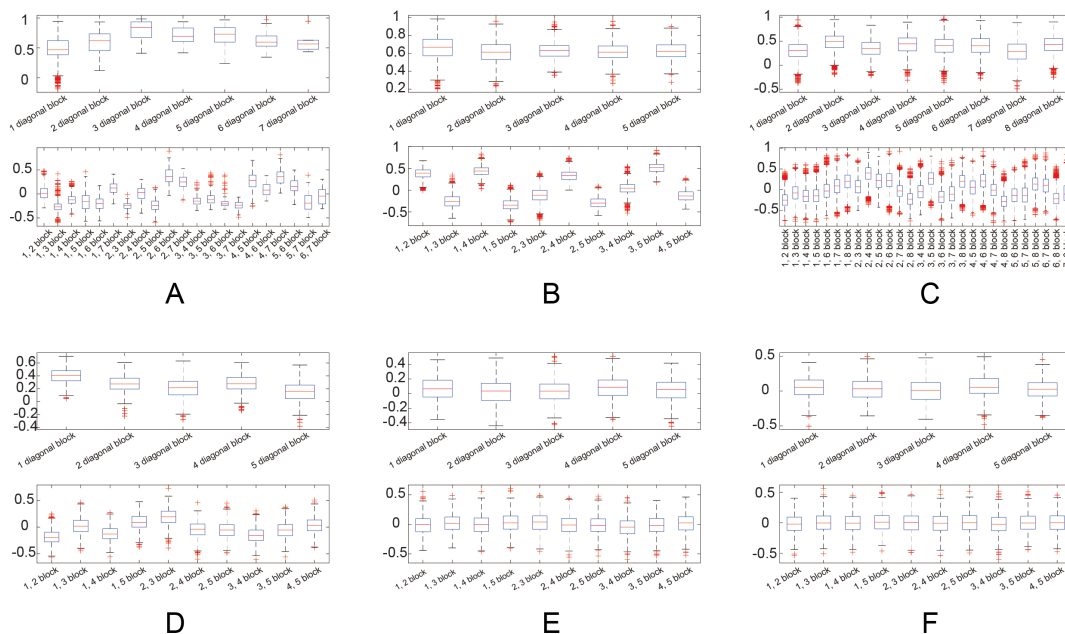


Figure C.1: We display box plots of the off-diagonal entries within the diagonal blocks and all entries in the off-diagonal blocks. A: Box plots for the proteomics dataset; B: Box plots for the brain imaging dataset; C: Box plots for the Spellman dataset; D: Box plots for the simulated dataset with $\sigma = 0.1$; E: Box plots for the simulated dataset with $\sigma = 0.5$; F: Box plots for the simulated dataset with $\sigma = 0.8$.

C.4 Justification of the proposed approach among alternative covariance structures

We assessed the performance of the proposed approach for three distinct community structures: unbalanced interconnected community structure denoted as “unbalanced”, independent community structure denoted as “independent”, and hierarchical community structure, denoted as “hierarchical”.

To generate the simulated datasets, we followed the procedure below. Initially, we defined the true covariance matrices:

(1) the true covariance matrix for unbalanced interconnected community (or uniform-block) structure $\Sigma_{0,U} = \mathbf{A}_{0,U} \circ \mathbf{I}(\mathbf{p}_4) + \mathbf{B}_{0,U} \circ \mathbf{J}(\mathbf{p}_4)$;

(2) the true covariance matrix for independent community structure $\Sigma_{0,I} = \mathbf{A}_{0,I} \circ \mathbf{I}(\mathbf{p}_4) + \mathbf{B}_{0,I} \circ \mathbf{J}(\mathbf{p}_4)$;

(3) the true covariance matrix for hierarchical community structure $\Sigma_{0,H} = \mathbf{A}_{0,H} \circ \mathbf{I}(\mathbf{p}_4) + \mathbf{B}_{0,H} \circ \mathbf{J}(\mathbf{p}_4)$.

In these expressions, the partition-size vector is defined by $\mathbf{p}_4 = (10, 15, 15, 20, 25)^\top$ indicating that $K = 5$, $p = 85$, and the unbalanced community sizes, $\mathbf{A}_{0,U} = \mathbf{A}_{0,I} = \mathbf{A}_{0,H} = \mathbf{A}_0$ are defined in Scenario 1, $\mathbf{B}_{0,U} = \mathbf{B}_0$ are defined in Scenario 1, $\mathbf{B}_{0,I} = \text{diag}(\mathbf{B}_0)$, and

$$\mathbf{B}_{0,H} = \begin{pmatrix} 6.731 & -1.690 & 0.530 & 0.530 & 0.530 \\ & 5.215 & 0.530 & 0.530 & 0.530 \\ & & 4.328 & 0.790 & 0.790 \\ & & & 6.788 & 0.790 \\ & & & & 3.954 \end{pmatrix}.$$

We then proceeded with generating datasets of size $n = 50$ with a mean vector $\boldsymbol{\mu} = \mathbf{0}_{p \times 1}$. Subsequently, we generated multivariate normal distributed datasets of size n with mean $\boldsymbol{\mu}$ and covariance matrices $\Sigma_{0,U}$, $\Sigma_{0,I}$, and $\Sigma_{0,H}$, respectively. To estimate the covariance parameters for each structure, we applied the proposed approach. Across 1000 replicates, we evaluated the average relative bias, Monte Carlo standard deviation, average standard error, and empirical

covariance probability based on 95% Wald-type confidence intervals for each parameter. The results are demonstrated in Table C.2. Furthermore, we visually represented the population, sample, and estimated covariance matrices for three structures in Figure C.2.

	Unbalanced				Hierarchical				Independent			
	bias	MCSD	ASE	95% CP	bias	MCSD	ASE	95% CP	bias	MCSD	ASE	95% CP
$a_{0,11}$	0.0	0.1	0.1	93.9	0.0	0.1	0.1	93.9	0.0	0.1	0.1	93.9
$a_{0,22}$	0.0	1.2	1.2	94.8	0.0	1.2	1.2	94.8	0.0	1.2	1.2	94.8
$a_{0,33}$	-0.2	4.0	4.0	93.9	-0.3	4.0	4.0	95.0	-0.3	4.0	4.0	95.0
$a_{0,44}$	0.0	0.3	0.3	94.3	0.0	0.3	0.3	94.3	0.0	0.3	0.3	94.3
$a_{0,55}$	0.0	0.4	0.4	95.1	0.0	0.4	0.4	95.1	0.0	0.4	0.4	95.1
$b_{0,11}$	3.9	137.3	136.8	94.0	7.7	138.9	137.6	93.7	6.3	132.9	137.3	94.2
$b_{0,12}$	-3.1	87.6	88.7	94.9	-4.1	91.8	88.5	93.9	-4.7	85.1	85.0	96.2
$b_{0,13}$	0.7	78.1	78.5	95.9	2.0	80.3	78.6	95.5	-2.1	77.7	77.9	96.2
$b_{0,14}$	0.2	103.7	105.2	94.3	-2.0	95.4	97.4	96.5	-0.1	101.0	97.2	94.9
$b_{0,15}$	-3.4	78.5	78.2	93.3	-6.6	75.0	74.2	96.0	3.2	73.7	73.9	96.3
$b_{0,22}$	4.2	108.3	106.5	94.2	-2.6	105.4	105.1	92.3	-1.5	105.0	105.3	92.2
$b_{0,23}$	2.1	88.1	87.7	94.2	-0.6	66.6	68.7	96.8	2.6	68.9	68.1	95.7
$b_{0,24}$	-2.4	86.7	86.6	95.0	2.1	84.9	85.3	95.6	-3.1	84.7	85.1	96.8
$b_{0,25}$	1.5	66.1	65.7	95.8	1.0	63.4	65.0	96.6	-4.0	66.2	64.8	95.5
$b_{0,33}$	1.2	88.3	88.7	92.7	2.1	91.1	88.9	93.3	-0.8	88.2	88.3	92.7
$b_{0,34}$	-1.0	92.1	91.3	93.8	1.4	81.0	78.9	95.8	-2.4	79.3	77.9	95.4
$b_{0,35}$	2.2	59.5	59.3	95.4	-1.6	59.6	60.3	95.3	-3.8	59.2	59.3	96.3
$b_{0,44}$	-1.5	136.1	136.9	93.5	0.7	138.1	137.3	93.3	1.5	139.4	137.5	92.4
$b_{0,45}$	-2.4	71.0	73.6	96.2	2.0	74.6	74.7	96.2	0.5	69.4	73.9	97.0
$b_{0,55}$	-4.0	79.4	79.2	93.3	-2.7	77.6	79.4	92.6	-1.7	79.6	79.6	92.8

Table C.2: We assess the estimated covariance parameters ($a_{0,kk}$ and $b_{0,kk'}$) using our proposed method across 1000 simulated datasets under $n = 50$ for the unbalanced interconnected community structure, the hierarchical community structure, and the independent community structure: “bias” represents the relative bias ($\times 100$); “MCSD” refers to the Monte Carlo standard deviation ($\times 100$); “ASE” stands for the average estimated standard error ($\times 100$); “95% CP” represents the empirical coverage probability (in %) based on a 95% Wald-type confidence interval. In all settings, the estimation biases of the covariance parameters are small, generally less than 5%. The standard errors, calculated using both MCSD and ASE, are close, indicating that our proposed variance estimators are accurate. This is further supported by the results of the 95% coverage probabilities.

To conduct the simulation studies discussed in Section 3 and Section C, we utilized the R packages “pfa” (Fan et al., 2012) (with some modifications), “CovTools” (Lee et al., 2021), “POET” (Fan et al., 2016), “CVTuningCov” (Wang, 2015) (with some modifications). The estimation procedures were implemented using the R software (R Core Team, 2021). The R code used for the simulation studies in Section 3 and the data examples in Section 4 can be accessed at <https://github.com/yiorfun/UBCovEst>. Moreover, all data examples are available at <https://github.com/yiorfun/UBCovEst>.

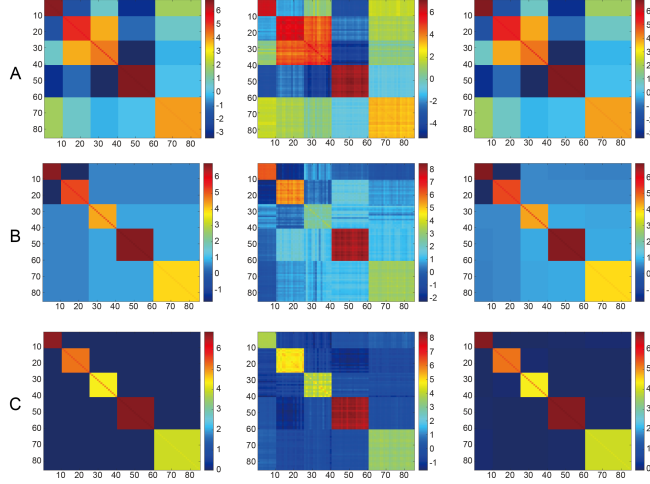


Figure C.2: We compare the estimated covariance matrix using our proposed method across 1000 simulated datasets under $n = 50$ for the unbalanced interconnected community structure, the hierarchical community structure, and the independent community structure. A: the unbalanced interconnected community structure, from the left to right: the population, the sample, and the estimated covariance matrices; B: the hierarchical community structure, from the left to right: the population, the sample, and the estimated covariance matrices; C: the independent structure, from the left to right: the population, the sample, and the estimated covariance matrices.

D PROOFS

D.1 Proofs of Lemma, Corollary, Corollary A.1

Please refer to the arguments and proofs in the work of [Yang et al. \(2023\)](#) for further details.

D.2 Derivations of the maximum likelihood estimators and their properties

Starting from equation (4),

$$\frac{\partial}{\partial \theta_j} \ell_n(\boldsymbol{\theta}; \mathbf{X}) = \frac{n}{2} \text{tr} \left[\left\{ \boldsymbol{\Sigma}(\mathbf{A}, \mathbf{B}, \mathbf{p}) - (\mathbf{S}_{kk'}) \right\} \left\{ \frac{\partial \mathbf{A}_\Omega}{\partial \theta_j} \circ \mathbf{I}(\mathbf{p}) + \frac{\partial \mathbf{B}_\Omega}{\partial \theta_j} \circ \mathbf{J}(\mathbf{p}) \right\} \right],$$

let $(\mathbf{M}_{kk'})$ denote $\mathbf{M} = \Sigma(\mathbf{A}, \mathbf{B}, \mathbf{p}) - (\mathbf{S}_{kk'})$ partitioned by \mathbf{p} . Then the system of the score equations is

$$\mathbf{S}_n(\boldsymbol{\theta}; \mathbf{X}) = \frac{n}{2} \begin{pmatrix} \text{tr} \left\{ (\mathbf{M}_{kk'}) \frac{\partial \Omega(\mathbf{A}_\Omega, \mathbf{B}_\Omega, \mathbf{p})}{\partial a_{11}} \right\} \\ \text{tr} \left\{ (\mathbf{M}_{kk'}) \frac{\partial \Omega(\mathbf{A}_\Omega, \mathbf{B}_\Omega, \mathbf{p})}{\partial a_{22}} \right\} \\ \vdots \\ \text{tr} \left\{ (\mathbf{M}_{kk'}) \frac{\partial \Omega(\mathbf{A}_\Omega, \mathbf{B}_\Omega, \mathbf{p})}{\partial a_{KK}} \right\} \\ \text{tr} \left\{ (\mathbf{M}_{kk'}) \frac{\partial \Omega(\mathbf{A}_\Omega, \mathbf{B}_\Omega, \mathbf{p})}{\partial b_{11}} \right\} \\ \vdots \\ \text{tr} \left\{ (\mathbf{M}_{kk'}) \frac{\partial \Omega(\mathbf{A}_\Omega, \mathbf{B}_\Omega, \mathbf{p})}{\partial b_{KK}} \right\} \end{pmatrix} = \mathbf{0}_{q \times 1}. \quad (\text{D.1})$$

Recall $\mathbf{P} = \text{diag}(p_1, \dots, p_K)$ and $\boldsymbol{\Delta} = \mathbf{A} + \mathbf{B}\mathbf{P}$. Using a fact $(\mathbf{A}\mathbf{P})^{-1} - \boldsymbol{\Delta}\mathbf{B}\mathbf{A}^{-1} = (\mathbf{P}\boldsymbol{\Delta})^{-1}$, and doing some algebra, we obtain the following derivatives,

$$\begin{aligned} \frac{\partial \mathbf{A}_\Omega}{\partial a_{kk}} &= -a_{kk}^{-2} \mathbf{E}_{kk}, & \frac{\partial \mathbf{B}_\Omega}{\partial a_{kk}} &= \boldsymbol{\Delta}^{-1} \mathbf{E}_{kk} \boldsymbol{\Delta}^{-1} \mathbf{B} \mathbf{A}^{-1} + a_{kk}^{-2} \boldsymbol{\Delta}^{-1} \mathbf{B} \mathbf{E}_{kk}, & \text{for every } k, \\ \frac{\partial \mathbf{A}_\Omega}{\partial b_{kk'}} &= \mathbf{0}_{K \times K}, & \frac{\partial \mathbf{B}_\Omega}{\partial b_{kk'}} &= \begin{cases} -\boldsymbol{\Delta}^{-1} \mathbf{E}_{kk} \mathbf{P} \boldsymbol{\Delta}^{-1} \mathbf{P}^{-1}, & k = k' \\ -\boldsymbol{\Delta}^{-1} (\mathbf{E}_{kk'} + \mathbf{E}_{k'k}) \mathbf{P} \boldsymbol{\Delta}^{-1} \mathbf{P}^{-1}, & k \neq k' \end{cases}, & \text{for every } k \text{ and } k'. \end{aligned}$$

Then, the individual equations in (D.1) can be simplified as

$$\begin{aligned} \text{tr} \left\{ (\mathbf{M}_{kk'}) \frac{\partial \Omega(\mathbf{A}_\Omega, \mathbf{B}_\Omega, \mathbf{p})}{\partial a_{kk}} \right\} &= (-a_{kk}^{-2}) \text{tr}(\mathbf{M}_{kk}) + \sum_{\ell=1}^K \sum_{\ell'=1}^K \text{sum}(\mathbf{M}_{\ell\ell'}) \left(\frac{\partial \mathbf{B}_\Omega}{\partial a_{kk}} \right)_{\ell', \ell} = 0, \\ \text{tr} \left\{ (\mathbf{M}_{kk'}) \frac{\partial \Omega(\mathbf{A}_\Omega, \mathbf{B}_\Omega, \mathbf{p})}{\partial b_{kk'}} \right\} &= \sum_{\ell=1}^K \sum_{\ell'=1}^K \text{sum}(\mathbf{M}_{\ell\ell'}) \left(\frac{\partial \mathbf{B}_\Omega}{\partial b_{kk'}} \right)_{\ell', \ell} = 0, \end{aligned}$$

for every k and k' , where $(\partial \mathbf{B}_\Omega / \partial a_{kk}), (\partial \mathbf{B}_\Omega / \partial b_{kk'}) \in \mathbb{R}^{K \times K}$ and the subscript (ℓ', ℓ) denotes the (ℓ', ℓ) element of $(\partial \mathbf{B}_\Omega / \partial a_{kk})$ or $(\partial \mathbf{B}_\Omega / \partial b_{kk'})$.

Now, we claim the system of score equations in (D.1) has a unique solution. Since $\mathbf{A} = \text{diag}(a_{11}, \dots, a_{KK})$, then $-\mathbf{A}^{-2} = \text{diag}(-a_{11}^{-2}, \dots, -a_{KK}^{-2})$, denoted by \mathbf{A}^* . Let $\boldsymbol{\beta}^* \in \mathbb{R}^q$

denote a vector as below,

$$\boldsymbol{\beta}^* = \{\text{tr}(\mathbf{M}_{11}), \dots, \text{tr}(\mathbf{M}_{KK}), \text{sum}(\mathbf{M}_{11}), \dots, \text{sum}(\mathbf{M}_{1K}), \text{sum}(\mathbf{M}_{22}), \dots, \text{sum}(\mathbf{M}_{KK})\}^\top.$$

Let $\mathbf{B}^{(1),*} \in \mathbb{R}^{K \times (q-K)}$ denote a matrix with k th row

$$\left\{ \begin{aligned} & \left(\frac{\partial \mathbf{B}_\Omega}{\partial a_{kk}} \right)_{1,1}, \left(\frac{\partial \mathbf{B}_\Omega}{\partial a_{kk}} \right)_{1,2} + \left(\frac{\partial \mathbf{B}_\Omega}{\partial a_{kk}} \right)_{2,1}, \dots, \left(\frac{\partial \mathbf{B}_\Omega}{\partial a_{kk}} \right)_{1,K} + \left(\frac{\partial \mathbf{B}_\Omega}{\partial a_{kk}} \right)_{K,1}, \left(\frac{\partial \mathbf{B}_\Omega}{\partial a_{kk}} \right)_{2,2}, \dots, \\ & \left(\frac{\partial \mathbf{B}_\Omega}{\partial a_{kk}} \right)_{K-1,K} + \left(\frac{\partial \mathbf{B}_\Omega}{\partial a_{kk}} \right)_{K,K-1}, \left(\frac{\partial \mathbf{B}_\Omega}{\partial a_{kk}} \right)_{K,K} \end{aligned} \right\},$$

for $k = 1, \dots, K$, and let $\mathbf{B}^{(2),*} \in \mathbb{R}^{(q-K) \times (q-K)}$ denote a matrix with rows

$$\left\{ \begin{aligned} & \left(\frac{\partial \mathbf{B}_\Omega}{\partial b_{kk'}} \right)_{1,1}, \left(\frac{\partial \mathbf{B}_\Omega}{\partial b_{kk'}} \right)_{1,2} + \left(\frac{\partial \mathbf{B}_\Omega}{\partial b_{kk'}} \right)_{2,1}, \dots, \left(\frac{\partial \mathbf{B}_\Omega}{\partial b_{kk'}} \right)_{1,K} + \left(\frac{\partial \mathbf{B}_\Omega}{\partial b_{kk'}} \right)_{K,1}, \left(\frac{\partial \mathbf{B}_\Omega}{\partial b_{kk'}} \right)_{2,2}, \dots, \\ & \left(\frac{\partial \mathbf{B}_\Omega}{\partial b_{kk'}} \right)_{K-1,K} + \left(\frac{\partial \mathbf{B}_\Omega}{\partial b_{kk'}} \right)_{K,K-1}, \left(\frac{\partial \mathbf{B}_\Omega}{\partial b_{kk'}} \right)_{K,K} \end{aligned} \right\}$$

for every $k \leq k'$. Thus, the system of the score equations in (D.1) can be rewritten as

$$\mathbf{S}_n(\boldsymbol{\theta}; \mathbf{X}) = \begin{pmatrix} \mathbf{A}^* & \mathbf{B}^{(1),*} \\ \mathbf{0}_{(q-K) \times K} & \mathbf{B}^{(2),*} \end{pmatrix} \boldsymbol{\beta}^* = \mathbf{0}_{q \times 1},$$

and $\text{rank} \begin{pmatrix} \mathbf{A}^* & \mathbf{B}^{(1),*} \\ \mathbf{0}_{(q-K) \times K} & \mathbf{B}^{(2),*} \end{pmatrix} = \text{rank}(\mathbf{A}^*) + \text{rank}(\mathbf{B}^{(2),*})$ due to $\mathbf{I}_K - \mathbf{A}^*(\mathbf{A}^*)^{-1} = \mathbf{0}_{K \times K}$, which satisfies the condition provided in [Buaphim et al. \(2018, Theorem 3.10, p.334\)](#).

On the one hand, $\text{rank}(\mathbf{A}^*) = K$ by the positive definiteness that $a_{kk} > 0$ for every k . On the other hand, to compute $\text{rank}(\mathbf{B}^{(2),*})$, use the fact $\text{vech}(AXB) = (B^\top \otimes A) \times \text{vech}(X)$, where the matrices A, B and X with suitable sizes, and \otimes denotes the Kronecker product. Since

$$\frac{\partial \mathbf{B}_\Omega}{\partial b_{kk'}} = \begin{cases} -\Delta^{-1} \mathbf{E}_{kk} \mathbf{P} \Delta^{-1} \mathbf{P}^{-1}, & k = k' \\ -\Delta^{-1} (\mathbf{E}_{kk'} + \mathbf{E}_{k'k}) \mathbf{P} \Delta^{-1} \mathbf{P}^{-1}, & k \neq k' \end{cases},$$

for every k and k' , where \mathbf{E}_{kk} and $\mathbf{E}_{kk'} + \mathbf{E}_{k'k}$ span the entire matrix space of symmetric

matrices with the size of K by K . Thus, $\text{rank}(\mathbf{B}^{(2),*}) = (K+1)K/2$ due to the equivalence of the matrix space and the vector space spanned by the matrices. Therefore, the coefficients matrix of the given homogeneous system of linear equations has full rank and has a unique solution $\beta^* = \mathbf{0}_{q \times 1}$. Finally, the solution to the system in (D.1), denoted by $\tilde{\theta}$, must be the maximum likelihood estimator due to the uniqueness.

Following (D.1), the first-order partial derivative of the score function with respect to θ is

$$\frac{\partial \mathbf{S}_n(\theta; \mathbf{X})}{\partial \theta} = \begin{pmatrix} \frac{\partial^2 \ell_n(\theta; \mathbf{X})}{\partial \theta^{(A)} \partial \theta^{(A), \top}} & \frac{\partial^2 \ell_n(\theta; \mathbf{X})}{\partial \theta^{(A)} \partial \theta^{(B), \top}} \\ \frac{\partial^2 \ell_n(\theta; \mathbf{X})}{\partial \theta^{(B)} \partial \theta^{(A), \top}} & \frac{\partial^2 \ell_n(\theta; \mathbf{X})}{\partial \theta^{(B)} \partial \theta^{(B), \top}} \end{pmatrix} = \frac{n}{2} \begin{pmatrix} \mathbf{H}_1 & \mathbf{H}_2 \\ \mathbf{H}_2^\top & \mathbf{H}_3 \end{pmatrix}, \quad (\text{D.2})$$

where $\theta^{(A)} = (a_{11}, \dots, a_{KK})^\top$, $\theta^{(B)} = (b_{11}, \dots, b_{1K}, b_{22}, \dots, b_{KK})^\top$, and therefore $\theta = (\theta^{(A), \top}, \theta^{(B), \top})^\top$, the blocks $\mathbf{H}_1 \in \mathbb{R}^{K \times K}$, $\mathbf{H}_2 \in \mathbb{R}^{K \times (q-K)}$, and $\mathbf{H}_3 \in \mathbb{R}^{(q-K) \times (q-K)}$. In particular, given k and k' ,

$$\mathbf{H}_1 = \begin{cases} \left[\begin{array}{l} 2a_{kk}^{-3} \text{tr}(\mathbf{M}_{kk}) - a_{kk}^{-2} \left\{ \frac{\partial}{\partial a_{mm}} \text{tr}(\mathbf{M}_{kk}) \right\} \\ + \sum_{\ell=1}^K \sum_{\ell'=1}^K \left[\left\{ \frac{\partial}{\partial a_{mm}} \text{sum}(\mathbf{M}_{\ell\ell'}) \right\} \left(\frac{\partial \mathbf{B}_\Omega}{\partial a_{kk}} \right)_{\ell', \ell} + \text{sum}(\mathbf{M}_{\ell\ell'}) \left\{ \frac{\partial}{\partial a_{mm}} \left(\frac{\partial \mathbf{B}_\Omega}{\partial a_{kk}} \right) \right\}_{\ell', \ell} \right] \end{array} \right], & m = k \\ \left[\begin{array}{l} \sum_{\ell=1}^K \sum_{\ell'=1}^K \left[\left\{ \frac{\partial}{\partial a_{mm}} \text{sum}(\mathbf{M}_{\ell\ell'}) \right\} \left(\frac{\partial \mathbf{B}_\Omega}{\partial a_{kk}} \right)_{\ell', \ell} + \text{sum}(\mathbf{M}_{\ell\ell'}) \left\{ \frac{\partial}{\partial a_{mm}} \left(\frac{\partial \mathbf{B}_\Omega}{\partial a_{kk}} \right) \right\}_{\ell', \ell} \right] \end{array} \right], & m \neq k \end{cases}$$

for $m = 1, 2, \dots, K$; and

$$\mathbf{H}_2 = \sum_{\ell=1}^K \sum_{\ell'=1}^K \left[\left\{ \frac{\partial}{\partial a_{mm}} \text{sum}(\mathbf{M}_{\ell\ell'}) \right\} \left(\frac{\partial \mathbf{B}_\Omega}{\partial b_{kk'}} \right)_{\ell', \ell} + \text{sum}(\mathbf{M}_{\ell\ell'}) \left\{ \frac{\partial}{\partial a_{mm}} \left(\frac{\partial \mathbf{B}_\Omega}{\partial b_{kk'}} \right) \right\}_{\ell', \ell} \right],$$

$$\mathbf{H}_3 = \sum_{\ell=1}^K \sum_{\ell'=1}^K \left[\left\{ \frac{\partial}{\partial b_{mm'}} \text{sum}(\mathbf{M}_{\ell\ell'}) \right\} \left(\frac{\partial \mathbf{B}_\Omega}{\partial b_{kk'}} \right)_{\ell', \ell} + \text{sum}(\mathbf{M}_{\ell\ell'}) \left\{ \frac{\partial}{\partial b_{mm'}} \left(\frac{\partial \mathbf{B}_\Omega}{\partial b_{kk'}} \right) \right\}_{\ell', \ell} \right],$$

for $m, m' = 1, 2, \dots, K$. The first-order partial derivatives $\partial \text{sum}(\mathbf{M}_{\ell\ell'}) / \partial a_{mm}$ and $\partial \text{sum}(\mathbf{M}_{\ell\ell'}) / \partial b_{mm'}$ are easily computed, where $\mathbf{M}_{\ell\ell'} = \Sigma_{\ell\ell'} - \mathbf{S}_{\ell\ell'}$ for $m, m', \ell, \ell' = 1, 2, \dots, K$. The second-order partial derivatives $\partial(\partial \mathbf{B}_\Omega / \partial a_{kk}) / \partial a_{mm}$, $\partial(\partial \mathbf{B}_\Omega / \partial b_{kk'}) / \partial a_{mm}$, and $\partial(\partial \mathbf{B}_\Omega / \partial b_{kk'}) / \partial b_{mm'}$ are

matrices for $m, m', k, k' = 1, 2, \dots, K$, shown respectively as below.

$$\frac{\partial}{\partial a_{mm}} \left(\frac{\partial \mathbf{B}_\Omega}{\partial a_{kk}} \right) = \begin{cases} -\Delta^{-1} \mathbf{E}_{kk} \Delta^{-1} (2\mathbf{E}_{kk} \Delta^{-1} \mathbf{B} \mathbf{A}^{-1} + \mathbf{B} \mathbf{A}^{-1} \mathbf{E}_{kk} \mathbf{A}^{-1}) \\ \quad - (2a_{kk}^{-3} \mathbf{I}_K + a_{kk}^{-2} \Delta^{-1} \mathbf{E}_{kk}) \Delta^{-1} \mathbf{B} \mathbf{E}_{kk}, & k = m \\ -\Delta^{-1} (\mathbf{E}_{mm} \Delta^{-1} \mathbf{E}_{kk} + \mathbf{E}_{kk} \Delta^{-1} \mathbf{E}_{mm}) \Delta^{-1} \mathbf{B} \mathbf{A}^{-1} \\ \quad - \Delta^{-1} \mathbf{E}_{kk} \Delta^{-1} \mathbf{B} \mathbf{A}^{-1} \mathbf{E}_{mm} \mathbf{A}^{-1} - a_{kk}^{-2} \Delta^{-1} \mathbf{E}_{mm} \Delta^{-1} \mathbf{B} \mathbf{E}_{kk}, & k \neq m \end{cases},$$

and,

$$\frac{\partial}{\partial a_{mm}} \left(\frac{\partial \mathbf{B}_\Omega}{\partial b_{kk'}} \right) = \begin{cases} \Delta^{-1} \mathbf{E}_{mm} \Delta^{-1} \mathbf{E}_{kk} \mathbf{P} \Delta^{-1} \mathbf{P} \\ \quad - \Delta^{-1} \mathbf{E}_{kk} \mathbf{P} \Delta^{-1} (\mathbf{E}_{mm} \Delta^{-1} \mathbf{B} - \mathbf{P} \mathbf{E}_{mm}) \mathbf{A}^{-1}, & k = k' \\ \Delta^{-1} \mathbf{E}_{mm} \Delta^{-1} (\mathbf{E}_{kk'} + \mathbf{E}_{k'k}) \mathbf{P} \Delta^{-1} \mathbf{P} \\ \quad - \Delta^{-1} (\mathbf{E}_{kk'} + \mathbf{E}_{k'k}) \mathbf{P} \Delta^{-1} (\mathbf{E}_{mm} \Delta^{-1} \mathbf{B} - \mathbf{P} \mathbf{E}_{mm}) \mathbf{A}^{-1}, & k \neq k' \end{cases}$$

and,

$$\frac{\partial}{\partial b_{mm'}} \left(\frac{\partial \mathbf{B}_\Omega}{\partial b_{kk'}} \right) = \begin{cases} \left\{ \begin{array}{ll} \Delta^{-1} (\mathbf{E}_{mm} + \mathbf{E}_{kk}) \mathbf{P} \Delta^{-1} (\mathbf{E}_{kk} + \mathbf{E}_{mm}) \mathbf{P} \Delta^{-1} \mathbf{P}, & m = m' \\ \Delta^{-1} (\mathbf{E}_{mm'} + \mathbf{E}_{m'm} + \mathbf{E}_{kk}) \mathbf{P} \Delta^{-1} (\mathbf{E}_{kk} + \mathbf{E}_{mm'} + \mathbf{E}_{m'm}) \mathbf{P} \Delta^{-1} \mathbf{P}, & m \neq m' \end{array} \right\}, & k = k' \\ \left\{ \begin{array}{ll} \Delta^{-1} (\mathbf{E}_{mm} + \mathbf{E}_{kk'} + \mathbf{E}_{k'k}) \mathbf{P} \Delta^{-1} (\mathbf{E}_{kk'} + \mathbf{E}_{k'k} + \mathbf{E}_{mm}) \mathbf{P} \Delta^{-1} \mathbf{P}, & m = m' \\ \Delta^{-1} (\mathbf{E}_{mm'} + \mathbf{E}_{m'm} + \mathbf{E}_{kk'} + \mathbf{E}_{k'k}) \mathbf{P} \Delta^{-1} (\mathbf{E}_{kk'} + \mathbf{E}_{k'k} + \mathbf{E}_{mm'} + \mathbf{E}_{m'm}) \mathbf{P} \Delta^{-1} \mathbf{P}, & m \neq m' \end{array} \right\}, & k \neq k' \end{cases}$$

By the unbiasedness from Theorem 1, the expectations of \mathbf{H}_1 , \mathbf{H}_2 , and \mathbf{H}_3 depend on the terms $E(\text{sum}(\mathbf{M}_{\ell\ell})) = (1 - c_n)p_\ell(a_{\ell\ell} + b_{\ell\ell}p_\ell)$, $E(\text{sum}(\mathbf{M}_{\ell\ell'})) = (1 - c_n)p_\ell p_{\ell'} b_{\ell\ell'}$ and $E(\text{tr}(\mathbf{M}_{\ell\ell})) = (1 - c_n)p_\ell(a_\ell + b_\ell)$ only, where $c_n = (n - 1)/n$. Then Fisher's information matrices for n observations and one observation can be calculated by $\mathbb{I}_n(\boldsymbol{\theta}) = -E(\partial \mathbf{S}_n(\boldsymbol{\theta}; \mathbf{X})/\partial \boldsymbol{\theta})$ and $\mathbb{I}_1(\boldsymbol{\theta}) = \mathbb{I}_n(\boldsymbol{\theta})/n$, respectively. Since both a determinant operator and a trace operator are continuous, the log-likelihood function $\ell_n(\boldsymbol{\theta}; \mathbf{X})$ is continuous with respect to $\boldsymbol{\theta}$. In addition,

there is a unique solution to the likelihood equation for every n . Thus, $\tilde{\boldsymbol{\theta}}$ is strongly consistent, asymptotically normal, and asymptotically efficient, following the classical arguments in [Ferguson \(1996\)](#); [Van Der Vaart and Wellner \(1996\)](#); [Stuart. et al. \(1999\)](#); [Bickel and Doksum \(2015a,b\)](#), i.e., $\tilde{\boldsymbol{\theta}} \rightarrow \boldsymbol{\theta}$ almost surely as $n \rightarrow \infty$ and $\sqrt{n}(\tilde{\boldsymbol{\theta}} - \boldsymbol{\theta}) \rightarrow N(\mathbf{0}_{q \times 1}, \mathbb{I}_1^{-1}(\boldsymbol{\theta}))$ in distribution as $n \rightarrow \infty$.

D.3 Proof of Theorem 1

Proof of Theorem 1. Recall an i.i.d. random sample $\mathbf{X}_i \sim N(\boldsymbol{\mu}, \boldsymbol{\Sigma}(\mathbf{A}, \mathbf{B}, \mathbf{p}))$ for $i = 1, \dots, n$, where $\boldsymbol{\Sigma}(\mathbf{A}, \mathbf{B}, \mathbf{p})$ is supposed to be a uniform-block matrix with diagonal matrix \mathbf{A} and symmetric matrix \mathbf{B} , and $\mathbf{p} = (p_1, \dots, p_K)^\top$ is a given partition-size vector with $p_k > 1$ for every k and $p = p_1 + \dots + p_K$. Let $\mathbf{X} \sim N(\boldsymbol{\mu}, \boldsymbol{\Sigma}(\mathbf{A}, \mathbf{B}, \mathbf{p}))$ and $\bar{\mathbf{X}} = (\mathbf{X}_1 + \dots + \mathbf{X}_n)/n$. Let $\mathbf{X}_{i,p_k}, \bar{\mathbf{X}}_{p_k}, \boldsymbol{\mu}_{p_k} \in \mathbb{R}^{p_k}$ satisfying $\mathbf{X}_i = (\mathbf{X}_{i,p_1}^\top, \dots, \mathbf{X}_{i,p_K}^\top)^\top$, $\bar{\mathbf{X}} = (\bar{\mathbf{X}}_{p_1}^\top, \dots, \bar{\mathbf{X}}_{p_K}^\top)^\top$, and $\boldsymbol{\mu} = (\boldsymbol{\mu}_{p_1}^\top, \dots, \boldsymbol{\mu}_{p_K}^\top)^\top$, respectively.

First, we prove that $\tilde{\boldsymbol{\theta}}$ is unbiased. By $\boldsymbol{\Sigma}(\mathbf{A}, \mathbf{B}, \mathbf{p}) = (\boldsymbol{\Sigma}_{kk'})$, we can obtain that

$$\begin{aligned}\boldsymbol{\Sigma}_{kk'} &= \text{cov}(\mathbf{X}_{p_k}, \mathbf{X}_{p_{k'}}) = \text{E}\{(\mathbf{X}_{p_k} - \boldsymbol{\mu}_{p_k})(\mathbf{X}_{p_{k'}} - \boldsymbol{\mu}_{p_{k'}})^\top\}, \\ \boldsymbol{\Sigma}_{kk'}/n &= \text{cov}(\bar{\mathbf{X}}_{p_k}, \bar{\mathbf{X}}_{p_{k'}}) = \text{E}\{(\bar{\mathbf{X}}_{p_k} - \boldsymbol{\mu}_{p_k})(\bar{\mathbf{X}}_{p_{k'}} - \boldsymbol{\mu}_{p_{k'}})^\top\}.\end{aligned}$$

for every k and k' . Let $\mathbf{C}_{kk'} = \sum_{i=1}^n (\mathbf{X}_{i,p_k} - \bar{\mathbf{X}}_{p_k})(\mathbf{X}_{i,p_{k'}} - \bar{\mathbf{X}}_{p_{k'}})^\top$ for every k and k' , which can be simplified to

$$\mathbf{C}_{kk'} = \sum_{i=1}^n (\mathbf{X}_{i,p_k} - \boldsymbol{\mu}_{p_k})(\mathbf{X}_{i,p_{k'}} - \boldsymbol{\mu}_{p_{k'}})^\top - n(\bar{\mathbf{X}}_{p_k} - \boldsymbol{\mu}_{p_k})(\bar{\mathbf{X}}_{p_{k'}} - \boldsymbol{\mu}_{p_{k'}})^\top.$$

Taking expectation on the both sides, we have $\text{E}(\mathbf{C}_{kk'}) = (n-1)\boldsymbol{\Sigma}_{kk'}$ for every k and k' .

Recall that, given k and k' , $\boldsymbol{\Sigma}_{kk} = a_{kk}\mathbf{I}_{p_k} + b_{kk}\mathbf{J}_{p_k}$ for $k = k'$ and $\boldsymbol{\Sigma}_{kk'} = b_{kk'}\mathbf{1}_{p_k \times p_{k'}}$. Define

$$\alpha_{kk} = a_{kk} + b_{kk} = \text{tr}(\boldsymbol{\Sigma}_{kk})/p_k, \quad \beta_{kk'} = \begin{cases} a_{kk}/p_k + b_{kk} = \text{sum}(\boldsymbol{\Sigma}_{kk})/p_k^2, & k = k' \\ b_{kk'} = \text{sum}(\boldsymbol{\Sigma}_{kk'})/(p_k p_{k'}), & k \neq k' \end{cases}.$$

By the definition of unbiased sample covariance matrix $(n - 1)\mathbf{S}_{kk'} = \mathbf{C}_{kk'}$, we have the following results:

$$\tilde{\alpha}_{kk} = p_k^{-1} \text{tr}(\mathbf{S}_{kk}), \quad \tilde{\beta}_{kk} = p_k^{-2} \text{sum}(\mathbf{S}_{kk}), \quad \tilde{\beta}_{kk'} = (p_k p_{k'})^{-1} \text{sum}(\mathbf{S}_{kk'})$$

are unbiased estimators for α_{kk} , β_{kk} for every k and for $\beta_{kk'}$ for every $k \neq k'$. Furthermore,

$$\tilde{a}_{kk} = \tilde{\alpha}_{kk} - \frac{p_k \tilde{\beta}_{kk} - \tilde{\alpha}_{kk}}{p_k - 1}, \quad \tilde{b}_{kk'} = \begin{cases} \frac{p_k \tilde{\beta}_{kk} - \tilde{\alpha}_{kk}}{p_k - 1}, & k = k' \\ \tilde{\beta}_{kk'}, & k \neq k' \end{cases},$$

are unbiased estimators for a_{kk} and $b_{kk'}$ every k and k' .

Next, we prove the optimal property of $\tilde{\boldsymbol{\theta}}$. Let $\mathbf{Y} = (\mathbf{X}_1^\top, \dots, \mathbf{X}_n^\top)^\top \in \mathbb{R}^{pn}$ denote a vector consisting of all observations. By normality assumption, $\mathbf{Y} \sim N(\boldsymbol{\mu}_y, \mathbf{V})$, where $\boldsymbol{\mu}_y = (\mathbf{1}_n \otimes \mathbf{I}_p) \boldsymbol{\mu} \in \mathbb{R}^{pn}$ and $\mathbf{V} = \mathbf{I}_n \otimes \boldsymbol{\Sigma}(\mathbf{A}, \mathbf{B}, \mathbf{p}) \in \mathbb{R}^{pn \times pn}$.

First, we prove $\tilde{\boldsymbol{\mu}} = \bar{\mathbf{X}}$ is the best linear unbiased estimator (BLUE). Equivalently, we need to check the conditions of Theorem 1 and Corollary 2 in [Zmysłony \(1976\)](#). Since $\boldsymbol{\Sigma}(\mathbf{I}_K, \mathbf{0}_{K \times K}, \mathbf{p}) = \mathbf{I}_p$, the identity matrix $\mathbf{I}_n \otimes \mathbf{I}_p \in \text{span}(\mathbf{V})$. Let M^- denote the generalized inverse for some matrix M , and let $\mathbf{P}_0 = (\mathbf{1}_n \otimes \mathbf{I}_p) \{(\mathbf{1}_n \otimes \mathbf{I}_p)^\top (\mathbf{1}_n \otimes \mathbf{I}_p)\}^- (\mathbf{1}_n \otimes \mathbf{I}_p)^\top$, which can be simplified to $n^{-1} \mathbf{J}_n \otimes \mathbf{I}_p$ by using the fact $\mathbf{1}_n^- = \mathbf{1}_n^\top / n$. Thus, \mathbf{P}_0 is an orthogonal projector because

$$\begin{aligned} \mathbf{P}_0^2 &= (n^{-1} \mathbf{J}_n \otimes \mathbf{I}_p) (n^{-1} \mathbf{J}_n \otimes \mathbf{I}_p) = n^{-2} (\mathbf{J}_n \times \mathbf{J}_n) \otimes \mathbf{I}_p = n^{-1} \mathbf{J}_n \otimes \mathbf{I}_p = \mathbf{P}_0, \\ \mathbf{P}_0^\top &= n^{-1} \mathbf{J}_n^\top \otimes \mathbf{I}_p^\top = \mathbf{P}_0. \end{aligned}$$

Then, \mathbf{V} and \mathbf{P}_0 are commutative, because

$$\begin{aligned} \mathbf{P}_0 \mathbf{V} &= (n^{-1} \mathbf{J}_n \otimes \mathbf{I}_p) \{\mathbf{I}_n \otimes \boldsymbol{\Sigma}(\mathbf{A}, \mathbf{B}, \mathbf{p})\} = n^{-1} (\mathbf{J}_n \mathbf{I}_n) \otimes \{\mathbf{I}_p \boldsymbol{\Sigma}(\mathbf{A}, \mathbf{B}, \mathbf{p})\} = n^{-1} \mathbf{J}_n \otimes \boldsymbol{\Sigma}(\mathbf{A}, \mathbf{B}, \mathbf{p}), \\ \mathbf{V} \mathbf{P}_0 &= \{\mathbf{I}_n \otimes \boldsymbol{\Sigma}(\mathbf{A}, \mathbf{B}, \mathbf{p})\} (n^{-1} \mathbf{J}_n \otimes \mathbf{I}_p) = n^{-1} (\mathbf{I}_n \mathbf{J}_n) \otimes \{\boldsymbol{\Sigma}(\mathbf{A}, \mathbf{B}, \mathbf{p}) \mathbf{I}_p\} = n^{-1} \mathbf{J}_n \otimes \boldsymbol{\Sigma}(\mathbf{A}, \mathbf{B}, \mathbf{p}). \end{aligned}$$

Hence, all estimable functions have the best estimator, which can be expressed in terms of the

solution to the following normal equation

$$(\mathbf{1}_n \otimes \mathbf{I}_p)^\top (\mathbf{1}_n \otimes \mathbf{I}_p) \boldsymbol{\mu} = (\mathbf{1}_n \otimes \mathbf{I}_p)^\top \mathbf{Y}.$$

So, $\tilde{\boldsymbol{\mu}} = \bar{\mathbf{X}}$ is BLUE. This coincides with the arguments of the proofs in [Roy et al. \(2016\)](#) and [Koziol et al. \(2017\)](#).

Second, we can prove $\tilde{\alpha}_{kk}$ and $\tilde{\beta}_{kk'}$ are best quadratic unbiased estimator (BQUE) for α_{kk} and $\beta_{kk'}$ for every k and k' . We need to check the conditions of Theorem 2 in [Zmyślony \(1976\)](#), or the lines of analogous arguments in [Roy et al. \(2016\)](#) and [Koziol et al. \(2017\)](#), that is, given $\mathbf{P}_0 \mathbf{V} = \mathbf{V} \mathbf{P}_0$ and $\mathbf{R}_0 = \mathbf{I}_{pn} - \mathbf{P}_0$, there exist BQUE for the parameters of quadratic covariance if and only if $\text{span}(\mathbf{P}_0 \mathbf{V} \mathbf{P}_0)$, i.e., the smallest linear space containing $\mathbf{P}_0 \mathbf{V} \mathbf{P}_0$, is a quadratic space. Since $\boldsymbol{\Sigma}(\mathbf{A}, \mathbf{B}, \mathbf{p})$ is a uniform-block matrix, $\{\boldsymbol{\Sigma}(\mathbf{A}, \mathbf{B}, \mathbf{p})\}^2$ is a uniform-block matrix, expressed by $(\boldsymbol{\Sigma}^2)(\mathbf{A}^2, \mathbf{A}\mathbf{B} + \mathbf{B}\mathbf{A} + \mathbf{B}\mathbf{P}\mathbf{B}, \mathbf{p})$, so $\text{span}\{\boldsymbol{\Sigma}(\mathbf{A}, \mathbf{B}, \mathbf{p})\}$ is a quadratic subspace and the identity matrix $\mathbf{I}(\mathbf{p})$ belongs to it. So, $\text{span}(\mathbf{V})$ is a quadratic subspace. In addition, it is clear that \mathbf{P}_0 is idempotent, because $\mathbf{P}_0^2 = (\mathbf{I}_{pn} - \mathbf{P}_0)^2 = \mathbf{I}_{pn}^2 - \mathbf{I}_{pn}\mathbf{P}_0 - \mathbf{P}_0\mathbf{I}_{pn} + \mathbf{P}_0^2 = \mathbf{I}_{pn} - 2\mathbf{P}_0 + \mathbf{P}_0 = \mathbf{I}_{pn} - \mathbf{P}_0 = \mathbf{P}_0$. By the result (2.e) from [Seely \(1971\)](#), $\text{span}(\mathbf{P}_0 \mathbf{V} \mathbf{P}_0) = \{\mathbf{P}_0 \mathbf{V} \mathbf{P}_0 : \mathbf{V} \in \text{span}(\mathbf{V})\}$ is a quadratic subspace. Since $\text{span}\{\boldsymbol{\Sigma}(\mathbf{A}, \mathbf{B}, \mathbf{p})\}$ and $\text{span}(\mathbf{V})$ are quadratic subspaces, we can find bases for them respectively. Recall the definition of the block Hadamard product. $\boldsymbol{\Sigma}(\mathbf{A}, \mathbf{B}, \mathbf{p})$ has a base as follows:

$$\mathbf{E}_{kk} \circ \mathbf{I}(\mathbf{p}), \quad \mathbf{E}_{kk} \circ \mathbf{J}(\mathbf{p}), \quad \text{for every } k, \quad (\mathbf{E}_{kk'} + \mathbf{E}_{k'k}) \circ \mathbf{J}(\mathbf{p}), \quad \text{for every } k \neq k',$$

where $\mathbf{E}_{kk'}$ denotes a K by K matrix in which (k, k') entry is 1 and the other entries are 0's for every k and k' . Thus, the base for $\text{span}(\mathbf{V})$ is

$$\mathbf{I}_n \otimes \{\mathbf{E}_{kk} \circ \mathbf{I}(\mathbf{p})\}, \mathbf{I}_n \otimes \{\mathbf{E}_{kk} \circ \mathbf{J}(\mathbf{p})\}, \text{ for every } k, \mathbf{I}_n \otimes \{(\mathbf{E}_{kk'} + \mathbf{E}_{k'k}) \circ \mathbf{J}(\mathbf{p})\}, \text{ for every } k \neq k'.$$

By Result 2 from [Roy et al. \(2016\)](#); [Koziol et al. \(2017\)](#), $(\mathbf{1}_n^\top \otimes \mathbf{I}_p) \mathbf{Y}$ is the complete and

minimal sufficient statistic for $\boldsymbol{\mu}$, and

$$\begin{aligned} \mathbf{Y}^\top \mathbf{P}_0 [\mathbf{I}_n \otimes \{\mathbf{E}_{kk} \circ \mathbf{I}(\boldsymbol{p})\}] \mathbf{P}_0 \mathbf{Y}, \quad \mathbf{Y}^\top \mathbf{P}_0 [\mathbf{I}_n \otimes \{\mathbf{E}_{kk} \circ \mathbf{J}(\boldsymbol{p})\}] \mathbf{P}_0 \mathbf{Y}, \quad \text{for every } k, \\ \mathbf{Y}^\top \mathbf{P}_0 [\mathbf{I}_n \otimes \{(\mathbf{E}_{kk'} + \mathbf{E}_{k'k}) \circ \mathbf{J}(\boldsymbol{p})\}] \mathbf{P}_0 \mathbf{Y}, \quad \text{for every } k \neq k', \end{aligned}$$

are the complete and minimal sufficient statistics for $\boldsymbol{\Sigma}$. Given the above base for $\text{span}(\mathbf{V})$, we follow the arguments about the coordinate-free approach (Roy et al., 2016; Koziol et al., 2017; Wichura, 2006), the BQEs for α_{kk} and $\beta_{kk'}$ are the least square estimators satisfying the normal equations as below:

$$\begin{aligned} & \text{vec}(\mathbf{P}_0 [\mathbf{I}_n \otimes \{\mathbf{E}_{kk} \circ \mathbf{I}(\boldsymbol{p})\}])^\top \text{vec}(\mathbf{P}_0 [\mathbf{I}_n \otimes \{\mathbf{E}_{kk} \circ \mathbf{I}(\boldsymbol{p})\}]) \alpha_{kk} \\ &= \text{vec}(\mathbf{P}_0 [\mathbf{I}_n \otimes \{\mathbf{E}_{kk} \circ \mathbf{I}(\boldsymbol{p})\}])^\top \text{vec}\{(\mathbf{P}_0 \mathbf{Y})(\mathbf{P}_0 \mathbf{Y})^\top\}, \\ & \text{vec}(\mathbf{P}_0 [\mathbf{I}_n \otimes \{\mathbf{E}_{kk} \circ \mathbf{J}(\boldsymbol{p})\}])^\top \text{vec}(\mathbf{P}_0 [\mathbf{I}_n \otimes \{\mathbf{E}_{kk} \circ \mathbf{J}(\boldsymbol{p})\}]) \beta_{kk} \\ &= \text{vec}(\mathbf{P}_0 [\mathbf{I}_n \otimes \{\mathbf{E}_{kk} \circ \mathbf{J}(\boldsymbol{p})\}])^\top \text{vec}\{(\mathbf{P}_0 \mathbf{Y})(\mathbf{P}_0 \mathbf{Y})^\top\}, \\ & \text{vec}(\mathbf{P}_0 [\mathbf{I}_n \otimes \{(\mathbf{E}_{kk'} + \mathbf{E}_{k'k}) \circ \mathbf{J}(\boldsymbol{p})\}])^\top \text{vec}(\mathbf{P}_0 [\mathbf{I}_n \otimes \{(\mathbf{E}_{kk'} + \mathbf{E}_{k'k}) \circ \mathbf{J}(\boldsymbol{p})\}]) \beta_{kk'} \\ &= \text{vec}(\mathbf{P}_0 [\mathbf{I}_n \otimes \{(\mathbf{E}_{kk'} + \mathbf{E}_{k'k}) \circ \mathbf{J}(\boldsymbol{p})\}])^\top \text{vec}\{(\mathbf{P}_0 \mathbf{Y})(\mathbf{P}_0 \mathbf{Y})^\top\}, \end{aligned}$$

for every k , every k , and every $k \neq k'$, respectively, where $\text{vec}(M)$ denotes a single vector by stacking the columns of M (Henderson and Searle, 1979). In addition to the fact that $\text{vec}(A)^\top \text{vec}(B) = \text{tr}(A^\top B)$, the idempotent matrix \mathbf{P}_0 commutes with the base of $\text{span}(\mathbf{V})$, the above equations can be simplified as below.

$$\begin{aligned} \text{tr}(\mathbf{P}_0 [\mathbf{I}_n \otimes \{\mathbf{E}_{kk} \circ \mathbf{I}(\boldsymbol{p})\}]^2) \alpha_{kk} &= (\mathbf{P}_0 \mathbf{Y})^\top [\mathbf{I}_n \otimes \{\mathbf{E}_{kk} \circ \mathbf{I}(\boldsymbol{p})\}] (\mathbf{P}_0 \mathbf{Y}), \quad \text{for every } k, \\ \text{tr}(\mathbf{P}_0 [\mathbf{I}_n \otimes \{\mathbf{E}_{kk} \circ \mathbf{J}(\boldsymbol{p})\}]^2) \beta_{kk} &= (\mathbf{P}_0 \mathbf{Y})^\top [\mathbf{I}_n \otimes \{\mathbf{E}_{kk} \circ \mathbf{J}(\boldsymbol{p})\}] (\mathbf{P}_0 \mathbf{Y}), \quad \text{for every } k, \\ \text{tr}(\mathbf{P}_0 [\mathbf{I}_n \otimes \{(\mathbf{E}_{kk'} + \mathbf{E}_{k'k}) \circ \mathbf{J}(\boldsymbol{p})\}]^2) \beta_{kk'} &= (\mathbf{P}_0 \mathbf{Y})^\top [\mathbf{I}_n \otimes \{(\mathbf{E}_{kk'} + \mathbf{E}_{k'k}) \circ \mathbf{J}(\boldsymbol{p})\}] (\mathbf{P}_0 \mathbf{Y}), \quad \text{for every } k \neq \end{aligned}$$

Define the residual vector $\mathbf{r}_0 = \mathbf{P}_0 \mathbf{Y} \in \mathbb{R}^{pn}$, the solutions to the simplified normal equations

are

$$\begin{aligned}\tilde{\alpha}_{kk} &= \frac{\mathbf{r}_0^\top [\mathbf{I}_n \otimes \{\mathbf{E}_{kk} \circ \mathbf{I}(\mathbf{p})\}] \mathbf{r}_0}{\text{tr}(\mathbf{P}_0 [\mathbf{I}_n \otimes \{\mathbf{E}_{kk} \circ \mathbf{I}(\mathbf{p})\}]^2)}, & \tilde{\beta}_{kk} &= \frac{\mathbf{r}_0^\top [\mathbf{I}_n \otimes \{\mathbf{E}_{kk} \circ \mathbf{J}(\mathbf{p})\}] \mathbf{r}_0}{\text{tr}(\mathbf{P}_0 [\mathbf{I}_n \otimes \{\mathbf{E}_{kk} \circ \mathbf{J}(\mathbf{p})\}]^2)} \quad \text{for every } k, \\ \tilde{\beta}_{kk'} &= \frac{\mathbf{r}_0^\top [\mathbf{I}_n \otimes \{(\mathbf{E}_{kk'} + \mathbf{E}_{k'k}) \circ \mathbf{J}(\mathbf{p})\}] \mathbf{r}_0}{\text{tr}(\mathbf{P}_0 [\mathbf{I}_n \otimes \{(\mathbf{E}_{kk'} + \mathbf{E}_{k'k}) \circ \mathbf{J}(\mathbf{p})\}]^2)} \quad \text{for every } k \neq k',\end{aligned}$$

where the denominators can be further simplified respectively (recall $\mathbf{P} = \text{diag}(p_1, \dots, p_K)$):

$$\begin{aligned}\text{tr}(\mathbf{P}_0 [\mathbf{I}_n \otimes \{\mathbf{E}_{kk} \circ \mathbf{I}(\mathbf{p})\}]^2) &= (n-1) \text{tr}\{\mathbf{E}_{kk} \circ \mathbf{I}(\mathbf{p})\} = (n-1)p_k \quad \text{for every } k, \\ \text{tr}(\mathbf{P}_0 [\mathbf{I}_n \otimes \{\mathbf{E}_{kk} \circ \mathbf{J}(\mathbf{p})\}]^2) &= (n-1) \text{tr}\{(\mathbf{E}_{kk} \mathbf{P} \mathbf{E}_{kk}) \circ \mathbf{J}(\mathbf{p})\} = (n-1)p_k^2 \quad \text{for every } k, \\ \text{tr}(\mathbf{P}_0 [\mathbf{I}_n \otimes \{(\mathbf{E}_{kk'} + \mathbf{E}_{k'k}) \circ \mathbf{J}(\mathbf{p})\}]^2) &= (n-1)(2p_k p_{k'}) \quad \text{for every } k \neq k'.\end{aligned}$$

Let $\mathbf{r}_i = (\mathbf{r}_{i,p_1}^\top, \mathbf{r}_{i,p_2}^\top, \dots, \mathbf{r}_{i,p_K}^\top)^\top \in \mathbb{R}^p$ denote the i th subvector of \mathbf{r}_0 satisfying that $\mathbf{r}_0 = (\mathbf{r}_1^\top, \mathbf{r}_2^\top, \dots, \mathbf{r}_n^\top)^\top$. For every k and k' ,

$$\begin{aligned}\tilde{\alpha}_{kk} &= \sum_{i=1}^n \mathbf{r}_{i,p_k}^\top \mathbf{r}_{i,p_k} / \{(n-1)p_k\}, \\ \tilde{\beta}_{kk} &= \sum_{i=1}^n \text{sum}(\mathbf{r}_{i,p_k}) \text{sum}(\mathbf{r}_{i,p_k}) / \{(n-1)p_k^2\} = \sum_{i=1}^n \text{sum}^2(\mathbf{r}_{i,p_k}) / \{(n-1)p_k^2\}, \\ \tilde{\beta}_{kk'} &= \sum_{i=1}^n 2(\text{sum}(\mathbf{r}_{i,p_k}) \text{sum}(\mathbf{r}_{i,p_{k'}})) / \{2(n-1)p_k p_{k'}\} = \sum_{i=1}^n \{\text{sum}(\mathbf{r}_{i,p_k}) \text{sum}(\mathbf{r}_{i,p_{k'}})\} / \{(n-1)p_k p_{k'}\}.\end{aligned}$$

By the facts that $\mathbf{r}_{i,p_k} = \mathbf{X}_{i,p_k} - \bar{\mathbf{X}}_{p_k}$ and $\mathbf{C}_{kk'} = \sum_{i=1}^n (\mathbf{X}_{i,p_k} - \bar{\mathbf{X}}_{p_k})(\mathbf{X}_{i,p_{k'}} - \bar{\mathbf{X}}_{p_{k'}})^\top = \sum_{i=1}^n \mathbf{r}_{i,p_k} \mathbf{r}_{i,p_{k'}}^\top$ for every k and k' , then,

$$\begin{aligned}k \neq k' : \text{sum}(\mathbf{C}_{kk'}) &= \text{sum}\left(\sum_{i=1}^n \mathbf{r}_{i,p_k} \mathbf{r}_{i,p_{k'}}^\top\right) = \sum_{i=1}^n \text{sum}\left(\mathbf{r}_{i,p_k} \mathbf{r}_{i,p_{k'}}^\top\right) = \sum_{i=1}^n \text{sum}(\mathbf{r}_{i,p_k}) \text{sum}(\mathbf{r}_{i,p_{k'}}), \\ k = k' : \text{sum}(\mathbf{C}_{kk'}) &= \text{sum}\left(\sum_{i=1}^n \mathbf{r}_{i,p_k} \mathbf{r}_{i,p_k}^\top\right) = \sum_{i=1}^n \text{sum}\left(\mathbf{r}_{i,p_k} \mathbf{r}_{i,p_k}^\top\right) = \sum_{i=1}^n \text{sum}^2(\mathbf{r}_{i,p_k}), \\ k = k' : \text{tr}(\mathbf{C}_{kk'}) &= \text{tr}\left(\sum_{i=1}^n \mathbf{r}_{i,p_k} \mathbf{r}_{i,p_k}^\top\right) = \sum_{i=1}^n \text{tr}\left(\mathbf{r}_{i,p_k} \mathbf{r}_{i,p_k}^\top\right) = \sum_{i=1}^n \mathbf{r}_{i,p_k}^\top \mathbf{r}_{i,p_k}.\end{aligned}$$

Finally, the estimators for $\boldsymbol{\mu}$ and $\boldsymbol{\Sigma}$ are respectively BLUE and BQUE, but also they are func-

tions of complete statistics. Thus, we have the following best unbiased estimators

$$\tilde{\boldsymbol{\mu}} = \frac{1}{n} \sum_{i=1}^n \mathbf{X}_i, \quad \tilde{\alpha}_{kk} = \frac{1}{n-1} \frac{\text{tr}(\mathbf{C}_{kk})}{p_k}, \quad \tilde{\beta}_{kk'} = \begin{cases} \frac{1}{n-1} \frac{\text{sum}(\mathbf{C}_{kk})}{p_k^2}, & k = k' \\ \frac{1}{n-1} \frac{\text{sum}(\mathbf{C}_{kk'})}{p_k p_{k'}}, & k \neq k' \end{cases},$$

for $\boldsymbol{\mu}$, α_{kk} , and $\beta_{kk'}$ for every k and k' . ■

D.4 Proof Corollary A.2

Proof of Corollary A.2. Roy et al. (2016) and Koziol et al. (2017) provided their formula (4.17) for calculating the variance of a quadratic form $\mathbf{Y} \mathbf{A} \mathbf{Y}^\top$ for some matrix \mathbf{A} satisfying $\mathbf{A} = \mathbf{P}_0 \mathbf{A} \mathbf{P}_0$,

$$\text{var}(\mathbf{Y}^\top \mathbf{A} \mathbf{Y}) = 2 \text{tr}(\mathbf{P}_0 \mathbf{A} \mathbf{V} \mathbf{A} \mathbf{V}),$$

where $\mathbf{Y} \sim N(\boldsymbol{\mu}_y, \mathbf{V})$ and $\mathbf{P}_0 = \mathbf{I}_{pn} - \mathbf{P}_0$ as defined in the proof of Theorem 1. Recall the proof of Theorem 1,

$$\begin{aligned} \tilde{\alpha}_{kk} &= \frac{\mathbf{r}_0^\top [\mathbf{I}_n \otimes \{\mathbf{E}_{kk} \circ \mathbf{I}(\mathbf{p})\}] \mathbf{r}_0}{(n-1)p_k}, \quad \tilde{\beta}_{kk} = \frac{\mathbf{r}_0^\top [\mathbf{I}_n \otimes \{\mathbf{E}_{kk} \circ \mathbf{J}(\mathbf{p})\}] \mathbf{r}_0}{(n-1)p_k^2}, \quad \text{for every } k \\ \tilde{\beta}_{kk'} &= \frac{\mathbf{r}_0^\top [\mathbf{I}_n \otimes \{(\mathbf{E}_{kk'} + \mathbf{E}_{k'k}) \circ \mathbf{J}(\mathbf{p})\}] \mathbf{r}_0}{(n-1)(2p_k p_{k'})}, \quad \text{for every } k \neq k'. \end{aligned}$$

Let $x = x(k, k)$, $y = y(k, k)$, and $z = z(k, k')$ denote the terms $\mathbf{E}_{kk} \circ \mathbf{I}(\mathbf{p})$, $\mathbf{E}_{kk} \circ \mathbf{J}(\mathbf{p})$, and $(\mathbf{E}_{kk'} + \mathbf{E}_{k'k}) \circ \mathbf{J}(\mathbf{p})$ respectively. Then, let ω denote any of x , y , and z and let $\mathbf{Q} = \mathbf{Q}(\omega) = \mathbf{P}_0(\mathbf{I}_n \otimes \omega)\mathbf{P}_0$. So, $\mathbf{P}_0 \mathbf{Q} \mathbf{P}_0 = \mathbf{P}_0^2(\mathbf{I}_n \otimes \omega)\mathbf{P}_0^2 = \mathbf{Q}$ due to the fact that $\mathbf{P}_0^2 = \mathbf{P}_0$. In addition, recall that $\mathbf{P}_0 \mathbf{V} = \mathbf{V} \mathbf{P}_0$. Thus, $\text{var}(\mathbf{Y}^\top \mathbf{Q} \mathbf{Y}) = 2 \text{tr}(\mathbf{P}_0 \mathbf{Q} \mathbf{V} \mathbf{Q} \mathbf{V})$, which can be simplified as below:

$$\begin{aligned} 2 \text{tr}(\mathbf{P}_0 \mathbf{Q} \mathbf{V} \mathbf{Q} \mathbf{V}) &= 2 \text{tr}[\mathbf{P}_0 \{\mathbf{P}_0(\mathbf{I}_n \otimes \omega)\mathbf{P}_0\} \mathbf{V} \{\mathbf{P}_0(\mathbf{I}_n \otimes \omega)\mathbf{P}_0\} \mathbf{V}] \\ &= 2 \text{tr}\{\mathbf{P}_0(\mathbf{I}_n \otimes \omega)\mathbf{V}(\mathbf{I}_n \otimes \omega)\mathbf{V}\}, \end{aligned}$$

where we use the fact that \mathbf{P}_0 commutes with $\mathbf{I}_n \otimes \omega$ and \mathbf{V} , respectively. Therefore,

$$\begin{aligned}
\text{var} \{ \mathbf{r}_0^\top (\mathbf{I}_n \otimes \omega) \mathbf{r}_0 \} &= \text{var} [\mathbf{Y}^\top \{ \mathbf{P}_0 (\mathbf{I}_n \otimes \omega) \mathbf{P}_0 \} \mathbf{Y}] \\
&= 2 \text{tr} \{ \mathbf{P}_0 (\mathbf{I}_n \otimes \omega) \mathbf{V} (\mathbf{I}_n \otimes \omega) \mathbf{V} \} \\
&= 2(n-1) \text{tr} \{ (\omega \boldsymbol{\Sigma}) (\omega \boldsymbol{\Sigma}) \} \\
&= 2(n-1) s_\omega,
\end{aligned}$$

where s_ω denotes $\text{tr} \{ (\omega \boldsymbol{\Sigma}) (\omega \boldsymbol{\Sigma}) \}$. Hence, using these notations,

$$\begin{aligned}
\text{var} (\tilde{\alpha}_{kk}) &= \frac{1}{(n-1)^2 p_k^2} \text{var} \{ \mathbf{r}_0^\top (\mathbf{I}_n \otimes x) \mathbf{r}_0 \} = \frac{2(n-1) s_x}{(n-1)^2 p_k^2} = \frac{2s_x}{(n-1) p_k^2} \quad \text{for every } k, \\
\text{var} (\tilde{\beta}_{kk}) &= \frac{1}{(n-1)^2 p_k^4} \text{var} \{ \mathbf{r}_0^\top (\mathbf{I}_n \otimes y) \mathbf{r}_0 \} = \frac{2(n-1) s_y}{(n-1)^2 p_k^4} = \frac{2s_y}{(n-1) p_k^4} \quad \text{for every } k, \\
\text{var} (\tilde{\beta}_{kk'}) &= \frac{1}{4(n-1)^2 p_k^2 p_{k'}^2} \text{var} \{ \mathbf{r}_0^\top (\mathbf{I}_n \otimes z) \mathbf{r}_0 \} = \frac{2(n-1) s_z}{4(n-1)^2 p_k^2 p_{k'}^2} = \frac{2s_z}{4(n-1) p_k^2 p_{k'}^2} \quad \text{for every } k \neq k',
\end{aligned}$$

where s_x, s_y and s_z are the traces of $(x\boldsymbol{\Sigma})^2, (y\boldsymbol{\Sigma})^2$ and $(z\boldsymbol{\Sigma})^2$ respectively. In fact, the expressions of the covariances among $\tilde{\alpha}$'s and $\tilde{\beta}$'s are associated with terms of the products of any two of $(x\boldsymbol{\Sigma}), (y\boldsymbol{\Sigma})$ and $(z\boldsymbol{\Sigma})$, where $x = x(k, k), y = y(k, k)$, and $z = z(k, k')$ for every k and every $k \neq k'$. We focus on the calculations of $(x\boldsymbol{\Sigma})^2, (y\boldsymbol{\Sigma})^2$, and $(z\boldsymbol{\Sigma})^2$ only.

First, we calculate the $\text{tr}(x\boldsymbol{\Sigma})^2$ as below:

$$\begin{aligned}
(x\boldsymbol{\Sigma})(x\boldsymbol{\Sigma}) &= \{ (\mathbf{E}_{kk}\mathbf{A}) \circ \mathbf{I}(\mathbf{p}) + (\mathbf{E}_{kk}\mathbf{B}) \circ \mathbf{J}(\mathbf{p}) \} \{ (\mathbf{E}_{kk}\mathbf{A}) \circ \mathbf{I}(\mathbf{p}) + (\mathbf{E}_{kk}\mathbf{B}) \circ \mathbf{J}(\mathbf{p}) \} \\
&= \{ (\mathbf{E}_{kk}\mathbf{A})(\mathbf{E}_{kk}\mathbf{A}) \} \circ \mathbf{I}(\mathbf{p}) + \{ (\mathbf{E}_{kk}\mathbf{A})(\mathbf{E}_{kk}\mathbf{B}) \} \circ \mathbf{J}(\mathbf{p}) + \{ (\mathbf{E}_{kk}\mathbf{B})(\mathbf{E}_{kk}\mathbf{A}) \} \circ \mathbf{J}(\mathbf{p}) \\
&\quad + \{ (\mathbf{E}_{kk}\mathbf{B})\mathbf{P}(\mathbf{E}_{kk}\mathbf{B}) \} \circ \mathbf{J}(\mathbf{p}) \\
&= \{ (\mathbf{E}_{kk}\mathbf{A})^2 \} \circ \mathbf{I}(\mathbf{p}) + \{ (\mathbf{E}_{kk}\mathbf{A})(\mathbf{E}_{kk}\mathbf{B}) + (\mathbf{E}_{kk}\mathbf{B})(\mathbf{E}_{kk}\mathbf{A}) + (\mathbf{E}_{kk}\mathbf{B})\mathbf{P}(\mathbf{E}_{kk}\mathbf{B}) \} \circ \mathbf{J}(\mathbf{p}),
\end{aligned}$$

therefore, for every k ,

$$\text{tr} \{ (x\boldsymbol{\Sigma})(x\boldsymbol{\Sigma}) \} = p_k (a_{kk}^2 + 2a_{kk}b_{kk} + p_k b_{kk}^2).$$

Then, we calculate the $\text{tr}(y\Sigma)^2$ as below:

$$\begin{aligned}(y\Sigma)(y\Sigma) &= \{(\mathbf{E}_{kk}\mathbf{A} + \mathbf{E}_{kk}\mathbf{PB}) \circ \mathbf{J}(\mathbf{p})\} \{(\mathbf{E}_{kk}\mathbf{A} + \mathbf{E}_{kk}\mathbf{PB}) \circ \mathbf{J}(\mathbf{p})\} \\ &= \{(\mathbf{E}_{kk}\mathbf{A} + \mathbf{E}_{kk}\mathbf{PB})\mathbf{P}(\mathbf{E}_{kk}\mathbf{A} + \mathbf{E}_{kk}\mathbf{PB})\} \circ \mathbf{J}(\mathbf{p}),\end{aligned}$$

therefore, for every k ,

$$\text{tr}\{(y\Sigma)(y\Sigma)\} = p_k^2(a_{kk} + p_k b_{kk})^2.$$

Finally, we calculate the $\text{tr}(z\Sigma)^2$ as below:

$$(z\Sigma)(z\Sigma) = [\{(\mathbf{E}_{kk'} + \mathbf{E}_{k'k})\mathbf{A} + (\mathbf{E}_{kk'} + \mathbf{E}_{k'k})\mathbf{PB}\} \mathbf{P} \{(\mathbf{E}_{kk'} + \mathbf{E}_{k'k})\mathbf{A} + (\mathbf{E}_{kk'} + \mathbf{E}_{k'k})\mathbf{PB}\}] \circ \mathbf{J}(\mathbf{p}),$$

therefore, for every $k \neq k'$,

$$\text{tr}\{(z_{kk'}\Sigma)(z_{kk'}\Sigma)\} = b_{k'k}^2 p_k^2 p_{k'}^2 + b_{kk'}^2 p_k^2 p_{k'}^2 + 2p_k p_{k'} (a_{kk} + p_k b_{kk})(a_{k'k'} + p_{k'} b_{k'k'}).$$

The expressions of the covariances among $\tilde{\alpha}$'s and $\tilde{\beta}$'s are associated with terms of the products of any two of $(x\Sigma)$, $(y\Sigma)$, and $(z\Sigma)$, where $x = x(k, k)$, $y = y(k, k)$, and $z = z(k, k')$ for every k and $k \neq k'$. One may obtain the covariance estimators by calculating $\text{tr}\{(x\Sigma)(y\Sigma)\}$, $\text{tr}\{(x\Sigma)(z\Sigma)\}$, and $\text{tr}\{(y\Sigma)(z\Sigma)\}$, respectively in a similar manner. We complete the proof of variance estimators. \blacksquare

D.5 Proof of Theorem 2

Lemma D.1. (*Gaussian Hanson-Wright inequality*) Let $X \in \mathbb{R}^p$ be a Gaussian vector with mean zero and covariance matrix Σ and $A \in \mathbb{R}^{p \times p}$. Then, for every $t \geq 0$, we have

$$\text{pr}(|X^\top AX - E(X^\top AX)| \geq t) \leq 2 \exp\left(-C \min\left\{\frac{t^2}{\|\Sigma^{1/2} A \Sigma^{1/2}\|_F^2}, \frac{t}{\|\Sigma^{1/2} A \Sigma^{1/2}\|_S}\right\}\right),$$

where the positive constant C does not depend on p , A , and t .

Proof of Lemma D.1. It can be derived from the case with sub-Gaussian variable. See the original proof in [Hanson and Wright \(1971\)](#) or [Wright \(1973\)](#) and a modern version in [Rudelson and Vershynin \(2013\)](#) or [Vershynin \(2018, Theorem 6.2.1\)](#). ■

We restate Theorem 2 as below.

Theorem 2 (Consistency of the modified hard-thresholding estimator). *Given a positive-definite covariance matrix with the uniform-block structure $\Sigma(\mathbf{A}, \mathbf{B}, \mathbf{p}) = (\sigma_{jj'})$, suppose $K = K(n) > n \rightarrow \infty$ and $\log(K)/n \rightarrow 0$ as $n \rightarrow \infty$, and there exist constants $0 < C_{p_0}, C_{q_0} < \infty$ such that $\sum_{j=1}^p \sum_{j'=1}^p |\sigma_{jj'}|^{p_0} \leq C_{p_0}$ and $\max_j \sum_{j'=1}^p |\sigma_{jj'}|^{q_0} \leq C_{q_0}$ for $0 < p_0 < 2$ and $0 < q_0 < 1$, then*

$$\text{pr} \left\{ \begin{aligned} \|\widehat{\Sigma}_\lambda(\widehat{\mathbf{A}}_\lambda, \widehat{\mathbf{B}}_\lambda, \mathbf{p}) - \Sigma(\mathbf{A}, \mathbf{B}, \mathbf{p})\|_F^2 &\leq C_{p_0} (2\lambda)^{2-p_0}, \\ \|\widehat{\Sigma}_\lambda(\widehat{\mathbf{A}}_\lambda, \widehat{\mathbf{B}}_\lambda, \mathbf{p}) - \Sigma(\mathbf{A}, \mathbf{B}, \mathbf{p})\|_S &\leq C_{q_0} (2\lambda)^{1-q_0} \end{aligned} \right\} \rightarrow 1,$$

as $K, n \rightarrow \infty$, where we choose $\lambda = C\{\log(K)/n\}^{1/2}$ for some positive constant C .

Proof of Theorem 2. We aim to prove it within 4 steps.

Step 1, we would like to find out the upper bounds for the absolute values of the biases for the modified hard-threshold estimators under different cases.

Case 1: for a fixed λ and every fixed k and k' , let $\sigma = b_{kk'}$ and $\tilde{\sigma} = \tilde{b}_{kk'}$, hence let $\hat{\sigma} = \tilde{\sigma}\mathbb{I}(|\tilde{\sigma}| > \lambda)$. Assuming that $|\tilde{\sigma} - \sigma| \leq \lambda/2$, or equivalently, $\sigma - \lambda/2 \leq \tilde{\sigma} \leq \sigma + \lambda/2$, we obtain: if $\sigma \in [-\lambda/2, \lambda/2]$, then $\tilde{\sigma} \in [-\lambda, \lambda]$, or equivalently, $|\tilde{\sigma}| \leq \lambda$, and therefore, $\hat{\sigma} = 0$ and $|\hat{\sigma} - \sigma| = |\sigma| \in [0, \lambda/2]$; if $\sigma \in (3\lambda/2, \infty)$, then $\tilde{\sigma} \in (\lambda, \infty)$, or equivalently, $|\tilde{\sigma}| > \lambda$, and therefore, $\hat{\sigma} = \tilde{\sigma}$ and $|\hat{\sigma} - \sigma| = |\tilde{\sigma} - \sigma| \in [0, \lambda/2]$; if $\sigma \in (-\infty, -3\lambda/2)$, then $\tilde{\sigma} \in (-\infty, -\lambda)$, or equivalently, $|\tilde{\sigma}| > \lambda$, and therefore, $\hat{\sigma} = \tilde{\sigma}$ and $|\hat{\sigma} - \sigma| = |\tilde{\sigma} - \sigma| \in [0, \lambda/2]$; if $\sigma \in (\lambda/2, 3\lambda/2]$, then $\tilde{\sigma} \in (0, 2\lambda]$ and it can be larger than λ or be smaller than λ , therefore $\hat{\sigma} \in \{0, \tilde{\sigma}\}$ and $|\hat{\sigma} - \sigma| = \begin{cases} |\tilde{\sigma} - \sigma| \in [0, \lambda/2], & \tilde{\sigma} \in (\lambda, 2\lambda] \\ |\sigma| \in (\lambda/2, 3\lambda/2], & \tilde{\sigma} \in (0, \lambda] \end{cases}$, which is between 0 and $3\lambda/2$;

if $\sigma \in [-3\lambda/2, -\lambda/2)$, then $\tilde{\sigma} \in [-2\lambda, 0)$ and it can be larger than $-\lambda$ or be smaller than $-\lambda$, therefore $\hat{\sigma} \in \{0, \tilde{\sigma}\}$ and $|\hat{\sigma} - \sigma| = \begin{cases} |\tilde{\sigma} - \sigma| \in [0, \lambda/2], & \tilde{\sigma} \in [-2\lambda, -\lambda) \\ |\sigma| \in [\lambda/2, 3\lambda/2], & \tilde{\sigma} \in [-\lambda, 0) \end{cases}$, which is also between 0 and $3\lambda/2$. Put the above arguments together, for a fixed λ , under the assumption $|\tilde{\sigma} - \sigma| \leq \lambda/2$,

$$|\hat{\sigma} - \sigma| = \begin{cases} |\tilde{\sigma} - \sigma| \in [0, \lambda/2], & \sigma \in (-\infty, -3\lambda/2) \\ \{|\tilde{\sigma} - \sigma|, |\sigma|\} \leq |\sigma| \vee (\lambda/2), & \sigma \in [-3\lambda/2, -\lambda/2) \\ |\sigma| \in [0, \lambda/2], & \sigma \in [-\lambda/2, \lambda/2] \\ \{|\tilde{\sigma} - \sigma|, |\sigma|\} \leq |\sigma| \vee (\lambda/2), & \sigma \in (\lambda/2, 3\lambda/2] \\ |\tilde{\sigma} - \sigma| \in [0, \lambda/2], & \sigma \in (3\lambda/2, \infty) \end{cases},$$

therefore the maximum of $|\hat{\sigma} - \sigma|$ might be either $|\sigma|$ if $\lambda/2 < |\sigma| \leq 3\lambda/2$ or $\lambda/2$ otherwise.

In other words, we may write $|\hat{\sigma} - \sigma| \leq |\sigma| \wedge (3\lambda/2)$.

Case 2: for a fixed λ and every fixed k , let $\sigma = a_{kk}$ and $\tilde{\sigma} = \tilde{a}_{kk}$, hence let $\hat{\sigma} = \tilde{\sigma} \mathbb{I}(|\tilde{\sigma}| > \lambda)$.

We assume that $|\tilde{\alpha}_{kk} - \alpha_{kk}| \leq \lambda/2$ and $|\tilde{b}_{kk} - b_{kk}| \leq \lambda/2$ holds simultaneously, then

$$|\tilde{a}_{kk} - a_{kk}| = |\tilde{\alpha}_{kk} - \tilde{b}_{kk} - (\alpha_{kk} - b_{kk})| = |(\tilde{\alpha}_{kk} - \alpha_{kk}) - (\tilde{b}_{kk} - b_{kk})| \leq |\tilde{\alpha}_{kk} - \alpha_{kk}| + |\tilde{b}_{kk} - b_{kk}| \leq \lambda.$$

So, the above assumption is equivalent implies that $|\tilde{\sigma} - \sigma| \leq \lambda$, or equivalently, $\sigma - \lambda \leq \tilde{\sigma} \leq \sigma + \lambda$: if $\sigma \in (-\infty, -2\lambda)$, then $\tilde{\sigma} \in (-\infty, -\lambda)$ and therefore $|\tilde{\sigma}| > \lambda$, and $\hat{\sigma} = \tilde{\sigma}$, and thus

$|\hat{\sigma} - \sigma| = |\tilde{\sigma} - \sigma| \in [0, \lambda]$; if $\sigma = 0$, then $|\tilde{\sigma}| \leq \lambda$ and therefore $\hat{\sigma} = 0$, and $|\hat{\sigma} - \sigma| = |\sigma| = 0$;

if $\sigma \in (0, 2\lambda]$, then $\tilde{\sigma} \in (-\lambda, 3\lambda]$ and therefore $|\tilde{\sigma}|$ can be larger than λ or be smaller than λ ,

thus $\hat{\sigma} = \{0, \tilde{\sigma}\}$, and thus $|\hat{\sigma} - \sigma| = \begin{cases} |\tilde{\sigma} - \sigma| \in [0, \lambda], & \tilde{\sigma} \in (\lambda, 3\lambda] \\ |\sigma| \in (0, 2\lambda], & \tilde{\sigma} \in (-\lambda, \lambda) \end{cases}$, which is between 0 and 2λ ;

if $\sigma \in [-2\lambda, 0)$, then $\tilde{\sigma} \in [-3\lambda, \lambda)$ and therefore $|\tilde{\sigma}|$ can be larger than λ or be smaller

than λ , thus $\hat{\sigma} = \{\tilde{\sigma}, 0\}$, and thus $|\hat{\sigma} - \sigma| = \begin{cases} |\tilde{\sigma} - \sigma| \in [0, \lambda], & \tilde{\sigma} \in [-3\lambda, -\lambda) \\ |\sigma| \in (0, 2\lambda], & \tilde{\sigma} \in [-\lambda, \lambda) \end{cases}$, which is

between 0 and 2λ ; if $\sigma \in (2\lambda, \infty)$, then $\tilde{\sigma} \in (\lambda, \infty)$ and therefore $|\tilde{\sigma}| > \lambda$, and $\hat{\sigma} = \tilde{\sigma}$, and thus $|\hat{\sigma} - \sigma| = |\tilde{\sigma} - \sigma| \in [0, \lambda]$. Put the above arguments together, for a fixed λ , under the assumption $|\tilde{\sigma} - \sigma| \leq \lambda$,

$$|\hat{\sigma} - \sigma| = \begin{cases} |\tilde{\sigma} - \sigma| \in [0, \lambda], & \sigma \in (-\infty, -2\lambda) \\ \{|\tilde{\sigma} - \sigma|, |\sigma|\} \leq |\sigma| \vee \lambda, & \sigma \in [-2\lambda, 0) \\ 0, & \sigma = 0 \\ \{|\tilde{\sigma} - \sigma|, |\sigma|\} \leq |\sigma| \vee \lambda, & \sigma \in (0, 2\lambda] \\ |\tilde{\sigma} - \sigma| \in [0, \lambda], & \sigma \in (2\lambda, \infty) \end{cases},$$

therefore the maximum of $|\hat{\sigma} - \sigma|$ might be either $|\sigma|$ if $0 < |\sigma| \leq 2\lambda$ or λ otherwise. In other words, we may write $|\hat{\sigma} - \sigma| \leq |\sigma| \wedge (2\lambda)$. Thus, at Step 1, we conclude that $|\hat{a}_{kk} - a_{kk}| \leq |a_{kk}| \wedge (2\lambda)$ and $|\hat{b}_{kk'} - b_{kk'}| \leq |b_{kk'}| \wedge (3\lambda/2)$ for a fixed λ and every k and k' under the assumptions: $\max_{1 \leq k \leq K} |\tilde{\alpha}_{kk} - \alpha_{kk}| \leq \lambda/2$ and $\max_{1 \leq k, k' \leq K} |\tilde{b}_{kk'} - b_{kk'}| \leq \lambda/2$. We denote the following event sets

$$\begin{aligned} \mathbf{E}_N^{(0)} &= \left\{ \max_{1 \leq k \leq K} |\tilde{a}_{kk} - a_{kk}| \leq \lambda \right\}, & \mathbf{E}_N^{(1)} &= \left\{ \max_{1 \leq k \leq K} |\tilde{\alpha}_{kk} - \alpha_{kk}| \leq \lambda/2 \right\}, \\ \mathbf{E}_N^{(2)} &= \left\{ \max_{1 \leq k \leq K} |\tilde{b}_{kk} - b_{kk}| \leq \lambda/2 \right\}, & \mathbf{E}_N^{(3)} &= \left\{ \max_{1 \leq k \neq k' \leq K} |\tilde{b}_{kk'} - b_{kk'}| \leq \lambda/2 \right\}, \end{aligned}$$

and the event sets $\mathbf{E}_N^{(1)}$ and $\mathbf{E}_N^{(2)}$ implies that $\mathbf{E}_N^{(0)}$. The probability of their complement sets can be bounded as below:

$$\begin{aligned} \text{pr} \left(\mathbf{E}_N^{(1), \mathbb{E}} \right) &= \text{pr} \left(\max_{1 \leq k \leq K} |\tilde{\alpha}_{kk} - \alpha_{kk}| > \lambda/2 \right) \stackrel{[1]}{\leq} K \text{pr} \left(|\tilde{\alpha}_{kk} - \alpha_{kk}| > \lambda/2 \right), \\ \text{pr} \left(\mathbf{E}_N^{(2), \mathbb{E}} \right) &= \text{pr} \left(\max_{1 \leq k \leq K} |\tilde{b}_{kk} - b_{kk}| > \lambda/2 \right) \leq K \text{pr} \left(|\tilde{b}_{kk} - b_{kk}| > \lambda/2 \right), \\ \text{pr} \left(\mathbf{E}_N^{(3), \mathbb{E}} \right) &= \text{pr} \left(\max_{1 \leq k \neq k' \leq K} |\tilde{b}_{kk'} - b_{kk'}| > \lambda/2 \right) \leq K(K-1) \text{pr} \left(|\tilde{b}_{kk'} - b_{kk'}| > \lambda/2 \right), \end{aligned}$$

where [1] holds due to the union bound.

Step 2, we would like to compute the upper bounds for the above three probabilities respec-

tively.

Let $\mathbf{E}_{kk'} \in \mathbb{R}^{K \times K}$ denote the matrix whose (k, k') entry is 1 and the other entries are 0 for every k and k' . Then, let $\mathbf{A}_{kk} = (p_k^{-1} \mathbf{E}_{kk}) \circ \mathbf{I}(\mathbf{p})$, $\mathbf{B}_{kk} = \{-p_k^{-1}(p_k - 1)^{-1} \mathbf{E}_{kk}\} \circ \mathbf{I}(\mathbf{p}) + \{p_k^{-1}(p_k - 1)^{-1} \mathbf{E}_{kk}\} \circ \mathbf{J}(\mathbf{p})$ and $\mathbf{B}_{kk'} = \{(p_k p_{k'})^{-1} \mathbf{E}_{kk'}\} \circ \mathbf{J}(\mathbf{p})$ for every k and $k \neq k'$. Let $\mathbf{W} = (\mathbf{X}_1^\top, \dots, \mathbf{X}_n^\top)^\top \in \mathbb{R}^{pn}$ and decompose $\mathbf{X} = (\mathbf{X}_{p_1}^\top, \dots, \mathbf{X}_{p_K}^\top)^\top$, where $\mathbf{X}_{p_k} = (\mathbf{X}_{\bar{p}_{k-1}+1}, \dots, \mathbf{X}_{\bar{p}_k})^\top \in \mathbb{R}^{p_k}$ for every k , $\bar{p}_0 = 0$ and $\bar{p}_k = \sum_{k'=1}^k p_{k'}$ denote the sum of the first k elements of \mathbf{p} for $k = 1, \dots, K$. Note that $\boldsymbol{\mu} = \mathbf{0}_{p \times 1}$ is known and $\mathbf{S} = \mathbf{X}^\top \mathbf{X} / n$, thus,

$$\begin{aligned} \mathbf{W}^\top (\mathbf{I}_n \otimes \mathbf{A}_{kk}) \mathbf{W} &= \sum_{i=1}^n \mathbf{X}_i^\top \mathbf{A}_{kk} \mathbf{X}_i = \frac{1}{p_k} \sum_{i=1}^n \text{tr}(\mathbf{X}_{i,p_k} \mathbf{X}_{i,p_k}^\top) = \frac{n}{p_k} \text{tr}(\mathbf{S}_{kk}) = n \tilde{\alpha}_{kk}, \\ \mathbf{W}^\top (\mathbf{I}_n \otimes \mathbf{B}_{kk}) \mathbf{W} &= \sum_{i=1}^n \mathbf{X}_i^\top \mathbf{B}_{kk} \mathbf{X}_i = \frac{n}{p_k(p_k - 1)} \{\text{sum}(\mathbf{S}_{kk}) - \text{tr}(\mathbf{S}_{kk})\} = n \tilde{b}_{kk}, \\ \mathbf{W}^\top (\mathbf{I}_n \otimes \mathbf{B}_{kk'}) \mathbf{W} &= \sum_{i=1}^n \mathbf{X}_i^\top \mathbf{B}_{kk'} \mathbf{X}_i = \frac{1}{p_k p_{k'}} \sum_{i=1}^n \text{sum}(\mathbf{X}_{i,p_k} \mathbf{X}_{i,p_{k'}}^\top) = \frac{n}{p_k p_{k'}} \text{sum}(\mathbf{S}_{kk'}) = n \tilde{b}_{kk'}, \end{aligned}$$

for every k and for every $k \neq k'$ respectively.

On the one hand, $\tilde{\alpha}_{kk}, \tilde{b}_{kk'}$ are unbiased estimators of α_{kk} and $b_{kk'}$ for every k and k' , let

$$\begin{aligned} Q_{kk}^{(\alpha)} &= \mathbf{W}^\top (\mathbf{I}_n \otimes \mathbf{A}_{kk}) \mathbf{W} - \mathbb{E} \{ \mathbf{W}^\top (\mathbf{I}_n \otimes \mathbf{A}_{kk}) \mathbf{W} \} = n (\tilde{\alpha}_{kk} - \alpha_{kk}), \\ Q_{kk'}^{(b)} &= \mathbf{W}^\top (\mathbf{I}_n \otimes \mathbf{B}_{kk'}) \mathbf{W} - \mathbb{E} \{ \mathbf{W}^\top (\mathbf{I}_n \otimes \mathbf{B}_{kk'}) \mathbf{W} \} = n (\tilde{b}_{kk'} - b_{kk'}), \end{aligned}$$

for every k and k' . On the other hand, applying the result of Lemma D.1, given a $\delta > 0$,

$$\begin{aligned}
& \text{pr} \left(|\tilde{\alpha}_{kk} - \alpha_{kk}| > \delta \right) \\
&= \text{pr} \left(\left| Q_{kk}^{(\alpha)} \right| > n\delta \right) \\
&\leq 2 \exp \left(-C \min \left\{ \frac{(n\delta)^2}{\left\| (\mathbf{I}_n \otimes \boldsymbol{\Sigma})^{1/2} (\mathbf{I}_n \otimes \mathbf{A}_{kk}) (\mathbf{I}_n \otimes \boldsymbol{\Sigma})^{1/2} \right\|_{\text{F}}^2}, \frac{n\delta}{\left\| (\mathbf{I}_n \otimes \boldsymbol{\Sigma})^{1/2} (\mathbf{I}_n \otimes \mathbf{A}_{kk}) (\mathbf{I}_n \otimes \boldsymbol{\Sigma})^{1/2} \right\|_{\text{S}}} \right\} \right), \\
& \text{pr} \left(|\tilde{b}_{kk} - b_{kk}| > \delta \right) \\
&\leq 2 \exp \left(-C \min \left\{ \frac{(n\delta)^2}{\left\| (\mathbf{I}_n \otimes \boldsymbol{\Sigma})^{1/2} (\mathbf{I}_n \otimes \mathbf{B}_{kk}) (\mathbf{I}_n \otimes \boldsymbol{\Sigma})^{1/2} \right\|_{\text{F}}^2}, \frac{n\delta}{\left\| (\mathbf{I}_n \otimes \boldsymbol{\Sigma})^{1/2} (\mathbf{I}_n \otimes \mathbf{B}_{kk}) (\mathbf{I}_n \otimes \boldsymbol{\Sigma})^{1/2} \right\|_{\text{S}}} \right\} \right), \\
& \text{pr} \left(|\tilde{b}_{kk'} - b_{kk'}| > \delta \right) \\
&\leq 2 \exp \left(-C \min \left\{ \frac{(n\delta)^2}{\left\| (\mathbf{I}_n \otimes \boldsymbol{\Sigma})^{1/2} (\mathbf{I}_n \otimes \mathbf{B}_{kk'}) (\mathbf{I}_n \otimes \boldsymbol{\Sigma})^{1/2} \right\|_{\text{F}}^2}, \frac{n\delta}{\left\| (\mathbf{I}_n \otimes \boldsymbol{\Sigma})^{1/2} (\mathbf{I}_n \otimes \mathbf{B}_{kk'}) (\mathbf{I}_n \otimes \boldsymbol{\Sigma})^{1/2} \right\|_{\text{S}}} \right\} \right),
\end{aligned}$$

for every k , for every k , and for every $k \neq k'$ respectively, where C is a positive constant. By the properties of Kronecker product and Frobenius norm,

$$\begin{aligned}
\left\| (\mathbf{I}_n \otimes \boldsymbol{\Sigma})^{1/2} (\mathbf{I}_n \otimes \mathbf{A}_{kk}) (\mathbf{I}_n \otimes \boldsymbol{\Sigma})^{1/2} \right\|_{\text{F}}^2 &= \left\| (\mathbf{I}_n \otimes \boldsymbol{\Sigma}^{1/2}) (\mathbf{I}_n \otimes \mathbf{A}_{kk}) (\mathbf{I}_n \otimes \boldsymbol{\Sigma}^{1/2}) \right\|_{\text{F}}^2 \\
&= n \left\| \boldsymbol{\Sigma}^{1/2} \mathbf{A}_{kk} \boldsymbol{\Sigma}^{1/2} \right\|_{\text{F}}^2 \\
&= n \text{tr} \left\{ (\boldsymbol{\Sigma}^{1/2} \mathbf{A}_{kk} \boldsymbol{\Sigma}^{1/2}) (\boldsymbol{\Sigma}^{1/2} \mathbf{A}_{kk} \boldsymbol{\Sigma}^{1/2}) \right\} \\
&= n \text{tr} \left(\boldsymbol{\Sigma}^{1/2} \mathbf{A}_{kk} \boldsymbol{\Sigma} \mathbf{A}_{kk} \boldsymbol{\Sigma}^{1/2} \right) \\
&= n \text{tr} \left(\mathbf{A}_{kk} \boldsymbol{\Sigma} \mathbf{A}_{kk} \boldsymbol{\Sigma} \right),
\end{aligned}$$

and

$$\begin{aligned}
\left\| (\mathbf{I}_n \otimes \boldsymbol{\Sigma})^{1/2} (\mathbf{I}_n \otimes \mathbf{B}_{kk}) (\mathbf{I}_n \otimes \boldsymbol{\Sigma})^{1/2} \right\|_{\text{F}}^2 &= n \text{tr} \left(\mathbf{B}_{kk} \boldsymbol{\Sigma} \mathbf{B}_{kk} \boldsymbol{\Sigma} \right), \\
\left\| (\mathbf{I}_n \otimes \boldsymbol{\Sigma})^{1/2} (\mathbf{I}_n \otimes \mathbf{B}_{kk'}) (\mathbf{I}_n \otimes \boldsymbol{\Sigma})^{1/2} \right\|_{\text{F}}^2 &= n \text{tr} \left(\mathbf{B}_{kk'} \boldsymbol{\Sigma} \mathbf{B}_{kk'} \boldsymbol{\Sigma} \right).
\end{aligned}$$

Then, calculate the traces,

$$n \operatorname{tr}(\mathbf{A}_{kk} \Sigma \mathbf{A}_{kk} \Sigma) = \frac{n}{p_k} (a_{kk}^2 + 2a_{kk}b_{kk} + p_k b_{kk}^2),$$

$$n \operatorname{tr}(\mathbf{B}_{kk} \Sigma \mathbf{B}_{kk} \Sigma) = \frac{n}{p_k(p_k - 1)^2} \{a_{kk}^2 - 2a_{kk}(a_{kk} - b_{kk} + p_k b_{kk}) + p_k(a_{kk} + p_k b_{kk} - b_{kk})^2\},$$

$$n \operatorname{tr}(\mathbf{B}_{kk'} \Sigma \mathbf{B}_{kk'} \Sigma) = n b_{kk'}^2.$$

By the properties of the operator norm, let $\lambda_{\max}(M)$ denote the largest eigenvalue of M ,

$$\begin{aligned} \left\| (\mathbf{I}_n \otimes \Sigma)^{1/2} (\mathbf{I}_n \otimes \mathbf{A}_{kk}) (\mathbf{I}_n \otimes \Sigma)^{1/2} \right\|_S^2 &= \left\| \mathbf{I}_n \otimes (\Sigma^{1/2} \mathbf{A}_{kk} \Sigma^{1/2}) \right\|_S^2 \\ &= \lambda_{\max} \left[\{ \mathbf{I}_n \otimes (\Sigma^{1/2} \mathbf{A}_{kk} \Sigma^{1/2}) \} \{ \mathbf{I}_n \otimes (\Sigma^{1/2} \mathbf{A}_{kk} \Sigma^{1/2}) \} \right] \\ &= \lambda_{\max} \left[\mathbf{I}_n \otimes \{ (\Sigma^{1/2} \mathbf{A}_{kk} \Sigma^{1/2}) (\Sigma^{1/2} \mathbf{A}_{kk} \Sigma^{1/2}) \} \right] \\ &= \lambda_{\max} \{ (\Sigma^{1/2} \mathbf{A}_{kk} \Sigma^{1/2}) (\Sigma^{1/2} \mathbf{A}_{kk} \Sigma^{1/2}) \} \\ &= \lambda_{\max} (\Sigma^{1/2} \mathbf{A}_{kk} \Sigma \mathbf{A}_{kk} \Sigma^{1/2}), \end{aligned}$$

and

$$\begin{aligned} \left\| (\mathbf{I}_n \otimes \Sigma)^{1/2} (\mathbf{I}_n \otimes \mathbf{B}_{kk}) (\mathbf{I}_n \otimes \Sigma)^{1/2} \right\|_S^2 &= \lambda_{\max} (\Sigma^{1/2} \mathbf{B}_{kk} \Sigma \mathbf{B}_{kk} \Sigma^{1/2}), \\ \left\| (\mathbf{I}_n \otimes \Sigma)^{1/2} (\mathbf{I}_n \otimes \mathbf{B}_{kk'}) (\mathbf{I}_n \otimes \Sigma)^{1/2} \right\|_S^2 &= \lambda_{\max} (\Sigma^{1/2} \mathbf{B}_{kk'} \Sigma \mathbf{B}_{kk'} \Sigma^{1/2}). \end{aligned}$$

Therefore, under the assumption about Σ , there exist positive constants $C_{1,*}$ and $C_{2,*}$ satisfying that

$$\begin{aligned} C_{1,*}^2 &= C_{\mathbf{A}, \mathbf{B}, \mathbf{p}}^2 = \max_K \max_{1 \leq k, k' \leq K} \\ &\{ \lambda_{\max} (\Sigma^{1/2} \mathbf{A}_{kk} \Sigma \mathbf{A}_{kk} \Sigma^{1/2}), \lambda_{\max} (\Sigma^{1/2} \mathbf{B}_{kk} \Sigma \mathbf{B}_{kk} \Sigma^{1/2}), \lambda_{\max} (\Sigma^{1/2} \mathbf{B}_{kk'} \Sigma \mathbf{B}_{kk'} \Sigma^{1/2}) \} < \infty, \end{aligned}$$

and

$$C_{2,*}^2 = C_{\mathbf{A}, \mathbf{B}, \mathbf{p}}^2 = \max_K \max_{1 \leq k, k' \leq K} \{ \operatorname{tr}(\mathbf{A}_{kk} \Sigma \mathbf{A}_{kk} \Sigma), \operatorname{tr}(\mathbf{B}_{kk} \Sigma \mathbf{B}_{kk} \Sigma), \operatorname{tr}(\mathbf{B}_{kk'} \Sigma \mathbf{B}_{kk'} \Sigma) \} < \infty.$$

Therefore,

$$\begin{aligned}
K \operatorname{pr} (|\tilde{\alpha}_{kk} - \alpha_{kk}| > \delta) &\leq 2K \exp \left(-C \min \left\{ \frac{n\delta^2}{C_{2,*}^2}, \frac{n\delta}{C_{1,*}} \right\} \right), \\
K \operatorname{pr} \left(\left| \tilde{b}_{kk} - b_{kk} \right| > \delta \right) &\leq 2K \exp \left(-C \min \left\{ \frac{n\delta^2}{C_{2,*}^2}, \frac{n\delta}{C_{1,*}} \right\} \right), \\
K(K-1) \operatorname{pr} \left(\left| \tilde{b}_{kk'} - b_{kk'} \right| > \delta \right) &\leq 2K(K-1) \exp \left(-C \min \left\{ \frac{n\delta^2}{C_{2,*}^2}, \frac{n\delta}{C_{1,*}} \right\} \right).
\end{aligned}$$

Step 3, let $U = Cn \min \{ \lambda^2 (2C_{2,*}^2)^{-1}, \lambda (2C_{1,*})^{-1} \} = Cn \min \{ \lambda^2, \lambda \}$, where constants $C_{1,*}$ and $C_{2,*}$ are absorbed into constant C . Set $n^{-1} \log(K) \rightarrow 0$ as $K > n \rightarrow \infty$. Let $\lambda = \eta \sqrt{\log(K)/n} \rightarrow 0^+$, then $n\lambda^2 = \eta^2 \log(K) \rightarrow \infty$, while $\lambda^2 < \lambda$ since $\lambda \rightarrow 0^+$. So, we have

$$\lim_{n \rightarrow \infty} \frac{U}{\log(K)} = \lim_{n \rightarrow \infty} \frac{Cn\lambda^2}{\log(K)} = \lim_{n \rightarrow \infty} \frac{C\eta^2 \log(K)}{\log(K)} = C\eta^2.$$

Therefore, the Forbenius norm is bounded as below,

$$\begin{aligned}
\left\| \widehat{\Sigma} - \Sigma \right\|_F^2 &= \sum_{k=1}^K p_k (\widehat{\alpha}_{kk} - \alpha_{kk})^2 + \sum_{k=1}^K p_k (p_k - 1) (\widehat{b}_{kk} - b_{kk})^2 + \sum_{k \neq k'} p_k p_{k'} (\widehat{b}_{kk'} - b_{kk'})^2 \\
&\leq \sum_{k=1}^K p_k \{ \alpha_{kk}^2 \wedge (2\lambda)^2 \} + \sum_{k=1}^K p_k (p_k - 1) \{ b_{kk}^2 \wedge (3\lambda/2)^2 \} + \sum_{k \neq k'} p_k p_{k'} \{ b_{kk'}^2 \wedge (3\lambda/2)^2 \},
\end{aligned}$$

and the spectral norm is bounded below

$$\begin{aligned}
\left\| \widehat{\Sigma} - \Sigma \right\|_s &\leq \left\| \widehat{\Sigma} - \Sigma \right\|_1 \\
&= \sup_{1 \leq j' \leq p} \left\{ \left| \alpha_{k(j')k(j')} \right| \wedge (2\lambda) + (p_{k(j')} - 1) \left| b_{k(j')k(j')} \right| \wedge (3\lambda/2) + \sum_{k \neq k(j')} p_k \left| b_{kk(j')} \right| \wedge (3\lambda/2) \right\},
\end{aligned}$$

where $k(j') = k$ if $j' \in \{ \bar{p}_{k-1} + 1, \bar{p}_{k-1} + 2, \dots, \bar{p}_k \}$ for every k .

Finally, step 4, set $0 < p_0 < 2$ and therefore x^{2-p_0} is monotonically increasing on $(0, \infty)$.

Let $\omega_{kk}^{(\alpha),2} = \alpha_{kk}^2 \wedge (2\lambda)^2$, $\omega_{kk'}^{(b),2} = b_{kk'}^2 \wedge (3\lambda/2)^2$ for every k and k' . After doing some algebra,

we have

$$\begin{aligned}
\sum_{k=1}^K p_k \{ \alpha_{kk}^2 \wedge (2\lambda)^2 \} &= \sum_{k=1}^K p_k \left| \omega_{kk}^{(\alpha)} \right|^{p_0} \left| \omega_{kk}^{(\alpha)} \right|^{2-p_0} \\
&\leq \sum_{k=1}^K p_k \left| \omega_{kk}^{(\alpha)} \right|^{p_0} \left(\max_{1 \leq k \leq K} \left| \omega_{kk}^{(\alpha)} \right| \right)^{2-p_0} \\
&= \left(\max_{1 \leq k \leq K} \left| \omega_{kk}^{(\alpha)} \right| \right)^{2-p_0} \left(\sum_{k=1}^K p_k \left| \omega_{kk}^{(\alpha)} \right|^{p_0} \right) \\
&\leq (2\lambda)^{2-p_0} \left(\sum_{k=1}^K p_k |\alpha_{kk}|^{p_0} \right),
\end{aligned}$$

and

$$\begin{aligned}
\sum_{k=1}^K p_k (p_k - 1) \{ b_{kk}^2 \wedge (3\lambda/2)^2 \} &\leq \left(\max_{1 \leq k \leq K} \left| \omega_{kk}^{(b)} \right| \right)^{2-p_0} \left\{ \sum_{k=1}^K p_k (p_k - 1) \left| \omega_{kk}^{(b)} \right|^{p_0} \right\} \\
&\leq (3\lambda/2)^{2-p_0} \left\{ \sum_{k=1}^K p_k (p_k - 1) |b_{kk}|^{p_0} \right\}, \\
\sum_{k \neq k'} p_k p_{k'} \{ b_{kk'}^2 \wedge (3\lambda/2)^2 \} &\leq \left(\max_{1 \leq k \neq k' \leq K} \left| \omega_{kk'}^{(b)} \right| \right)^{2-p_0} \left(\sum_{k=1}^K p_k p_{k'} \left| \omega_{kk'}^{(b)} \right|^{p_0} \right) \\
&\leq (3\lambda/2)^{2-p_0} \left(\sum_{k \neq k'} p_k p_{k'} |b_{kk'}|^{p_0} \right).
\end{aligned}$$

Put them together,

$$\begin{aligned}
&\left\| \widehat{\Sigma} - \Sigma \right\|_F^2 \\
&\leq \sum_{k=1}^K p_k \{ \alpha_{kk}^2 \wedge (2\lambda)^2 \} + \sum_{k=1}^K p_k (p_k - 1) \{ b_{kk}^2 \wedge (3\lambda/2)^2 \} + \sum_{k \neq k'} p_k p_{k'} \{ b_{kk'}^2 \wedge (3\lambda/2)^2 \} \\
&\leq (2\lambda)^{2-p_0} \left(\sum_{k=1}^K p_k |\alpha_{kk}|^{p_0} \right) + (3\lambda/2)^{2-p_0} \left(\sum_{k=1}^K p_k (p_k - 1) |b_{kk}|^{p_0} \right) + (3\lambda/2)^{2-p_0} \left(\sum_{k \neq k'} p_k p_{k'} |b_{kk'}|^{p_0} \right) \\
&\leq (2\lambda)^{2-p_0} \left\| \Sigma \right\|_{p_0}^{p_0, (\text{vector})},
\end{aligned}$$

where $\|\cdot\|_p^{(\text{vector})}$ denotes the entrywise norm. For the spectral norm, consider $0 < q_0 < 1$,

$$\begin{aligned}
& \left\| \widehat{\Sigma} - \Sigma \right\|_s \\
&= \sup_{1 \leq j' \leq p} \left\{ \left| \alpha_{k(j')k(j')} \right| \wedge (2\lambda) + (p_{k(j')} - 1) \left| b_{k(j')k(j')} \right| \wedge (3\lambda/2) + \sum_{k \neq k(j')} p_k \left| b_{kk(j')} \right| \wedge (3\lambda/2) \right\} \\
&\leq \sup_{1 \leq j' \leq p} \left\{ (2\lambda)^{1-q_0} \left| \alpha_{k(j')k(j')} \right|^{q_0} + (3\lambda/2)^{1-q_0} (p_{k(j')} - 1) \left| b_{k(j')k(j')} \right|^{q_0} + (3\lambda/2)^{1-q_0} \sum_{k \neq k(j')} p_k \left| b_{kk(j')} \right|^{q_0} \right\} \\
&\leq (2\lambda)^{1-q_0} \sup_{1 \leq j' \leq p} \left\{ \left| \alpha_{k(j')k(j')} \right|^{q_0} + (p_{k(j')} - 1) \left| b_{k(j')k(j')} \right|^{q_0} + \sum_{k \neq k(j')} p_k \left| b_{kk(j')} \right|^{q_0} \right\} \\
&\leq (2\lambda)^{1-q_0} \|\Sigma^{q_0}\|_1,
\end{aligned}$$

where $\|\cdot\|_1^{q_0}$ denotes the maximum absolute column sum (with q_0 -th power entrywisely).

In summary, given $\log(K)/n \rightarrow 0$ as $K = K_n > n \rightarrow \infty$, we select $C\eta^2 = 5$ and $\lambda = \eta\sqrt{\log(K)/n} \rightarrow 0$, then $2K(K-1)\exp(-U) \rightarrow 0$. Furthermore, for $0 < p_0 < 2$ and $0 < q_0 < 1$, $\|\widehat{\Sigma} - \Sigma\|_F^2 \leq (2\lambda)^{2-p_0} \|\Sigma\|_{p_0}^{p_0, (\text{vector})}$ and $\|\widehat{\Sigma} - \Sigma\|_s \leq (2\lambda)^{1-q_0} \|\Sigma^{q_0}\|_1$ with probability 1. ■

References

- Bickel, P. J. and Doksum, K. A. (2015a). *Mathematical statistics: basic ideas and selected topics*, volume 1. CRC Press, 2 edition.
- Bickel, P. J. and Doksum, K. A. (2015b). *Mathematical statistics: basic ideas and selected topics*, volume 2. CRC Press, 2 edition.
- Buaphim, N., Onsaard, K., So-ngoan, P., and Rungratgasame, T. (2018). Some reviews on ranks of upper triangular block matrices over a skew field. In *International Mathematical Forum*, volume 13, pages 323–335.
- Fan, J. and Han, X. (2017). Estimation of the false discovery proportion with unknown de-

- pendence. *Journal of the Royal Statistical Society: Series B (Statistical Methodology)* **79**, 1143–1164.
- Fan, J., Han, X., and Gu, W. (2012). Estimating false discovery proportion under arbitrary covariance dependence. *Journal of the American Statistical Association* **107**, 1019–1035.
- Fan, J., Liao, Y., and Mincheva, M. (2016). *POET: Principal Orthogonal ComplEment Thresh-
olding (POET) Method*. R package version 2.0.
- Ferguson, T. (1996). *A Course in Large Sample Theory*. Chapman & Hall Texts in Statistical Science Series. Springer US.
- Hanson, D. L. and Wright, F. T. (1971). A Bound on Tail Probabilities for Quadratic Forms in Independent Random Variables. *The Annals of Mathematical Statistics* **42**, 1079 – 1083.
- Henderson, H. V. and Searle, S. R. (1979). Vec and vech operators for matrices, with some uses in jacobians and multivariate statistics. *The Canadian Journal of Statistics / La Revue Canadienne de Statistique* **7**, 65–81.
- Koziol, A., Roy, A., Zmyślony, R., Leiva, R., and Fonseca, M. (2017). Best unbiased estimates for parameters of three-level multivariate data with doubly exchangeable covariance structure. *Linear Algebra and its Applications* **535**, 87–104.
- Lee, K., Lin, L., and You, K. (2021). *CovTools: Statistical Tools for Covariance Analysis*. R package version 0.5.4.
- R Core Team (2021). *R: A Language and Environment for Statistical Computing*. R Foundation for Statistical Computing, Vienna, Austria.
- Roy, A., Zmyślony, R., Fonseca, M., and Leiva, R. (2016). Optimal estimation for doubly multivariate data in blocked compound symmetric covariance structure. *Journal of Multivariate Analysis* **144**, 81–90.
- Rudelson, M. and Vershynin, R. (2013). Hanson-Wright inequality and sub-gaussian concentration. *Electronic Communications in Probability* **18**, 1 – 9.

- Seely, J. (1971). Quadratic Subspaces and Completeness. *The Annals of Mathematical Statistics* **42**, 710 – 721.
- Stuart, A., Ord, J., and Arnold, S. (1999). *Advanced Theory of Statistics, Volume 2A: Classical Inference and the Linear Model*. London: Oxford University Press.
- Van Der Vaart, A. W. and Wellner, J. A. (1996). *Weak convergence and empirical processes*. Springer.
- Vershynin, R. (2018). *High-Dimensional Probability: An Introduction with Applications in Data Science*. Cambridge Series in Statistical and Probabilistic Mathematics. Cambridge University Press.
- Wang, B. (2015). *Regularized Estimators of Covariance Matrices with CV Tuning*. R package version 1.0.
- Wichura, M. J. (2006). *The coordinate-free approach to linear models*, volume 19. Cambridge University Press.
- Wright, F. T. (1973). A bound on tail probabilities for quadratic forms in independent random variables whose distributions are not necessarily symmetric. *The Annals of Probability* **1**, 1068–1070.
- Yang, Y., Lee, H., and Chen, S. (2023). A new representation of uniform-block matrix and applications.
- Zmyślony, R. (1976). On estimation of parameters in linear models. *Applicationes Mathematicae* **3**, 271–276.